The New Gradient Wave

soluble compound screening using microfluidic gradients for regenerative medicine research

Björn Harink

The New Gradient Wave

Björn Harink

Graduation committee

Chair	Prof. Dr. Hans Hilgenkamp
Promoter	Prof. Dr. Clemens van Blitterswijk
Assistant promoter	Dr. Pamela Habibovic
Members	Prof. Dr. Albert van den Berg (University of Twente)
	Dr. Séverine Le Gac (University of Twente)
	Prof. Dr. Liam Grover (University of Birmingham)
	Prof. Dr. Leon Terstappen (University of Twente)
	Prof. Dr. Sabeth Verpoorte (University of Groningen)

Colophon

Title: The New Gradient Wave
Author: Björn Harink
Cover and layout design: Björn Harink
Publication date: 1st of November, 2014
ISBN: 978-90-365-3756-8
DOI: 10.3990/1.9789036537568
Website: www.bjornharink.info/the-new-gradient-wave
E-mail: bjorn@harink.info
Publisher: Gildeprint, Enschede, The Netherlands

Publication of this thesis was financially supported by the faculty of Science & Technology of the University of Twente and the Netherlands Society for Biomaterials & Tissue Engineering.

The New Gradient Wave

soluble compound screening using microfluidic gradients for regenerative medicine research

DISSERTATION

to obtain
the degree of doctor at the University of Twente
on the authority of the rector magnificus
Prof. Dr. H. Brinksma,
on account of the decision of the graduation committee,
to be publicly defended
on Thursday the 27th of November, 2014 at 12:45

by

Matthijs Björn Marijn Harink

born on the 8th of March, 1983
in Groningen, The Netherlands

This dissertation has been approved by:

Promoter	Prof. Dr. Clemens van Blitterswijk
Assistant promoter	Dr. Pamela Habibovic

"A ship is always safe at the shore -
but that is NOT what it is built for."

Albert Einstein

to my family and friends

Table of Contents.

1 Introduction.

"Every science begins as philosophy and ends as art."

Will Durant

An introduction into gradients in biology and microfluidics

The aim of RM is to restore or establish normal function of damaged tissues or organs, using cell therapy, tissue engineered constructs and synthetic graft substitutes. Since the population of the western world is ageing, there is an increasing need for RM therapies, which are readily available in large quantities. In general, the search for such strategies is based on the candidate approach, in which a limited number of candidates (e.g. biomaterials, growth factors and cells) are selected, based on a rationale. As a result, a limited number of candidates is investigated, and therefore development and clinical implementation of novel, significantly improved strategies is relatively slow. Microfluidics is a field that offers new tools to accelerate progress in RM research, by enabling higher throughput of screening through parallelisation, miniaturisation, and tailoring of a physical and chemical microenvironment. One such a tool is the use of microfluidic concentration gradients that can be generated using flow- or diffusion-based techniques.

Introduction.

An introduction into gradients in biology and microfluidics

In an emergent aging population, the demand for regenerative strategies is increasing. Although a patient's own tissue (autograft) is still considered the best choice in most regenerative applications, its use is often associated with important drawbacks, such as limited availability and poor suitability, especially in elderly patients. Therefore, the need for regenerative strategies that relieve the use of autograft material is imperative, for example in the form of cell therapy, tissue-engineered constructs and synthetic graft substitutes. Synthetic biomaterials and inorganic soluble molecules are of particular interest as regenerative strategy, owing to their unlimited and off-the-shelf availability and relatively low cost.

Classically, the search for alternatives to natural tissue grafts occurs following the so-called "candidate approach". This approach is a serial process, whereby a limited number of compounds or their combinations are chosen with the rationale to mimic the function of the native tissue, followed by a long and costly path from characterisation to biological assessment *in vivo* and *in vitro*. This rational design is limited by the lack of knowledge of complex signalling networks and can only be applied to compounds that already have a known effect, making this approach conceptually weak. Furthermore, during this process, many decisions are made based on assumptions, which may lead to omission of potentially good candidates or late apprehension of poor candidates. For this reason, the need exists to accelerate and improve the efficacy of this search by better substantiating the choices made and eventually replacing the conventional candidate approach by other approaches that allow for increase of throughput in screening.

Currently many techniques arise that provide possibilities to screen large libraries of compounds and materials, which are either readily available or custom-made using methods like combinatorial chemistry and micro-array technologies.[2–6] In addition to individual compounds, by employing combinatorial chemistry approaches,

"**Regenerative Medicine (RM)** is the interdisciplinary field of research and clinical applications focused on the repair, replacement or regeneration of cells, tissues or organs to restore impaired function resulting from any cause, including congenital defects, disease, trauma and ageing. It uses a combination of several converging technological approaches, both existing and newly emerging, that moves it beyond traditional transplantation and replacement therapies. The approaches often stimulate and support the body's self-healing capacity. These approaches may include, but are not limited to, the use of soluble molecules, gene therapy, stem and progenitor cell therapy, tissue engineering and the reprogramming of cell and tissue types."

Quoted from: Daar and Greenwoord 2007.[1]

> "**Synergy** *is the interaction of discrete agents (as drugs) such that the total effect is greater than the sum of the individual effects."*
>
> *Quoted from: Merriam-Webster (Medical).*

libraries of bulk materials, surface-bound or soluble factors can be completed with mixtures of individual compounds, with possibly a synergistic effect.

The given definition comes from pharmacology, where combinations of drugs are used to achieve an enhanced effect, also known as multicomponent therapeutics.[7] Generally, these therapies use compounds that have already proven their individual therapeutic effect or have a clear rationale behind the chosen combination. An example is the successful identification of drug pairs that show a synergistic effect against resistant melanoma phenotypes by Held and co-workers.[8] After analysing 150 potential drugs as single agents, 40 were chosen for pair-wise combination screening, which resulted in 820 conditions. This combinatorial screen showed that the combination of statin class drugs, clinically used to lower cholesterol, and cyclin-dependent kinases, protein kinases involved in cell cycle regulation, led to a substantial reduction in growth of normally resistant melanoma. Despite general knowledge that combinations exist with synergistic effects, modern drug discovery remains mainly driven by single molecule therapeutics.

Systems biology, however, shows that mammalian cells and tissues are composed of complex biochemical networks, having multiple convergent, divergent and redundant signalling pathways.[9] In embryogenesis of the common fruit fly, combinations of compounds guide tissue formation. For example, the overlapping gradients of the Bicoid and Hunchback morphogens, described in detail in the next section, are both required to generate the specific polarity along the embryonic axis and the subsequent anterior patterning.[10] It is therefore logical to consider screening for combinations of materials and compounds in regenerative strategies as well.

Synergistic screening can be described as the search for combinations of compounds that have a synergistic effect. This is in itself not a complex process, but becomes challenging when it comes to sheer numbers. In general, the number of conditions in such material/compound libraries exponentially increases as compared to conventional, candidate-approach tests, making automation, using robotics, an essential part of the screen. This approach is already widely used, for example in pharmaceutical industry, where large rooms are filled with pipetting robots and support personnel, much like the early computers. As an example, taking 10 different compounds and testing them all will result in 1,023 unique conditions:

$$2^n - 1 \; \forall \; n \in \mathbb{Z}^+ \tag{1.1}$$

For an experiment with these conditions performed for multiple time points, the number of conditions will further increase drastically, requiring analysis approaches different from conventional pipetting or robotics. Where testing of all combinations is not an option, usually a limited number of combinations is chosen based on existing knowledge and assumptions. Two different steps exist in this process, namely methods to substantiate choices and actual screening. Computational modelling or virtual screening (VS)[11,12] can be used to screen for specific protein virtual interactions with simple compounds to substantiate choices. Then screens can be performed by robotic systems using proven 96-, 384- or even 1536-well-plate technology. Although the well-plate technology already significantly reduced reagent use and miniaturisation is ongoing, this method is still very expensive and slow.

A field that offers a multitude of possibilities to increase throughput in screening of regenerative strategies, without the need for classical robotics-based automation, is microfluidics, owing to extensive opportunities for integration, parallelisation and miniaturisation.[13,14] Additionally, an important advantage of microfluidics is that it allows tailoring (biological) microenvironments with high fidelity, closely mimicking the *in vivo* situation. The biological microenvironment is a complex environment, which comprises different cell types surrounded by a milieu of physical and chemical signals. This environment is of great importance for the fate of the individual cell, as well as for communication among individual cells in the 3D environment of a tissue or organ.[15–17] In this thesis, a novel microfluidics-based multi-gradient system is presented to study the effects of different combinations of soluble compounds on mammalian cells. As a background, in this chapter, an introduction into microfluidics and gradients is given before describing aims and objectives of the thesis and introducing its content.

1.1. Microfluidics

Mammalian cells experience the world at the microlevel down to the nanolevel. They have a typical volume ranging from 10^{-13} to 10^{-11} litres, right in the range of microfluidics.[19] This makes microfluidics an ideal candidate for mimicking the biological microenvironment, allowing spatial and temporal control at the micro-level with high fidelity, creating unique physical conditions that are not available in macro-tools. Another advantage that makes it an interesting candidate is the possibility to create integrated fluidic circuits comparable to those in the semiconductor industry, allowing for fast and parallel assays suitable for high-throughput screening strategies.

> "**Microfluidics** is the science and technology of systems that process or manipulate small (10^{-9} to 10^{-18} litres) amounts of fluids, using channels of tens to hundreds of micrometers."
> Quoted from: Whitesides 2006.[18]

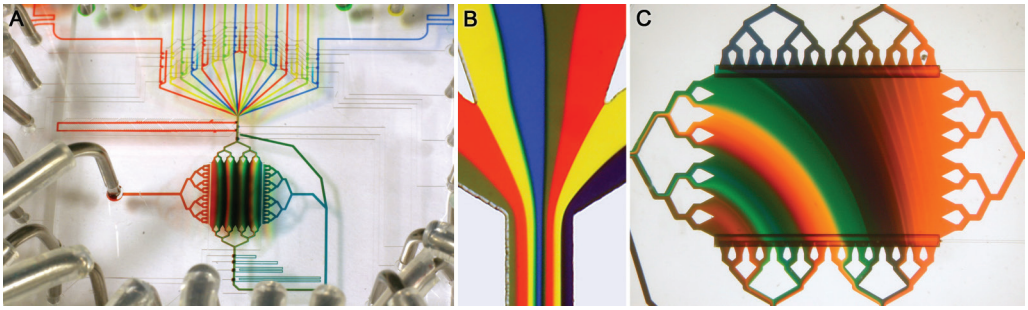

Fig. 1.1 (A) Microfluidic device with different colour dyes. (B) Zoomed-in image of the different colour dyes meeting in a single channel, showing laminar flow behaviour, therefore the colours do not readily mix. (C) Switching different streams and changing pumps speeds can results in complex fluidic flow-patterns. Courtesy of Albert Foclh LAB ART.

Properties

Shrinking the dimensions in fluidics rapidly changes the fundamental physics. To illustrate this, it is important to introduce scaling laws, which express physical quantities in relation to size (l), like volume forces, such as gravity and inertia; and surface forces, such as viscosity and surface tension.[20] When scaling down, surface forces become dominant over volume forces:

$$\frac{surface\ forces}{volume\ forces} \propto \frac{l^2}{l^3} = l^{-1} \underset{l \to 0}{\longrightarrow} \infty \qquad (1.2)$$

Scaling laws that are predominant in the macro-world, such as gravity, become insignificant in the micro-world and forces that are mostly insignificant, such as surface tension, become dominant. For example, the dominant force of mass transport in microfluidics is viscous dissipation (surface), whereas inertial forces (volume) are negligible.[21] This creates unique opportunities, since inertia is responsible for turbulence and therefore absent, making it possible to generate solely laminar flow streams that only mix by diffusion. Although laminar flows are present in the macro-world, they do not exist without turbulent flow and therefore mix quickly. In microfluidics, different streams from different channels brought together do not mix, creating lanes of different liquids in the same channel (Fig. 1.1).

The Reynolds number (Re) is an important number in microfluidics, it is the ratio between laminar and turbulent flow. This is a dimensionless number that indicates inertial forces (f_i) over viscous forces (f_v):

$$\frac{f_i}{f_v} = \frac{\rho U_0 L_0}{\eta} \equiv \mathrm{Re} \qquad (1.3)$$

In regimes operated in microfluidic systems (with typical length L_0 < 1 mm and flow speed U_0 < 10 mm·s^{-1}) the Reynolds number stays well below Re < 10, (using the density ρ 1.0 kg·m^{-3} and viscosity η 1.0 Pa·s of water at 1 atm and 20°C), which is considered well below the transition phase from

laminar to turbulent flow (Re > 2000).[21] The lack of turbulence makes mixing only possible by diffusion. The Péclet number (Pe) expresses the relative importance between advection ($U_0 w$) over diffusion (D):

$$\frac{L}{w} \sim \frac{U_0 w}{D} \equiv \mathrm{Pe} \qquad (1.4)$$

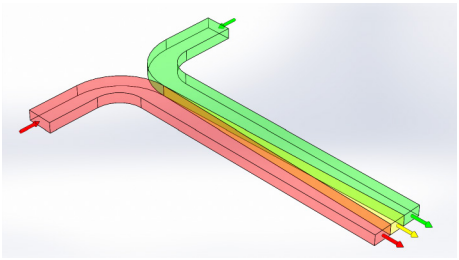

Fig. 1.2 Schematic depiction of a microfluidic T-sensor with two fluidic entrances and one exit. The red and green colours depict different dies entering from either side into a single channel with a laminar flow. The yellow colour is the region where the two dies meet and mix solely due to diffusion. The arrows depict the flow directions.

When bringing two liquid streams together in a single channel, in a so-called T-sensor (Fig. 1.2), the liquids will mix depending on the diffusivity, speed and the typical dimension of the single channel.[22] For instance, an ion (diffusion D = 2 x 10^3 μm^2·s^{-1}) in one of the streams at a speed of 100 μm·s^{-1} (speed U_0) will take approximately 25 mm (length L) in a 100 μm wide (characteristic length w) channel to completely mix.[21]

The fact that flow in microfluidic systems is predominately laminar, and therefore mixing only occurs through diffusion, may be an undesired effect, for example, when fast mixing is required for faster reaction times. However, this behaviour, using multiple laminar flow streams, allows for highly precise local delivery of compounds, without disturbing the surroundings. For example, Van der Meer and co-workers used three laminar streams to remove part of a monolayer of endothelial cells by focused delivery of trypsin, an enzyme used to detach adherent cells (Fig. 1.3A&B).[23] This type of assay, better known as a wound healing assay, is used to follow migration and proliferation of endothelial cells

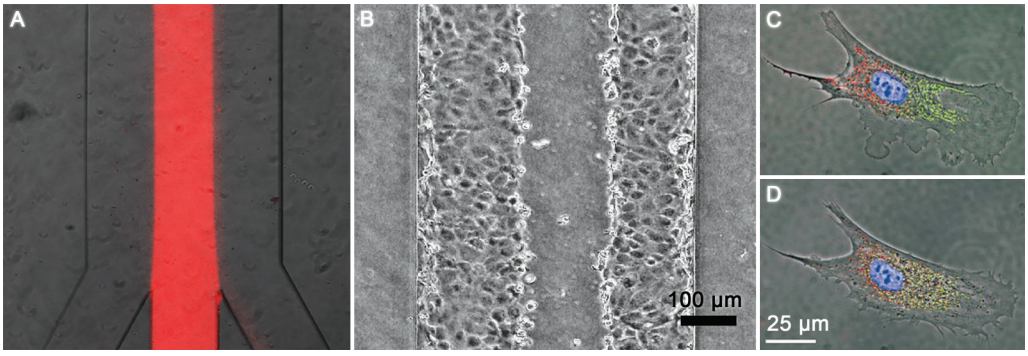

Fig. 1.3 (A) Local delivery of trypsin over a monolayer of endothelial cells, including an added fluorescent dye for visualisation. (B) Effect after local trypsin delivery: removing part of endothelial monolayer. Reproduced with permission, copyright 2010 American Physiological Society.[23] (C) Fluorescence images of a single cell after treatment with Mitotracker Green FM on the left and Mitotracker Red on the right. (D) Image of the same cell 2.5 h after staining, showing intermixing of red and green subpopulations of mitochondria. Reproduced with permission, copyright 2001 Macmillan Publishers Ltd.[24]

into the 'wound', for example upon exposure to compounds that affect cell proliferation or migration. Conventionally, wound healing assays are created by making a scratch in a cell monolayer. The advantage of using microfluidics is that cells are gently detached without damaging the surface, the cells themselves and the surrounding cells.

Application of focused streams also allows single cell experiments in which, for instance, different parts of the cell are exposed to different compounds. Takayama et al. demonstrated this by passing two streams over a single cell, with on one side Mitotracker-Red, a mitochondria stain, and on the other Mitotracker-Green (Fig. 1.3C&D). This experiment allowed them to follow mitochondria migration and distribution within a single cell.

The effects of laminar flow and diffusion-limited mixing make it possible to generate unique microenvironments not possible in macro-tools, making microfluidics an interesting alternative for many applications in biology and regenerative medicine. Therefore, microfluidics allows for tailoring the fluidic and therewith chemical microenvironment at sub-cellular dimensions, generating highly complex fluidic streams and chemical patterns, which might even be considered art (Fig. 1.1).

Materials and manufacturing

Materials and fabrication methods used to develop microfluidic systems for biomedical research originate from the semiconductor industry. Developments from the semiconductor industry delivered mature manufacturing techniques in rigid materials like silicon and glass, which allow high spatial resolution and control, even in the nanometre range, far smaller than any mammalian cell. Examples demonstrating unique possibilities of spatial control are the capture of a single cell in a trapezoid (Fig. 1.4A),[25] to study cell-cell interactions over a distance, or recreating part of the structure of an organ, such as the hepatic cord of the liver (Fig. 1.4B&C), in a so-called organ-on-a-chip.[26,27]

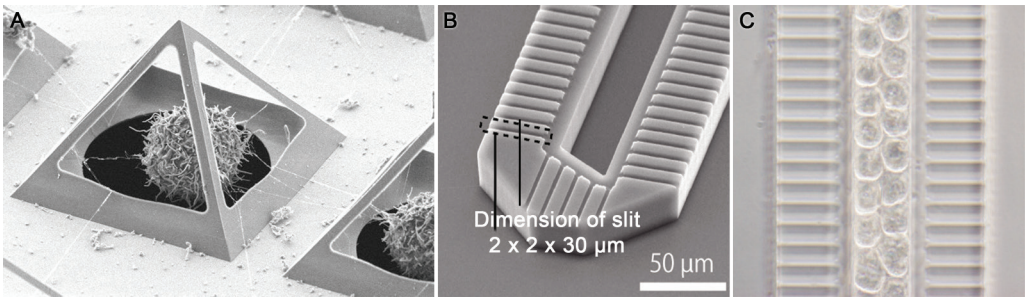

Fig. 1.4 (A) Scanning electron microscope (SEM) image of a captured chondrocyte in complex spatial design, using corner lithography.[25] Courtesy of the University of Twente. (B) SEM image of a spatial design of a liver lobule in a so-called Liver-on-a-Chip. (C) Hepatocytes in the culture area of the artificial liver lobule. Reproduced with permission, copyright 2011 AIP Publishing LLC.[26]

Following rigid silicon and glass materials, polymers were introduced as a material of choice for microfluidic systems, such as SU-8 epoxy, polyimide photoresist and polydimethylsiloxane (PDMS).[28–30] Only with the introduction of PDMS and soft lithography techniques, such as replica moulding, microfluidic devices became more widely available, since advanced cleanroom facilities are not required to make such devices.[31] Replica moulding techniques involve a monomer solution mixed with a cross-linker that is poured over a master-mould and allowed to solidify. The master is usually a silicon wafer with SU-8 features, an epoxy resin photoresist. PDMS is an optically transparent elastomeric silicone rubber that is relatively inexpensive. It instantly became a popular material in cell culture systems, because it is inert and inexpensive enough to be used as a disposable. Another important advantage of PDMS is that it is gas-permeable, allowing cell culture in microfluidic devices within conventional incubators providing pH-stability by CO_2 and temperature control. In addition, PDMS can be used for realisation of integrated valves, allowing for fabrication of highly integrated and multiplexed microfluidic systems.[32]

Although PDMS is currently the most frequently used material in microfluidic systems, its application comes with important drawbacks. The elastomeric nature of the material limits design possibilities because of deformation, allowing only low aspect ratios and limited over-span. The gas-permeability of PDMS can also be a downside, since it also causes evaporation of liquid through the material, resulting in osmolality fluctuations and unwanted convection. Furthermore, due to permeability of the material it is not possible to test hydrophobic low molecular weight compounds in the system as they can be absorbed and released by the material.[33–35] This makes the material choice of fundamental importance for the intended application (Fig. 1.5). Therefore, materials traditionally used in biological research are gaining popularity, like polystyrene (PS), glass and even certain biomaterials.

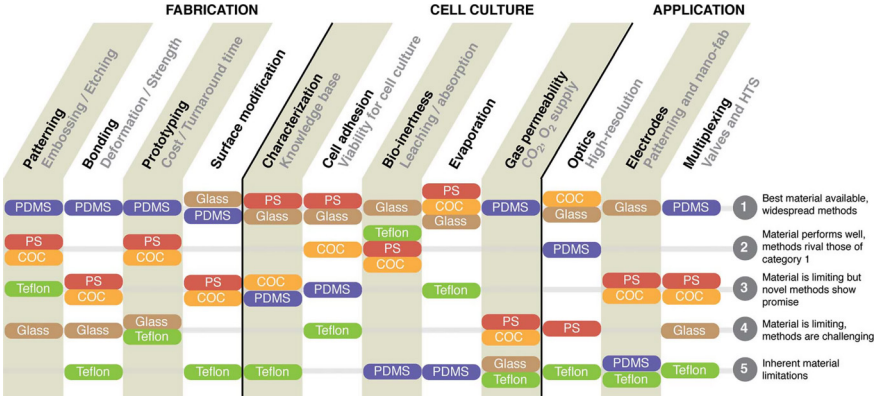

Fig. 1.5 Comparative list of materials used in microfluidics and their apparent advantages or disadvantages in fabrication, cell culture and application. Reproduced with permission, copyright 2012 The Royal Society of Chemistry.[36]

"**A gradient** can be defined as the rate of change of one variable relative to another. For instance a physical quantity, like chemical concentration, increases or decreases relative to a given variable, like distance."

Proposed definition.

Berthier, Young and Beebe,[36] as well as Bettinger and Borenstein[37] have recently elegantly reviewed the advantages and disadvantages of materials used in microfluidics.

Lately, materials used in conventional biological experiments have been investigated as building material for microfluidic devices, such as hydrogels.[38–41] They have gained interest owing to their tunable stiffness, which can be applied to influence stem-cell fate by creating artificial niches, as demonstrated by Lutolf and co-workers.[42]

By combining physics of microfluidics, i.e. features at the micro-level and the right material choice, it is possible to create complex, but controlled microenvironments that mimic certain aspects or functions of the biological microenvironment, as is demonstrated by for instance the organ-on-a-chip concept of the hepatic cord and the ability to create artificial stem-cell niches to maintain stem-cell fate. As suggested by van der Meer and van den Berg certain complexity is necessary to investigate fundamental biological processes or to screen for compounds, but needs to be reduced to still create reproducible results with reliable and relevant assays.[27]

High Throughput Systems

The biggest promise of microfluidics is to bring highly integrated and parallelised systems for high-throughput screening (HTS) strategies. Since the beginning of microfluidics, this has been the ultimate goal, to produce systems that can compete with current room-filling robotics systems in the pharmaceutical industry, with the advantages of reduced reagent use and shorter incubation times.[43]

With the introduction of the microfluidic valves[13,14] a big step forward in multiplexing was made. The pneumatic membrane valve first introduced by the laboratory of Quake, consists of two perpendicular overlaying channels in a flexible material like PDMS, one for fluids and one for pneumatics.[14] By applying pressure in the pneumatic layer, the flexible membrane between the channels collapses into the fluidic channel, closing the circuit. This system allowed for development of integrated circuits using fluidic micro-channels, introducing the promised age of HTS.[44] Fig. 1.6, demonstrates a system with 256 individually addressable chambers, introduced by Thorsen et al.[13]

Using these techniques, systems were developed and commercialised, especially successful in polymerase chain reaction (PCR) analysis and pharmacological screening. For instance, Dalerba and collaborators used

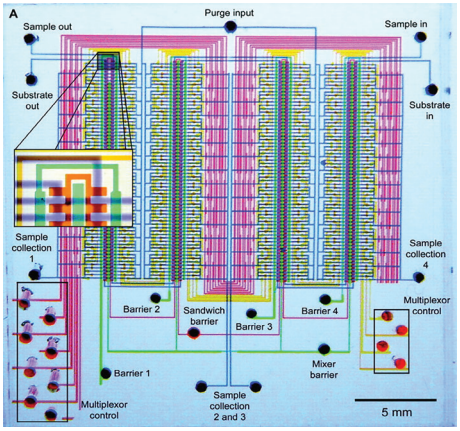

Fig. 1.6 Multiplexed microfluidics system with 256 individually addressable chambers using 2,056 microvalves. Reproduced with permission, copyright 2007 AAAS.[13]

a commercially available single-cell quantitative PCR system to investigate transcriptional heterogeneity in colon cancer tissue. They showed that tumour tissues generated from a single cell show the lineage diversity of parent tumors.[45]

Although microfluidic HTS systems are highly promising when it comes to acceleration of progress in biomedical applications, including RM, they require elaborate manufacturing techniques, equipment and most importantly, a great amount of expertise. Therefore, many have sought for systems that do not rely on valves or even open systems that allow access with a pipette. For example, Folch and co-workers developed systems with open-access or open-air microfluidic devices. Hsu et al. demonstrated micro-canals accessible with a pipette[46] and Cate et al. showed a system that can generate sharp gradients over an open-access microfluidic culture chamber.[47] Even though these systems may not have the automation and throughput as previous described systems, they are more compatible with equipment and protocols already used by biologists.

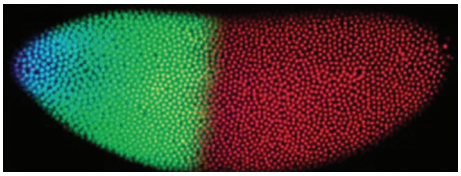

Fig. 1.7 Microscopy image of triple labelled Drosophila embryo, 2 h after fertilisation. The Bicoid protein (blue) gradient, emanating from the left, produces a shallow gradient towards the right, resulting in a sharp difference of expression in Hunchback protein (green), seen by the sharp transition from green to red (DNA). Reproduced with permission, copyright 2007 Elsevier.[53]

1.2. Gradients

To justify the choice for developing a microfluidic system in which gradients of soluble compounds are generated and screened, a short introduction of the importance of chemical gradients in biology and their use and relevance in experiments is given. In addition, a brief overview is provided of conventional systems and microfluidic alternatives to generate molecular gradients and investigate their effect on cells.

Gradients in biology

The cellular microenvironment consists of different cell types in a complex milieu of physical and chemical signals. These signals frequently exist in the form of gradients, like molecular concentration gradients, leading to chemotaxis, guidance and morphogenesis. Such mechanisms play an important role in immune response, axon guidance, and development and regeneration of organs and tissues.

In immune response, leukocytes (white blood cells) are dependent on directed migration, by the release of chemokines, cytokines released by cells around the inflammation site. Since these chemokines propagate from a localised source, they exist in gradients and leukocytes will move in the direction of increasing concentration, in a process called chemotaxis. Cell migration and guidance by surface (or matrix) bound gradients of compounds (ligands) is referred to as haptotaxis.

Gradients of chemo-attractants are also important in guidance of axons from neuronal cells (neurogenesis) and sprouting of microvessels (angiogenesis). For instance, a gradient of the protein netrin-1 makes a diffusible guidance cue for axon outgrowth,[48] and a gradient of vascular endothelial growth factor (VEGF) guides tip cells, specialised endothelial cells at the tip of the vascular sprout.[49,50]

Besides migration and guidance, the organisation and development of tissues is also governed by locally secreted signalling molecules, named morphogens, in a process called morphogenesis.[51] Through gradient formation from a localised source, morphogens contribute to the arrangement of tissue by determining cell fate as a response to different concentrations in the gradient.[52] The most researched and understood organism in biology, Drosophila melanogaster, the common fruit fly, illustrates this effect very drastically, as can be seen in Fig. 1.7 that shows a fluorescently stained microscopy image of a Drosophila embryo, two hours after fertilisation. Cells on the left side release a morphogen protein, called Bicoid (stained blue), generating a shallow gradient towards the right. This protein regulates the expression of another protein, Hunchback (stained red). In this case, the Hunchback regulation is not a linear response, but generates a discrete response, visible in the sharp cut-off from red to green, in which green represents the stained nuclei of the individual cells.[53] This generates discrete phenotypes of cells on the anterior (Left side in Fig. 1.7) and posterior (Right side in Fig. 1.7), resulting in early stage organisation of the developing organism.

Examples given above demonstrate that many soluble factors in the biological environment exist in gradients rather than in the bulk and create different effects from those seen by bulk addition of factors. To investigate the response of cells upon exposure to a concentration gradient of different compounds, a variety of tools has been developed.

Conventional Gradient Generators

A number of different conventional, macro-scale chemotaxis assays have been developed in the past, the majority of which is based on delivery by diffusion. One simple method involves use of a gel substrate, like an agar

plate, in which two holes are punched and cells are added on one side and the compound of interest on the other side, followed by the study of cell migration towards or away from the compound source.[54] The gel limits the speed of diffusion, but is open enough for cells to migrate through, creating gradients that remain there for minutes to hours, depending on the density of the gel. Another way is to cut paths in the gel, guiding gradient and cell-migration, called the double P technique, using a P-shaped cutter to increase reproducibility.[55] Methods like these are inexpensive and easy to make and can give a first insight into effects of the chosen compound. The major disadvantage of such models, however, is the unpredictability and irreproducibility of the formed gradient. The gradients are transient, constantly changing, and eventually reach equilibrium after minutes to hours.

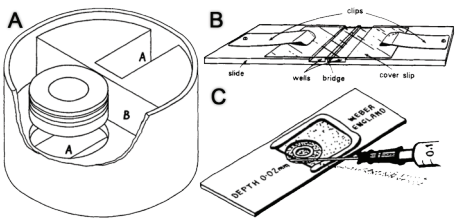

Fig. 1.8 (A) Original schematic drawing of the Boyden chamber. Compartment B holds a membrane with the test solution on top. Compartment A holds the cells, migrating towards or away from B.[56] (B) Zigmond chamber, which uses lanes divided by shallow bridges, to limit mass transport.57 (C) Dunn chamber, similar to the previous chamber, but in the form of concentric rings.[58]

Chamber-based methods offer better control of directionality of the gradient and are more predictable. One such system, proposed by Boyden (Fig. 1.8A),[56] uses a membrane between two chambers, similar to a trans-well system, with the compound of interest on one side and cells on the other. Boyden used this system to investigate chemotaxis of granulocytes in the presence of antibody and antigen gradients and this system is considered one of the standard methods for comparable studies. Zigmond later suggested a device in which chambers, or lanes, were separated by shallow bridges in a poly-methylmethacrylate (PMMA) slide, limiting mass transport by high relative size difference between chamber and bridge (Fig. 1.8B).[57] This device was also used for chemotactic research on granulocytes and became another standardised method for performing chemotaxis assays, especially because it is easier to image and compatible with microscopy systems in comparison with gel methods and the Boyden chamber. A similar method was introduced by Dunn and co-workers (Fig. 1.8C),[58] in which the chambers were circular concentric rings, instead of lanes, connected by shallow circular bridges. Next to a proof of concept experiment, using a gradient of the positively chemotactic compound N-formylmethionylleucylphenylalanine (FMLP) on neutrophils, the authors showed extensive modelling data of the formation and decay of the formed gradients, with the aim to improve predictability and reliability of the system.

Although chamber-based systems offer better spatial control and predictability than classical gel-based systems, gradients in chambers are still transient and will reach equilibrium after minutes to hours, depending on the membrane characteristics and size of the shallow bridges.

Microfluidic Gradient Generators

To overcome the limitations of conventional gradient systems, microfluidics can be employed to create stable gradient systems with high spatial control and reproducibility, making them predictable and quantifiable. In microfluidics, gradients of molecules can enter a cell culture area in two ways, namely: advection, i.e. mass transport by fluid bulk motion; or solely by diffusion, i.e. spreading of unequally distributed molecules by biased random walk induced by Brownian motion. Microfluidic gradient devices can therefore be generally divided into flow-based and diffusion-based platforms.[59]

Flow-Based Systems

In flow-based systems, streams of different chemical concentrations are combined and introduced in a single channel, by advection, where cells can be cultured, for instance. In this way different concentrations are flown over the cells, whereby cells experience shear stress. The simplest system is the T-sensor, as previously described (Fig. 1.2). In such a system two different concentrations of the same or different compounds can flow next to each other in a laminar-flow regime, therefore two streams do not mix and compounds in the streams are only exchanged by diffusion. This generates a gradient inside the main channel in the shape of a sigmoid function, starting with a sharp vertical divide that flattens as a function of distance in the channel. Even though these systems are used to investigate gradient effects on cells, they are limited to sigmoid shaped gradients and change while progressing through the channel; thereby each cell further down the channel experiences another concentration. In this way only individual cells can be tested, not cell populations.

For that reason other flow-based gradient generators were developed, as demonstrated by Dertinger et al.[60] By using a microfluidic mixer-network, different concentrations of two (or more) compounds can be generated (Fig. 1.1). Combining the streams of different compound concentrations into one channel can generate complex shaped gradients in a laminar flow.

These types of gradients have been used to investigate the response of cells to complex gradient shapes, for example in the field of neurogenesis. Chung and co-workers demonstrated guidance of proliferation and differentiation of human neuronal stem cells by gradients of growth factors.[61] Alternatively, a more complex gradient, shown by Wang and co-workers, demonstrated

the effect of an N-shaped deposited gradient of laminin, an adhesion promoter, inside a linear soluble gradient of brain-derived neurotrophic factors (BDNF), a known axon attractant, on directional outgrowth of axons from neuronal cells.[62]

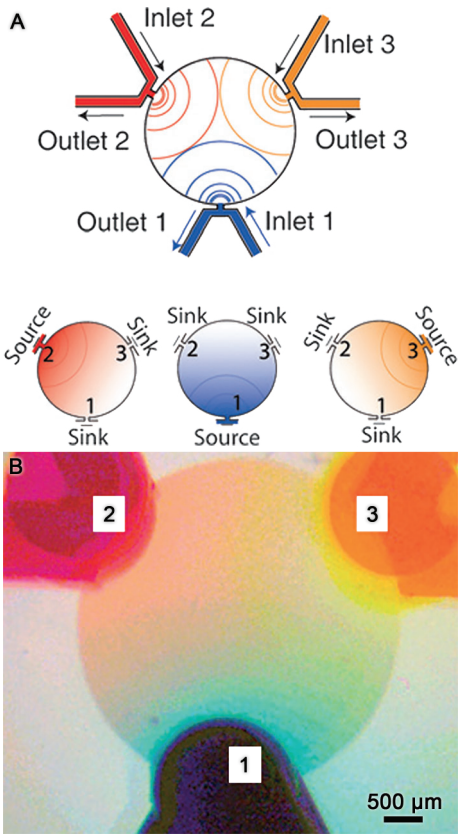

Fig. 1.9 (A) Schematic representation of a diffusion-based multi-gradient microfluidic device, depicting sources and sinks from different entry-points, and the positions of inlets and outlets. (B) Microscope image of the device with three different colour dyes, creating three overlapping gradients solely by diffusion. Reproduced with permission, copyright 2009 Royal Society of Chemistry.

Diffusion-Based Systems

Since some cell types are highly sensitive to shear stress, flow-based systems are not suitable for culture of such cells. Furthermore, the flow direction in flow-based gradient generators may bias the direction of cell migration. In these cases, diffusion-based gradient generation is a better option, in which compounds only enter the culture area by diffusion. Diffusion-based gradient generators rely on a source-to-sink system. At the source a higher concentration of soluble factors is introduced into the central channel or chamber, while on the sink side, the compound at the decreased concentration is removed (Fig. 1.9A).

Samloo and co-workers demonstrated a system in which small channels or bridges connecting the source and sink channels to the central chamber were used.[63] Since the fluid is flowing in a laminar fashion through the channel, and the relative resistance between the channel and the chamber is high, due to large difference in channel diameter, delivering compounds solely by diffusion. Using this device, chemotaxis and filopodia outgrowth of endothelial cells in vascular endothelial growth factor (VEGF) gradients was studied.

This source-to-sink system can also be utilised to generate multiple gradients in a single chamber, as proposed by Atencia et al.[64] In this case, a circular chamber was surrounded by three gradient generators (Fig. 1.9). The gradient generators exist of a channel connected to the chamber by a small orifice, having relative high resistance compared to the channel. By applying the same pressure to all three generators, no net advective

flow exists over the circular chamber. Together with the ability of rapidly changing the compounds in the gradient generators, the rapid chemotaxis of bacteria could be followed, using glucose gradients.

Another method to introduce compounds by using only diffusion is the use of a gel barrier, as for instance a hydrogel. Cheng and co-workers produced a relatively simple three-channel microfluidic device made of agarose gel by using soft lithography from photoresist features on a silicon substrate as a mould, similar to PDMS molding.[65] By using one side-channel as the source, with a high concentration of the compound, and the other as a sink, with low concentration, the compound diffuses through the gel, separating the three channels, and generating a gradient in the middle channel. The authors used this device to study neutrophil behaviour in a gradient of formyl-Met-Leu-Phe (fMLP), a chemo-attractant.

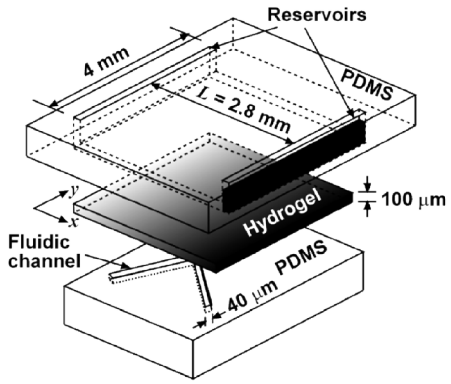

Fig. 1.10 Schematic representation of a microfluidic device with a hydrogel membrane sandwiched between two different fluidic layers, which enables the creation of complex shaped chemical gradients by diffusion. Reproduced with permission, copyright 2006 American Society of Chemistry.[66]

Another way to utilise an agarose-gel barrier is to use it as a membrane sandwiched between two fluidic layers. Such a system allows generation of various shapes of diffusive-gradients inside flow-free microfluidic channels, in which the underlying channel determines the shape of the gradient, as demonstrated by Wu et al (Fig. 1.10).[66]

Depending on the requirements of the experiment either a flow-based or a diffusion-based system can be chosen for generating gradients. Advantages of the flow-based systems are: the possibility to create complex shaped gradients or chemical environments; fast, within seconds, switching of gradient shape and direction; and no diffusion limitation of nutrients. As compared to diffusion-based systems, which are: only able to generate a limited amount of shapes; establishing of the gradient is dependent on 'slow' diffusion, which can take minutes to hours; and nutrients are diffusion limited. On the other hand, diffusion-based systems: do not create shear stress, which is especially important when dealing with delicate cells and can create undesired effects; can be used on part of a cell population, testing more cells with the same condition; and can generate multiple overlapping gradients, allowing combinations of compounds.

1.3. Aim and objectives

The aim of the work described in this thesis was to develop a novel strategy to screen the effects of soluble factors on the behaviour of mammalian cells, for use in regenerative medicine research. The following objectives were defined with regard to the properties of the system:

i. **Temporal screening:** The system should provide temporal information about the effect of compounds on mammalian cells;

ii. **Combination and concentrations screening:** the system should allow testing different concentrations of a compound and/or combinations of different compounds at varying concentrations in a single assay;

iii. **In situ assay and analysis:** The system should be adaptable to different assays, allowing study of various cell functions (e.g. proliferation, differentiation, extracellular matrix production);

iv. **Mimicking biological microenvironment:** The system should mimic the biological microenvironment of the mammalian cells to enable better translation of *in vitro* results to *in vivo* situation.

To realise these objectives, a microfluidic platform was designed that provides nutrients and compounds of interest by diffusive delivery from four sides surrounding cell culture chamber whereby overlapping and orthogonal gradients of four compounds are created, allowing study of combinations of compounds at different concentrations (Fig. 1.11). Furthermore, the platform is suitable for live-imaging to assess the effect on cells in time.

Various aspects of the platform are described in detail in the thesis. Chapter 2 is a review on the use of microfluidics in RM, including possibilities and limitations, and future perspectives. Chapter 3 covers the development of a standalone chip holder, which also functions as an incubator, that allows temperature and gas control in the closed gas-impermeable microfluidic system. In Chapter 4, the design and fabrication steps of the microfluidic gradient chip are described, together with the analysis and verification of the generated gradients. In Chapter 5, an example of a screening assay development applicable to the platform is described. Finally, Chapter 6 presents the conclusions from the research performed here and an outlook towards future research.

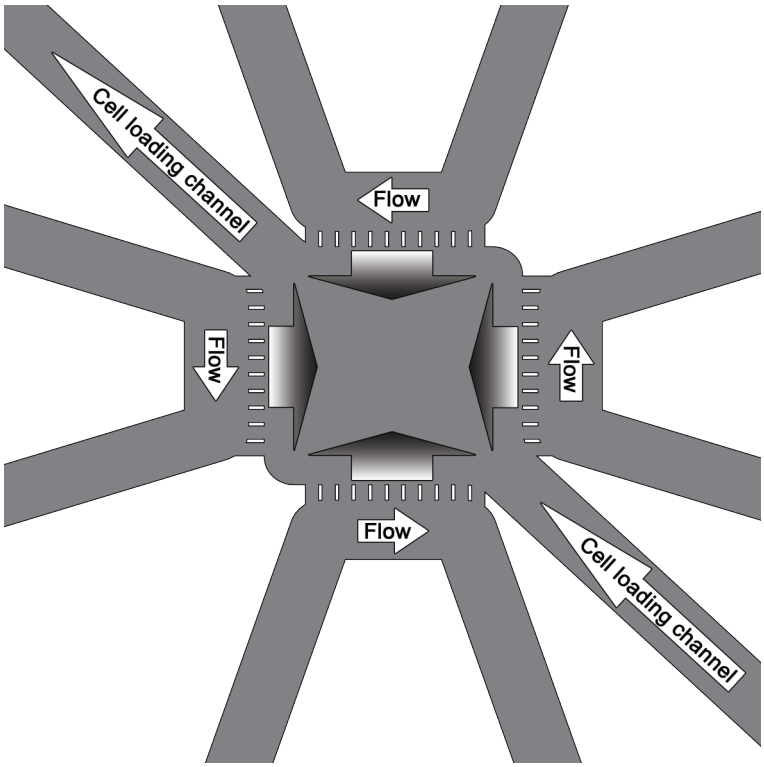

Fig. 1.11 Schematic representation of microfluidic diffusion-based multi-gradient device. White arrows depict the flow directions and gradient-filled arrows the direction of the overlapping gradients.

2 Regeneration-on-a-Chip?

"Eine neue wissenschaftliche Wahrheit pflegt sich nicht in der Weise durchzusetzen, daß ihre Gegner überzeugt werden und sich als belehrt erklären, sondern vielmehr dadurch, daß ihre Gegner allmählich aussterben und daß die heranwachsende Generation von vornherein mit der Wahrheit vertraut gemacht ist."

Max Planck

The perspectives on use of microfluidics in regenerative medicine

Currently, tremendous efforts are made in development of novel regenerative strategies, which are becoming increasingly important as a consequence of ageing. To facilitate accelerated development of new strategies, fast and reliable assessment of (biological) performance is sought for, not only to select the potentially promising candidates, but also to rule out poor ones at an early stage of development. Microfluidics can provide the tools to accelerate RM research, as proven in its maturity for the realisation of high-throughput screening platforms. In addition, microfluidic systems are suitable for recreating in vivo-like microenvironments. Application of microfluidics to RM research is, however, a challenging process. One needs to take into account the complexity of organs or tissues that need to be regenerated, but also the complexity of regenerative strategies themselves. The question therefore arises whether so much complexity can be integrated into microfluidic systems without compromising reliability and throughput of assays.

This chapter is based on the publication: "Regeneration-on-a-Chip? The perspectives on use of microfluidics in regenerative medicine", Lab Chip 2013

Regeneration-on-a-Chip?

The perspectives on use of microfluidics in regenerative medicine

While the world population is continuously ageing, demand for novel strategies to repair and regenerate damaged and diseased tissues and organs has tremendously grown. Transplantation of a patient's own tissue is still considered the best option in most cases; however, limited availability becomes an increasingly problematic issue, especially for elderly patients. As a consequence, the field of regenerative medicine (RM) has emerged to address these currently growing demands.

RM is a highly multidisciplinary field, with a number of aims and distinguishing features. This is obvious from the definition proposed by Daar and Greenwood, in an attempt to facilitate understanding among various stakeholders. The authors defined RM as "an interdisciplinary field of research and clinical applications focused on the repair, replacement or regeneration of cells, tissues or organs to restore impaired function resulting from any cause, including congenital defects, disease, trauma and ageing. It uses a combination of several converging technological approaches, both existing and newly emerging, that moves it beyond traditional transplantation and replacement therapies. The approaches often stimulate and support the body's self-healing capacity. These approaches may include, but are not limited to, the use of soluble molecules, gene therapy, stem and progenitor cell therapy, tissue engineering and the reprogramming of cell and tissue types".[1]

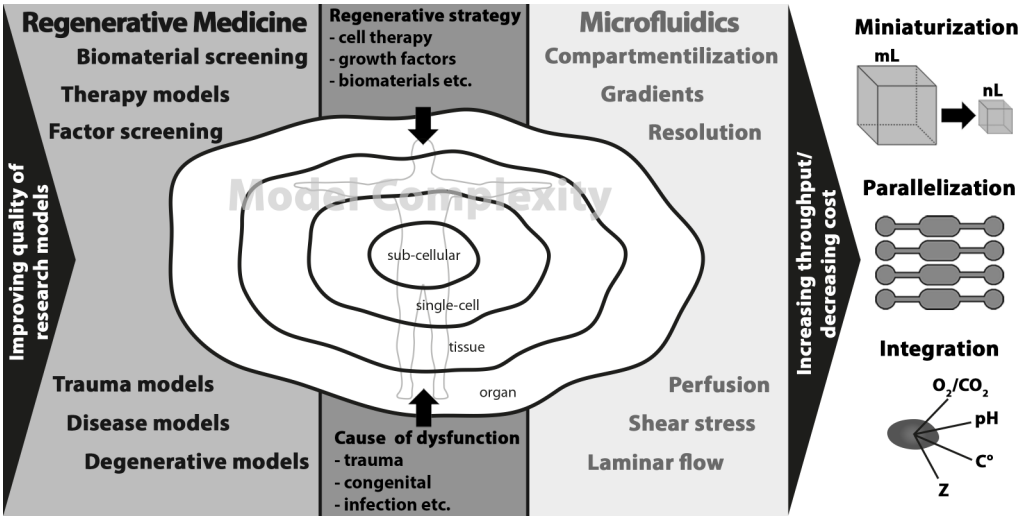

Fig. 2.1 The needs of regenerative medicine research and the tools microfluidics offers to meet them.

This definition clearly demonstrates different facets researchers working in the RM field need to deal with. While the final aim of RM research is improvement of the existing strategies and clinical applications, understanding of fundamental mechanisms of developmental, (stem) cell and molecular biology is imperative to reach this goal. A variety of research models is required in the field, differing not only in the type of tissue or organ to be regenerated, but also in the cause of dysfunction or damage. Finally, strategies toward regeneration are multiple, including cells, soluble factors, natural and synthetic biomaterials, and combinations thereof. For all these different aspects in RM research: (i) cell/tissue/organ type, (ii) cause of damage and (iii) regenerative strategy, reliable models are needed that resemble the *in vivo* situation as closely as possible, which comes with a high level of complexity.

Next to this quest for improving the quality of the existing research models, a recurring issue encountered in the field of RM is a need to considerably increase the rate at which new approaches are developed and implemented, while decreasing the cost thereof. This implies notably fast and reliable assessment of (biological) performance to select potentially interesting candidates, but also to rule out poor ones at an early stage of development, something that is not possible when using classical research approaches.

Microfluidics, defined by Whitesides as "the science and technology of systems that process or manipulate small (10^{-9} to 10^{-18} litres) amounts of fluids, using channels with dimensions of tens to hundreds of micrometers",[67] offers an extensive toolbox that may be useful for developing novel, more representative *in vitro* models for RM research. Microfluidic devices have already been used as platforms for cell-based screens, in particular for studying fundamental biological processes and for drug testing owing to advantages they offer over classical cell culture systems: temporal and spatial control over fluids and physical parameters, and integration of sensors to obtain direct and *in situ* readout. Moreover, microfluidics may provide a new avenue to accelerate research in the field of RM, as it has proven its maturity for the realisation of high-throughput screening (HTS) platforms,[68] through development of multiplexed platforms, parallelisation of the assays as well as automation.

While microfluidics as technology is obviously attractive for many reasons, it is important to investigate whether, and if so, how it can be routinely utilised in RM research. One of the questions that needs to be answered is whether the biological complexity of real tissues, including heterogeneous cell population, extracellular matrix (ECM), chemical and physical cues in 3D, and systemic effects can be implemented in microfluidic devices. Recent work on engineered cellular microenvironments and in particular organs-

on-chips suggest that this certainly is possible.[69,70] Equally important is the question whether the cause and the nature of the injury can be mimicked in a reliable way. Timing is also important: can such culture systems run long enough to study clinically relevant regeneration? Lastly, is it possible to investigate different regenerative strategies in microfluidic devices? While these systems are probably suitable for drug-based therapies and, to a certain extent, cell therapies, introduction of bioactive, natural or synthetic 3D biomaterials into the system may cause issues such as the loss of transparency of the device, flow regime retention, and if applicable, control over gradients and their stability. The aspect of biomaterials should not be ignored in this context, as the need for synthetic alternatives to natural tissue and biological approaches, which suffer from issues of immunogenicity, lot-to-lot variability, high cost and most importantly, limited availability, is growing rapidly. Fig. 2.1 illustrates why novel research tools are needed in RM and where microfluidic tools can make a valuable contribution to the field.

This review is aimed at providing the state-of-the-art of the application of microfluidics in RM research. Presented here is an overview on the potential of microfabricated and microfluidic tools to advance research in RM, followed by examples of established microfluidic models for neuronal, vascular, musculoskeletal and hepatic regeneration. Possibilities and limitations of these techniques will be discussed in view of requirements from the RM field. Finally, a view on the future perspectives of microfluidics for RM will be presented, and the remaining challenges that have to be overcome before microfluidics can become a commonly applied tool for RM research highlighted.

2.1. Properties of microfluidic systems and their applicability

Lab-on-a-chip technology and microengineering approaches, both derived from the microelectronics field, provide a unique and unprecedented toolbox to be used in cell biology and related fields, including RM. As mentioned before, in order to improve quality of the RM research models, it is important to both mimic the cell biological microenvironment, which presents a high level of confinement, and to incorporate soluble or surface-bound gradients and natural or synthetic materials to reach a high level of tissue/organ complexity. To increase the rate at which research is performed, the development of HTS systems is of great value, and the integration of read-out sensors into such systems enables to have direct feedback on the cell state and microenvironment. In the following paragraphs, these different features offered by microfluidic systems are presented.

Physical cell microenvironment

Microfluidic devices present a high level of confinement, which resembles the environment cells experience *in vivo*. Compared to classical open microwells, these confined, closed and convection-free vessels enable local accumulation of substances secreted by cells, and have proven consequently to be more efficient to study autocrine-paracrine signaling.[71] Furthermore, the micrometre-sized structures are characterised by a larger surface-to-volume ratio, which offers a higher level of control over various physical parameters, such as temperature or gas concentrations in solution (e.g., oxygen tension).[72] This capability has notably been exploited to create hypoxic conditions,[73] which are particularly important to recapitulate ischemia as found in injured tissues. A simple approach to deliver well-defined oxygen amounts in the cell culture medium has been reported, which relies on the use of a membrane-based oxygenator:[74] this device consists of a three-layer structure with a thin gas-permeable PDMS membrane placed between a fluidic channel and a gas channel. The oxygen tension is precisely controlled in the gas channel, and thanks to the gas-permeability of PDMS, the same oxygen conditions are found in the fluidic channel.

Similarly, the predictability and control of flows, due to their laminar character, offer new experimentation schemes. First, cells can be cultured under dynamic conditions with continuous perfusion of fresh medium, and they can be subjected to biologically relevant shear stresses.[75] This experimentation scheme is not conceivable in classical culture platforms, where cells are grown in a static environment, without any active super- or perfusion. At the same time, microfluidic platforms can be designed so that nutrient-delivery and gas-exchange are solely governed by diffusion,[76] circumventing thereby shear stress and associated issues[75] and reproducing conditions found *in vivo*. Next, cells and microtissues can be exposed simultaneously to different flow compositions in a microfluidic platform, by exploiting the laminar character of the flow.[24] This approach has been applied to create a temperature step in a microchannel, which has provided new understanding on the development of *Drosophila Melanogaster* embryos and on the importance of the temperature on the process of embryogenesis.[77,78] More recently, an embryonic body has been cultured at the interface between a differentiating solution and standard culture medium to induce neural cellular differentiation in half of the tissue while leaving the other half undifferentiated.[79] Finally, the utilisation of microfluidic culture conditions is highly attractive to rapidly exchange the fluid in the cell surrounding, which is precluded in standard microwells, and to control the cell microenvironment in a temporal manner.[80]

Soluble gradients

In vivo, chemical signals are mainly found in the form of gradients, which elicit highly different cell responses than simple bulk addition. For instance, during embryogenesis, organ and tissue development and, similarly, during regeneration and wound healing, gradients of morphogens or their repetitive periodic patterns are responsible for cell recruitment and ECM production and organisation.[81,82] Conventional gradient generators, such as Zigmond[83] and Dunn[84] systems consisting of side-by-side or concentric chambers connected by a narrow bridge are poorly controlled, irreproducible, and unquantifiable. In contrast, the laminar character of the flows at the microscale facilitates the generation of continuous, stable and precise gradients. Two approaches are mostly used to generate gradients of soluble compounds in microfluidic systems:[85] (i) serial dilutions[61] between a solution containing a soluble factor of interest and a "buffer" or (ii) via diffusion from a source structure, e.g., a chamber or a channel to a sink,[86] this often occurring through a barrier with a high fluidic resistance such as an array of channels with a low square-micron cross-section[87] or a hydrogel material.[41] As is illustrated by examples in the section on various tissues, this capability to generate gradients has enabled so far the study of chemotaxis,[88] outgrowth of axons in neuronal cells[61] or filopodia in endothelial cells,[89] as well as the determination of optimal culture conditions by varying the concentration of specific factors in growth medium.[90]

Material-related considerations

In a similar way as they respond to (bio)chemical factors and gradients thereof, cells are highly sensitive to the mechanical properties of the substrate they are grown on, and possible variations in its stiffness/softness. Initially, microfluidic systems have been fabricated from rigid materials such as silicon and glass, for which mature microfabrication processes derived from the microelectronic field were available, for both the realisation of structures and substrate assembly. Slightly later, polymer materials entered the field, those being photo- or heat-curable such as SU-8 epoxy, polyimide photoresist and the polydimethylsiloxane (PDMS) elastomer,[28–30] respectively, and thermoplastics such as polymethylmethacrylate (PMMA), polycarbonate, polystyrene (PS),[91] cyclic-olefin-copolymers, or Teflon®.[92] Interestingly, PDMS has rapidly become the most popular substrate to realise cell culture platforms since it is biocompatible, gas-permeable, transparent, cheap, its processing does not require any dedicated cleanroom environment, and it lends itself well to the realisation of integrated valves.[32] However, PDMS suffers from a number of limitations, as recently acknowledged: it is highly hydrophobic; its porous structure works as a "sponge" for small and hydrophobic compounds, resulting in osmolality and concentration shifts in the cell environment; small oligomers can be

released from the bulk PDMS into the solution in the devices; it is highly gas-permeable, which impedes the creation of hypoxic conditions;[91] and its deformability makes it challenging to reliably realise either low micrometre-sized structures or shallow and wide channels or chambers, or even to align and bond a PDMS layer with another structured substrate.[33–35] In that context, PS, of which commercially available culture dishes are made and which is fully characterised for cell culture experiments, is gaining interest even though it is gas-impermeable.[33] Alternatively, biopolymers such as silk fibroin have been utilised to build microfluidic devices intended for biological experiments.[93] More details on these material-related aspects of microfluidic systems can be found in elegant reviews by Berthier et al.[33] and Bettinger and Borenstein.[37]

In addition to these materials, soft polymer substrates which are frequently encountered in classical biological experiments, such as gelatin,[38] hydrogels,[39,41] and silk fibroin[94,95] have also been employed to fabricate relatively simple microfluidic structures, as discussed in the next sections. The main interest in these materials lies in their tunable mechanical properties which are obtained by tailoring their composition and polymerisation conditions. This capability is notably exploited to introduce mechanical gradients into microfluidic systems and to study influence of stiffness on cell fate, as demonstrated by Lutolf and co-workers.[42] Furthermore, soluble active factors can be encapsulated in the polymer matrix, and progressively releases in a controlled manner during experiments.[96] Alternatively, the material can be pre-loaded with cells. Finally, biological response to these polymers can be tuned through embedding of functional groups into the backbone of the material.[97] Such soft materials are usually processed either by using a combination of moulding and polymerisation techniques comparable to soft-lithography[98] with the polymerisation being initiated using, e.g., light, heat, pH or salt concentrations, or by soft embossing.[99]

Surface-bound chemical signals

The chemical nature of the substrate plays an important role, and interactions with the ECM environment are essential for the proper functioning of the cells. Surface coating is routinely applied in standard culture dishes as a uniform layer covering the whole dish. While this approach enables control of cell adhesion, it is not suitable to screen various ECM components, especially in a combinatorial manner, to understand the influence of the cell-ECM interaction on cell fate and to find optimal ECM conditions due to the number of independent dishes required and the price of ECM proteins. Using microfabrication and microprinting techniques, any kind of molecule can be patterned on a substrate along well-defined geometries. As a result, in a single culture dish, a large amount of ECM conditions can be

tested, and their influence on the cell fate assessed. This micropatterning approach has brought valuable knowledge on the influence of the shape, surface area and chemical nature of the patterns on the cell behaviour. It has for example been shown that surface area directly correlates with cell viability and growth rate,[100] as well as with cell differentiation into various tissue lineages.[101] Furthermore, Bhatia and co-workers have systematically screened mixtures of various ECM components, such as laminin and collagen, for their ability to promote human mesenchymal stromal cells (hMSC) to differentiate into hepatic lineages.[102]

From single cell to sophisticated organ models

Microfluidic devices have already been applied to a variety of cell-based *in vitro* systems including individual cells,[103] cell monolayers, complex and sophisticated multicellular tissues[104] or even organ-like models.[69,70]

Single cell level experiments are of particular interest in the field of RM to extend our knowledge on stem cells, in the quest to create artificial niches to preserve cell stemness,[105–107] and to ultimately be able to control cell-fate. Microengineering approaches and lab-on-a-chip technology have enabled generation of single cell platforms, as discussed in several reviews,[103,108–110] in opposition to standard laboratory approaches which typically deal with large cell populations. In a microfluidic format, individual cells can be isolated from a large population, trapped in dedicated structures, which make it possible to both follow their fate[111,112] and to analyse their content, possibly in a parallel manner.[111,113,114] Lutolf and co-workers, for example, systematically studied the influence of various parameters such as substrate stiffness,[16,108,115] cell-cell interactions and ECM proteins on hMSC differentiation and mouse neural stem cell self-renewal.[42] Similarly, Chen. et al. have recently trapped a MCF-7 cancer cell in a microfluidic chamber and allowed it to expand *in situ* into a tissue/spheroid filling the microchamber.[116] While developed as a cancer model, this approach could also be used to grow microtissues starting from a handful of primary cells isolated from a patient, to study the process of injury and the effect of regenerative strategies.

At the opposite side of the spectrum, studies on 3D cellular aggregates or microtissues,[117] which are currently gaining significant interest also greatly benefit from the utilisation of microfabrication and lab-on-a-chip technology. Where standard hanging-drop[118] and rotary bioreactor-based[119,120] microtissue formation techniques fail for the large scale preparation of microtissues with homogeneous size and shape, microfabricated well arrays,[121] microfluidic channels[122,123] or droplet platforms[124] have proven their suitability for the spontaneous, rapid and massive generation of microspheroids with a highly controlled size and

shape.[117] These microengineering approaches have notably been applied to the field of cancer research for drug screening assays,[125] as well as for creating elementary building blocks which upon successive self-assembly can give rise to more complex tissues with a clinically relevant size,[121] or even to get new insights into biological processes such as angiogenesis. When generated in a microfluidic format, such microtissues have been successfully employed to study cell-cell interactions and the ability of specific cell lines to form co-culture multicellular aggregates.[126] In another approach, microtissues have been prepared by directly including cells into a hydrogel.[127] A main advantage of this hydrogel-based strategy is its suitability to generate tissue structures with a great variety of shapes[128] when using photolithography-like polymerisation, including high-aspect ratio structures like long fibres,[129] which are not possible to create using conventional microfabrication techniques. Furthermore, such hydrogel microtissues also lend themselves well to self-assembly processes to generate larger pieces of tissue.[130] Finally, by combining cellular systems with microfabricated structures, different groups have been able to create sophisticated models that emulate the organ-physiological architecture.[131–134] Owing to their complexity, these organs-on-chip models have found applications for drug screening and nanotoxicology assays, as biologically relevant alternatives to animal experimentation, or for understanding of particular diseases, but their use in RM research is still limited.

Large-scale integration platforms for HTS

While the features of microfluidic systems discussed so far are mainly useful to improve quality of the *in vitro* models for RM, the most important advantage of microfluidic devices to accelerate progress of RM research is their high level of integration. This can be seen two-fold: on one hand, for the parallelisation of the assays via the multiplexing of the device, in the same way as 96-well plates include 96 individual vessels for independent assays, and, on the other hand, for the implementation of a series of successive steps on one single platform. For both types of integration, it is essential to compartmentalise the fluids and cells. This is realised by either adding valves[32,135] or using droplet-based microfluidics.[136,137] Interestingly, this on-chip compartmentalisation strategy is considered as a promising alternative to robotic fluidic handling.

The realisation of robust valves in microfluidic platforms has long been a major challenge from a fabrication point of view. However, nowadays, a few standard strategies are routinely used: (i) the Quake valves made using multilayer soft-lithography,[32] which exist in the push-up and push-down "flavours"; (ii) "normally closed" valves[135] consisting of a thin polymer membrane sandwiched between two substrates; and (iii) the pin-Braille

valves.[138] Interestingly, these valves, originally aimed at isolating small fluidic chambers, can serve a few other purposes such as pumping[139] using a peristaltic approach, mixing[138,140] (while pumping), or fluid metering.[141] Adding valves in a microfluidic platform can enable the drastic reduction of the number of fluidic connections for a given multiplexed device, as well as between devices, while increasing the multiplexing and integration capability. Furthermore, as discussed in recent reviews,[14,142] combining series of valves in a smart way enables to decrease the number of actuation/control lines for microfluidic large scale integration (mLSI).[14] This mLSI strategy has proven to be very promising for a wide spectrum of applications. In the field of RM, it enables screening of a great variety of soluble factors and their concentrations, and assessment of their influence on cell growth and fate.

Concerning HTS in microfluidic systems, it is worth mentioning that, while these systems are highly suitable for parallelisation and assay integration, issues exist with compatibility with classical high-throughput equipment, including robotic fluid handling for 96-, 384-, or 1536-well plates, and with conventional assay and biological readout equipment. Thus, despite the expected decrease in cost due to miniaturisation and reduced reagent and biological material use, to compete with existing industry, screening in microfluidic systems must first be adopted more routinely by different fields to justify the required initial investment in suitable automated systems. Alternatively, microfluidic systems should be designed in such a way that they are compatible with standard laboratory equipment.

Integrated sensors for cell culture monitoring

Integration in microfluidic platforms also includes the implementation of smart capabilities or sensors realised using microelectromechanical system (MEMS) technology to precisely monitor *in situ*, in real-time and in a non-invasive way the cell microenvironment and the cell activity, a feature which is also of great importance when increasing throughput of screening. Of particular interest in this context for the field of RM are[143] (i) oxygen sensors to regulate the oxygen tension in the cell surrounding or to follow the cell respiratory activity;[144] (ii) or, in general sensors to control the physical parameters (e.g., carbon dioxide, temperature, pH) in the cell culture medium; (iii) sensors to measure the cellular stress level and the production of reactive oxygen species (ROS); (iv) sensors to determine the cell metabolism; (v) electrochemical sensors to track the chemical activity of neurons and neural tissues;[145] and (vi) sensors to determine in a non-invasive way the differentiation status of stem cells by detecting specific markers for differentiation such as alkaline phosphatase[146] or to assess proper functioning of the tissues by quantifying proteins secreted by the tissue such as albumin in the case of liver. Sensing generally

Table. 2.1 Important differences between conventional (monolayer) and microfluidic in vitro cell culture.

Conventional	Microfluidics
Cell microenvironment	
No confinement (open wells).	No confinement (open wells).
Limited level of spatial control (e.g. only single well or trans-well systems).	High level of spatial control (e.g. compartmentalisation for co-culture, 3-dimensionality and sub-cellular resolution).
No fluid control (only static or chaotic).	High level of control over fluids (e.g. laminar flow, perfusion, and temporal control over fluid exchange).
Limited possibilities for creating physical stimuli.	Various physical stimuli possible (e.g. stiffness, shear, compression).
Low temporal and spatial control over chemical stimuli (only bulk addition).	Possibility to create highly defined spatial and temporal chemical stimuli (e.g. soluble or surface gradients).
Established and characterised culture substrate materials.	Limited characterisation of applied substrate materials and limited use of biologically characterised materials.
Biological read-out	
Compatible with conventional standardised biological assays.	Compatibility issues with conventional standardised biological assays.
Compatible with established read-out equipment.	Compatibility issues with established read out equipment.
Comparable to large amount of data from historical experiments.	Low number of available historical experiments limits comparison.
Limited possibilities for *in situ* readout of biological processes.	Possibility to integrate sensors and assays for *in situ* readout of biological processes.
High throughput screening (HTS)	
High reagent and biological (cell) material use in HTS setting.	Reduced reagent and biological (cell) material use in HTS setting.
Limited possibilities to parallelise and integrate assays.	Highly applicable to parallelisation and integration of assays.
Compatible to conventional high throughput (robotics) equipment.	Not compatible to conventional high throughput (robotics) equipment.

relies on either electrochemical/electrical principles or on optical readout, and sometimes includes enzymatic degradation processes for metabolic measurements of specific substrates (e.g., glucose, lactate or pyruvate). Jeong and co-workers reported an electrochemical sensor for long-term monitoring of alginate-based 3D lung cellular models for viability assays, which could be applied for the detection of any electro-active species.[147] In another approach, pancreatic islets were encapsulated in an alginate-based shell including oxygen-sensitive fluorescent moieties, using a microfluidic droplet-based platform.[148] This HTS approach, which can bring valuable information on the pancreatic islet activity, can easily be applied for the detection of other analytes than oxygen alone. Finally, Krommenhoek et al. reported an integrated sensor device with a footprint of $< 1\ cm^2$ to monitor in parallel different parameters in a bioreactor such as the temperature, the pH, the oxygen concentration, and the biomass.[149] Although this device has originally been developed for yeast culture, it could easily be employed in an integrated bioreactor for closely monitoring the growth environment of microtissues.

This brief overview of properties of microfluidic devices is an attempt to indicate how they can contribute to advancement of RM research. Table. 2.1 summarises some important differences between microfluidic and classical cell culture models. In the next section some examples of microfluidic systems are discussed which have been developed for RM research, specifically to study neuronal, vascular, musculoskeletal and hepatic regeneration.

2.2. Neuronal regeneration

Microfluidic systems have a long history in the field of neuronal regeneration. Therefore, this application illustrates particularly well advancements in microfluidic technology to better meet biological demands.

When studying neuronal degeneration and regeneration, the geometry of the microenvironment is of utmost importance. Enclosed and separated compartments are usually employed to study axon outgrowth and their response to stimuli. Compartmentalised devices such as Campenot chambers (Fig. 2.2) have for instance been employed for that purpose.[150,151] In these devices, a fluoropolymer divider is attached to a standard culture dish using vacuum grease. Neuronal bodies are plated in the central compartment, while axons can grow out to surrounding compartments, through either the vacuum grease sealing or "rough" scratches in the surface of the culture dish previously generated with a knife. Although these systems have provided new insights into neuronal development and degeneration,[151] they suffer from a number of limitations including limited resolution at the scale of the size of neurons, cumbersome assembly with high risk for leakage,

and easy axon growth disruption upon the slightest mechanical strain.

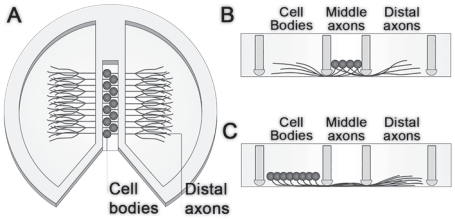

Fig. 2.2 Schematic diagram of a Campenot chamber. (A) Top-view with cell-bodies in the centre and axons spreading to the outer chambers by scratches in the surface or through vacuum grease. (B) Side-view of situation in A. (C) Alternative seeding possibility from the left chamber, so the middle part of the axons can be exposed to treatment, separately. Reproduced with permission, copyright 2005 Macmillan Publishers Ltd.[151]

The emergence of microtechnology has brought up alternative microfluidics-based systems, with dimensions that could be precisely controlled. For instance, compartmentalised systems can easily be realised using soft lithography rapid prototyping in PDMS with micron-sized structures such as grooves through which axon growth is guided, while neuronal bodies are retained.[152–155] Interestingly, the same design has enabled cell co-culture, each compartment being used for a different cell type, as well as cell-cell interaction studies. Such systems have been notably applied to study the creation of synapses between neurons (Fig. 2.3),[156,157] chronic excitotoxin-dependent axon degeneration, excessive stimulation by neurotransmitters,[155] and degeneration induced by paclitaxel, a mitotic inhibitor.[158]

After a third compartment has been added between the two initial chambers, the axonal part of the neurons has been locally exposed to a flow of detergent, creating thereby precise "injuries", with the rationale of mimicking trauma-induced degeneration.[153]

In an even more complex device, neurons were co-cultured with glial cells, like astrocytes or Schwann cells, introduced in another compartment, while a fourth chamber was employed to flow acrylamide to induce axotomy. Thereafter, neuron regeneration was studied, and interestingly, axons showed a higher tolerance to acrylamide than neuronal bodies, especially compared to reported toxicity values for standard culture. This observation could be explained by the fact that microfluidics enabled local delivery of toxins to either the axon or the neuronal body.[159] Alternatively, axotomy was achieved using a femto-second laser for localised heat-induced ablation.[160]

A different strategy to guide axons and study their outgrowth is known as the Bonhoeffer strip assay, which relies on specific chemical patterns to promote or inhibit axon growth.[161] While this assay enables the identification of inhibiting factors for axon outgrowth, this technique, where neurons are simply plated, exhibits low reproducibility, and moreover, neurons are randomly oriented. By combining microfluidics with chemical patterning of polylysine and aggrecan to promote and guide axon growth, or to alter it, better cell alignment was achieved.[162] Furthermore, nutrients are supplied

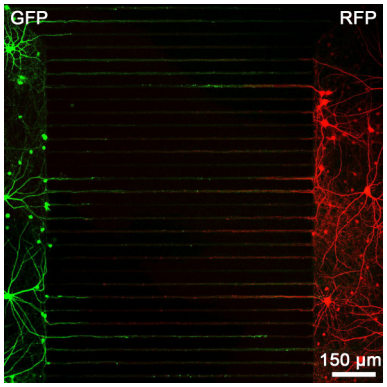

Fig. 2.3 Fluorescent microscopy image of a compartmentalised microfluidic device in which two chambers are connected with micro-grooves of 7.5 µm x 3 µm x 900 µm. Neurons, from rat hippocampus, on the left produce Green Fluorescent Protein (GFP) and neurons on the right Red Fluorescent Protein (RFP). Such a system allows the investigation and manipulation of synapses between neurons. Reproduced with permission, copyright 2010 Elsevier.[152]

in such a system using flow regimes that resemble the *in vivo* situation, and compounds can precisely and specifically be delivered to different cell sub-populations.

As biological and chemical cues predominantly occur in the form of gradients in native tissue, an extensive amount of research has focused on the creation of gradients of factors that promote neuron growth,[61,62] guide it,[163] stimulate cellular differentiation,[61] establish synapses,[164,165] or induce diseases.[166] Gradients were generated through various approaches, using a resistance mixer network,[61] hydrogel-based barriers,[164,165,167] or arrays of high resistance microchannels,[163,166] some of which are fully compatible with standard compartmentalised devices.[166] The influence of mechanical gradients on neurite growth was similarly studied in an H-shaped channel configuration.[168] The device was filled with a collagen gel, and a gradient of cross-linking agent was created across the connecting channel, resulting thereby in a gradient of gel stiffness. Seeding neural cells in the middle of the cross-channel allowed the study of collagen gel stiffness on axon outgrowth. In an updated version, the same device was employed to study gradients of adhesive ligands on the collagen gel.[169] In another approach to assess the sensitivity of neural cells to mechanical forces, cells were grown on a stretchable PDMS membrane; this allowed the investigation of stretch-related growth of integrated axons,[170] dynamic stretch injury of axons,[171] mechanical breaking of microtubules[172] and localised mechanotransduction on sensory nerves.[173]

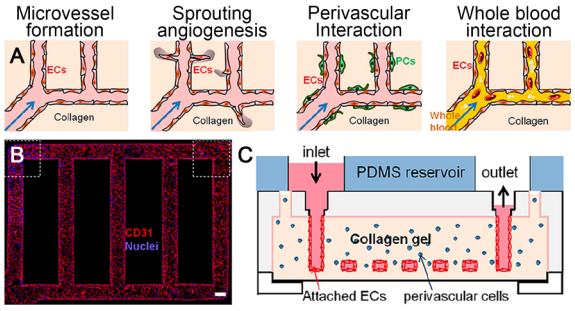

Fig. 2.4 Gel-based 3D microvascular network made of collagen type-I gel. (A) Schematic representation of research possibilities on this platform. (B) Fluorescent microscopy image of human umbilical vein endothelial cells (HUVEC) on the walls of the gel-based networks, stained for the nuclei (blue) and CD31 (red), an angiogenic marker. (C) Schematic side-view representation of the microvascular networks. Reproduced with permission, copyright 2012 National Academy of Sciences, U.S.A.[180]

As an advantage over the so far discussed 2D culture approaches, 3D neuronal tissues or neurospheres are

supposed to more closely resemble the *in vivo* environment of neurons, making the study of their function more relevant. A microfluidic device with compartment chambers separated by micropillars was employed to trap spheroids derived from aggregates of adipose tissue-derived stem cells (ATSC). The tissues were subsequently stimulated to differentiate into neurospheres, with neurons sprouting through the pillar network.[90,174]. A similar approach was utilised for the co-culture of Schwann Cells (SC) derived from human embryonic stem cell (hESC) with hESC-derived neurospheres to obtain spheroid formation.[175]

A number of attempts to develop HTS systems have been reported by combining microfluidics with microarray technology. For example, Shi and co-workers demonstrated a microarray platform with microfluidic channel connections in a 96-well plate format for screening the effect of small molecules on synaptogenesis.[176] This system is a particularly good example, where microfluidics is made compatible with conventional laboratory equipment for well-plate culture dishes, while offering HTS solutions to search for potentially interesting factors for neural regeneration. In another example, a microfluidic concentration gradient generator network with multiple downstream culture chambers was used to screen for optimal combinations of soluble factors to induce differentiation of rat MSCs into Schwann cells.[177]

Although all microfluidic systems discussed so far do have the potential to become valuable RM models, they have predominantly been used for studying fundamentals of degeneration and drug screening for prevention of degeneration. Interestingly, one of the early reported devices combined microfluidics and microengineering and aimed at creating a retinal-neural interface in an attempt to create a true RM model.[178] In this work, the authors developed an artificial synapses system by micropatterning substrates to guide neurite growth, with localised neurotransmitter delivery while using soft materials. It is envisioned that more of such systems will appear in the future specifically for the purpose of studying regenerative strategies.

2.3. Vascular regeneration and wound healing

Vascularisation is of great importance in regenerative medicine for proper oxygen and nutrient supply, and most cells in the human body are not much further than 100-200 µm from a capillary.[179] Without proper vascularisation, tissue constructs of larger than 200-400 µm are not viable because of oxygen and nutrient depletion. Therefore, new blood vessel formation is a relevant part of every regenerative strategy. Since the dimensions in microfluidic conduits are comparable to those of natural microvessels, which typically range from a few micrometres to tenths of millimetres, microdevices are particularly attractive to realise capillary vessels or to study the processes

of vasculogenesis and angiogenesis. For instance, an *in vitro* microvessel network has been successfully created from collagen type-1 gel using soft lithography techniques (Fig. 2.4).[180] After device fabrication, human umbilical vein endothelial cells (HUVEC) were seeded in the 100 µm x 100 µm microchannels, and left to attach and proliferate on their walls to yield an endothelialised lumen, and the channels were thereafter perfused with culture medium or whole blood. To study interactions between HUVECs and perivascular cells, the latter were added to the collagen gel before device fabrication. Upon treatment with growth factors such as vascular endothelial growth factor (VEGF), which is a signal protein produced by cells at low-oxygen or hypoxic conditions as well as a well-known angiogenic factor, sprouting angiogenic structures were observed in the gel matrix. Similarly, the same microdevice has successfully been applied to study cell-cell interactions between pericytes and smooth muscle cells, and as a model for thrombosis upon chemical induction of blood clogging in the created microvessels. This artificial capillary network is of utmost interest not only to test materials and compounds for RM strategies but also as a potential implant candidate. Alternatively, microfluidic devices have been produced by combining two different types of gels, each containing one cell type (fibroblasts or endothelial cells). The aim was to provide additional versatility in creating ECM microenvironments in the bulk and the channel network in one device to investigate implantable candidates and to study cell-cell interactions.[181]

To recreate the perivascular stem cell niche[182] as a model for vasculogenesis, a microfluidic approach was applied where HUVECs and stromal cells were co-cultured in parallel gel lanes. Specifically, the device system included five independent lanes, the three middle lanes consisting of fibrin-gel while the external lanes were kept for medium perfusion. When cells were separately added to lanes two and four, the formation of vessel-like structures into the middle gel lane was observed. Interestingly, this study was one of the first to demonstrate vascular generation with lumen formation and an actual hollow capillary-network inside a microfluidic system by simply co-culturing cells in gel without any patterning of the cells in a microchannel network.

As mentioned before, VEGF gradients are known to elicit angiogenic sprouting. To study this phenomenon, Shamloo et al. designed a simple three-channel gradient device, with cells being cultured in the middle channel as a monolayer and exposed to gradients of VEGF created upon diffusion from the side channels via an array of low-micrometre channels.[75] VEGF gradients have alternatively been created across a 3D gel structure in a 3-lane microfluidic device:[89,183–186] collagen type-1 gel phase in the middle lane was exposed to a medium flow on one side, and VEGF-supplemented

medium on the other side, to yield a VEGF gradient in the gel. Cells cultured on the wall of the gel on the lower end of the gradient migrated in the gel structure to 3D blood vessels. This platform has additionally been employed for a variety of other studies to quantitatively analyse vascular growth in an endothelial monolayer using VEGF alone[89] or in combination with either the angiogenic regulator sphingoshine-1-phosphate (S1P)[184] or ANG-1, a co-factor known to be involved in stabilizing vessels.[185] In the same platform, co-culture of endothelial cells in collagen gel with fibroblasts in alginate beads yielded capillary bed-like structures.[187]

Sprouting of vessels relies on the migration of endothelial cells; this process has been studied separately in devices focusing on wound healing models. In a classical wound healing assay, which was one of the earliest methods to study directional cell migration *in vitro* after 'injury',[188] a scratch is made with a sharp object in a cell monolayer to remove cells along a sub-millimetre to millimetre sized line. Thereafter, the rate and efficiency of cell migration to close this artificial wound is monitored. This assay has proven to be interesting for testing the effects of drugs as well as co-culture settings on cell proliferation and migration; however, it suffers from a poor reproducibility due to the uncontrolled way "damage" is realised in the cell monolayers. In that context, laminar flows, as found at the micrometre scale, are particularly attractive to create wounds in a highly controlled manner.[189,190] For instance, van der Meer et al. and Felder et al. employed a 3-phase flow configuration, the centre solution containing trypsin to promote cell detachment from the surface in a well-defined way only in the middle of the channel while leaving cells on the side unaffected.[189,190]

For vascular regeneration, microfluidics can provide improved *in vitro* models mainly for fundamental research on diseases such as thrombosis and for testing RM strategies such as soluble compounds and combinations of hydrogel materials. Furthermore, hydrogel-based microdevices could be employed as implantable constructs for organ repair, and they provide a strategy for connecting artificial organs to the vascular network.

2.4. Musculoskeletal regeneration

Developing reliable models to study regeneration of musculoskeletal tissues, including bone, cartilage and skeletal muscle presents additional challenges of complex 3D architecture and strong dependence on mechanical stimuli such as compression and stretching, since these tissues are part of the human locomotion system, giving rigidity and mobility to the human body.

Relatively simple culture devices have been proposed to investigate the effect of microfluidic confinement and continuous perfusion on osteogenesis. For example, devices were developed containing a single microchannel in which

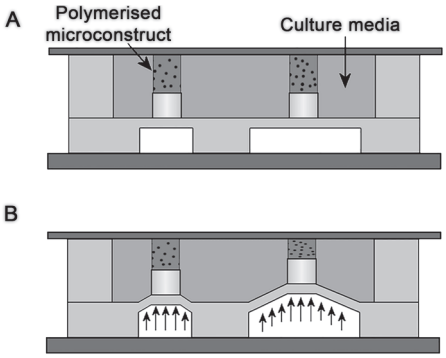

Fig. 2.5 High-throughput screening platform for compression analysis of cells in hydrogel materials. (A) Schematic representation of the compression array in rest and (B) in compressed state. Reproduced with permission, copyright 2010 Elsevier.[196]

osteoblasts, bone-forming cells, were cultured and continuously perfused with osteogenesis-inducing factors such as dexamethasone, bone morphogenetic protein-2 (BMP-2) or a combination of both factors, to study their effect on osteogenic differentiation, as compared to static cell culture systems.[191–193] Similarly, Leclerc et al. studied the effect of perfusion with different shear stress intensities on the behaviour of murine osteoblasts[194] in a 3D microfabricated capillary network. Interestingly, elevated levels of alkaline phosphatase, a marker for osteogenic differentiation, were found in the microfluidic format, either upon exposure to flow or simply under static conditions, as compared to static culture in 2D flasks. These examples demonstrated that confinement already had an influence on cell differentiation, which was further promoted in the presence of a shear flow. In a recent review, Riehl and Lim have discussed in detail these differences between macro- and microfluidic *in vitro* systems for skeletal RM research.[195]

In another approach to evaluate the effect of mechanical stimuli on the process of osteogenesis in a high-throughput manner, Moraes et al. built a microfluidic-based compression array, specifically designed to expose cells encapsulated in a hydrogel to mechanical strain (Fig. 2.5).[196,197] Separate polyethylene glycol (PEG) hydrogel plugs loaded with murine MSCs were formed in a microfluidic chamber using photopolymerisation. Application of a pressure on a PDMS membrane led to compression of the hydrogel plugs, and subsequently of the cells and nuclei. This and similar high-throughput platforms are likely to provide valuable information on the effect of compression on cellular differentiation by using various hydrogels.

Not only mechanical signals are important to steer osteogenesis or chondrogenesis, but chemical signals can also contribute to differentiation processes. To investigate this, a 3D microtissue was generated from primary human bone marrow-derived MSCs between two rows of pillars in a microfluidic channel to study the process of osteogenesis.[174,198] After one week of exposure to osteoinductive chemical stimuli in the platform, calcium deposition was observed, which indicates bone formation. The influence of insulin growth factor 1 (ILGF-1) on chondrocyte proliferation was studied in separate chambers made from collagen gel, in a concentration-dependent

manner.[199] For that purpose, an ILGF-1 gradient was generated upstream to the culture chamber using a microfluidic resistor mixer network.

In an attempt to introduce a high-throughput strategy for screening relevant biomaterials and their effect on 3D culture of osteoblasts, various biomaterials were deposited using inkjet printing in independent microfluidic chambers. Thereafter, MC3T3-E1 osteoblastic cells were seeded in the chamber, and tested for their ability to form mineral nodules (Fig. 2.6).[200] In a further study, the same system was employed to investigate the effect of bacteria and antibiotics on the process of osteogenesis, as well as biofilm-related infections, which are frequently the reason for failure of, for example, orthopaedic implants.[201,202]

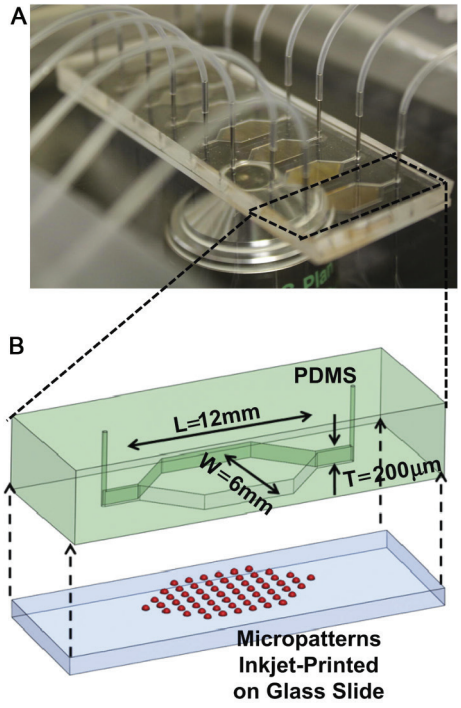

Fig. 2.6 High-throughput screening platform for cell-biomaterial interactions, using parallel microfluidic chambers with different inkjet printed materials. (A) Photograph of the microfluidic platform, depicting multiple chambers. (B) Schematic representation of a single chamber with printed micropatterns. Reproduced with permission, copyright 2012 Elsevier.[200]

During embryonic development of muscular tissue, or myogenesis, myoblasts fuse together to form myotubes, which are early skeletal muscle fibres. This myoblast-to-myotube fusion was emulated in microfluidic format by Folch and co-workers using a long-term culture strategy.[203] In a first step, cells were seeded on a patterned surface combining fibronectin linear structures with a PEG cell-repellent coating, to guide the attachment of murine myoblast cells (C2C12) along specific lines in a microfluidic chamber. After 7 days of culture under diffusion-based perfusion, myotubes were formed in the chamber along the fibronectin lines. This device was particularly useful to study the mechanisms behind synaptogenesis, after local delivery of agrin and neureglin-1, both known to be involved in neuro-muscular junctions during development, mimicking the path-finding dynamics between muscle cells and neurons.[204–206] In contrast to conventional culture approaches, the microfluidic format enabled single myotube interaction study in a highly reproducible way. Finally, this platform also proved to be amenable to HTS assays for the simultaneous study of multiple factors.[205]

To study myogenesis itself over prolonged periods, microbioreactors proved to be particularly attractive. Figallo et al. proposed a PDMS-based device having the footprint of a standard microscope slide and containing 12 independent wells. These wells acted as independent bioreactors[207] in which C2C12 cells were kept in culture for up to 10 days. Compartmentalisation into individual bioreactors while limiting fluidic connections was reported using another strategy relying on a pin Braille display, serving the purposes of creating valves and of pumping fluids. This system was notably applied for a highly automated and multiplexed myogenesis study,[138] cells being seeded and reagents mixed using the pin Braille display, and dynamic culture conditions achieved at various shear rates.

In the musculoskeletal system, damage often occurs in more than one tissue, making regeneration of defects an extra complex process. For example, osteochondral defects require regeneration of both bone and cartilage tissue and when replacing a ligament, integration of ligament tissue into surrounding bone is as important for the success of the procedure as the quality of ligament itself. Therefore, combinations of individual musculoskeletal tissues into one system is expected to be highly valuable for RM research purposes.

2.5. Hepatic regeneration

In vitro liver models have received much attention owing to the important role of this organ in processes of metabolism and detoxification, with the motivation to develop relevant and functional alternatives to animal experiments for HTS of drugs, chemicals, nanoparticles, etc.[208] In that context, liver tissue models are also combined with models of other target tissues for inter-organ interaction studies.[209,210] However, from a RM point of view, engineering liver tissue is only driven by the fact that in case of liver failure, transplantation is the only available option, since no maintenance therapy exists. Since a few reviews were published in the last years on microfluidic liver *in vitro* models, only selected examples are presented in this section and the reader is referred to these reviews for complementary information.[209,211,212]

One of the earlier attempts to use micromachining to create a liver tissue was reported by Kaihara and colleagues.[213] They applied microfabricated vascular networks in silicon and glass substrates coated with Matrigel or Vitrogen as templates to grow endothelial cells and hepatocytes monolayers. These monolayers which were shown to maintain their albumin production, were lifted from the platform after 4-5 days of culture, and folded as 3D vascularised tissues prior to implantation into rats. Since this seminal work aiming at regeneration, a variety of microbioreactors has been described for 2D and 3D culture of hepatocytes under perfusion conditions, for long-

term culture,[214–221] and sometimes subsequent coupling to a gradient generator for concentration-dependent toxicity studies.[222,223] In general, the use of a microfluidic format is accompanied by an enhancement in liver function compared to conventional culture, as measured by albumin/urea production[211] and relevant gene expression.[224] However, direct exposure of the cells to the perfusion proved to lead to cell damage; therefore, most of the reported reactors contain a porous membrane between the medium flow and the cell culture for diffusion-based and shear-free delivery of fresh nutrients to the tissues.

For instance, Ostrovidov et al. employed a PDMS membrane functioning as a scaffold for the growth of hepatocytes, while providing maximum surface area for perfusion on the opposite side.[219] With this approach the authors demonstrated formation of hepatic cellular aggregates which were viable for more than two weeks. Alternatively, etched silicon[220] or polymer membranes[225] have been reported for the same purpose. Using the same perfusion-based culture approach through a porous membrane, Griffith and co-workers developed a multiplexed platform compatible with standard well-plate equipment; the device included 12 independent microreactors in which primary hepatocytes could be kept in 3D culture for several weeks, while maintaining important liver specific functions.[220,226] In another approach, 3D hepatocyte tissues were combined with microfabricated PDMS structures recapitulating the liver sinusoidal space that is naturally made from endothelial cells.[132] Medium was perfused in a microchannel separated from the cell culture chamber by the microfabricated liver sinusoid. Functional liver tissue was obtained, after seeding of hepatocytes, and culture was demonstrated for over 7 days. In a more refined device, rat primary hepatocytes or human Hep/G2/C3A cells were cultured in connection to a rat vasculature via a membrane.[227] The model which was tested for short-term survival and function maintenance, was seen as a promising *ex vivo* model for clinical settings.

Hepatospheres or hepatocyte-based spheroids were also reported as an *in vitro* approach to culture liver cells, while keeping their functions.[228] As for other tissues, hepatospheres were formed in microfabricated well arrays[228] or microfluidic devices.[115] For instance, culture of hepatospheres in microchannels equipped with microwells allowed the spheres to keep their geometry and function, in a parallelised fashion for HTS, while assessing the effect of flow, and testing co-culture.[229–232]

The different liver models presented are excellent candidates for drug screening at first, but for the future it is envisioned that assembling and implanting such microtissues may support or overtake certain liver functions as an RM strategy.

Besides liver, systems for kidney and lung/airways are well known examples of tissues built by employing microfluidics and other microengineering technologies, predominantly to test a specific function of the organ or for drug screening, rather than as a model to test regenerative strategies. For example, microfluidic systems were used to study renal cell behaviour under influence of shear stress and chemical gradients.[233–235] Huh and co-workers demonstrated a device to investigate lung injury by fluid mechanical stresses,[131] as well as mechanical stretching and used the system as a model to test for toxic aerosols.[133] Tatiana et al. demonstrated a microfluidic approach for a respiratory assist device, using high surface-to-volume ratio of microfluidic channel networks in a gas-permeable silicone.[236]

2.6. Future perspectives

Examples of platforms used as a model to study regenerative processes in neuronal, vascular, musculoskeletal and hepatic applications discussed so far, are illustrative of the advantages of microfluidics over classical, static cell cultures in a Petri dish. The power to predict and control flows has been utilised for purposes of creating artificial tissue 'defects', biologically relevant shear stresses, gradients of compounds of interest, and manipulation of cell orientation and movement, all with high precision. Besides, examples of parallelisation demonstrated exciting opportunities to increase screening throughput by a multitude of what is achieved in conventional settings.

While fluid regimes applied are often very smart and create well-defined gradients, the features of most platforms are relatively simple in terms of geometry and cell population. Cells are often cultured as a monolayer, on the bottom of a channel/chamber or on a membrane. Experiments are predominantly performed on one cell-type, and when two cell-types are involved, they are either separated in the device or mixed in a random manner. Experimental results from such studies are undoubtedly useful to obtain some fundamental information on cell-cell interactions or response of cells to (bio)chemicals, but the question remains if they are sophisticated enough to test and develop regenerative strategies. This question is highly relevant considering that even in the case of a comparatively simple injury like a skin wound, damage involves much more than a monolayer and one cell type. Other tissues like for example bone are even more complex owing to their well-defined 3D structure but also because steps leading to complete regeneration of bone tissue, including, for example, callus formation and mineralisation, are multiple.

For these reasons, models that combine the 3D geometrical complexity including ECM and cell heterogeneity with the already discussed advantages of microfluidics seem like the way to go in order for microfluidics to become a standard tool in the RM research. But is this feasible?

Organs-on-chips, developed as advanced *in vitro* models with the aim to mimic the potential key-aspects of human physiology with respect to a certain tissue or organ, and combining realistic biological readout with simplicity, low cost, high throughput and reproducibility may potentially make a large impact on RM research. For this, in contrast to conventional cell culture, microfluidic chips provide features such as organ-level organisation of cells or tissues, physiological gradients of growth factors or cytokines, shear stress from pulsatile fluid flow or cyclic stretch from elastic membranes. While some of such models were briefly discussed in the previous section, a more detailed review of various examples of successful organs-on-chips has recently been published by Baker.[69]

As mentioned earlier, the existing organs-on-chips are excellent models to study fundamental physiological processes and for drug/toxicity screens, but do they meet the needs of RM research? In a conventional approach for organs-on-chips, the major cells or tissues contributing to the overall function of a certain organ are cultured in separate microfluidic compartments, and through connections between the compartments, fundamental physiological processes are studied upon exposure to stimuli. As is the case for 'regular' on-chip systems, the cells or tissues in the compartments are mainly cultured in comparatively poorly defined environments. These have simple 2½D geometries as derived from anisotropic micro-structuring processes and are made from materials which are biocompatible or inert. To increase the potential relevance of such systems for studying regenerative processes, it would be useful for example to engineer more complex artificial cellular microenvironments. These engineered environments should have hierarchical multi-scale 3D or curved geometries such as the unique structure of the hepatic cord of the liver,[237] supporting a corresponding spatial organisation and consequently communication of the cells as it is similarly found in the vast majority of the mammalian tissues. Within each compartment, heterogeneous populations of cells could be created by co-culture of cells in the form of simultaneous cell culture in the same environment,[238] physically separated,[159] or in a unique configuration,[239] to provide tissue organisation and function, or to recreate an artificial cell niche. But also compartments themselves could possibly be positioned in such a way that they more closely resemble the three-dimensionality of native tissue. By doing so, an environment would be created in which cells can be cultured for longer, clinically relevant time periods to allow for studying all processes leading to successful regeneration. In such, more complex systems, it is also envisioned that some of the effects of the immune system during regeneration could be mimicked. These effects are of great importance for the natural process of regeneration of any tissue, and yet, they are lacking in all available *in vitro*

models. Increasing structural complexity of model tissues or organs may bring along issues of inadequate oxygen and nutrient supply and additional active perfusion or engineering of artificial vessels may be required.

Most importantly, such 3D models should be suitable to test any type of regenerative strategy of interest. While testing of growth factor based therapies will probably be most easily applied, therapies including bioactive materials, either alone or as tissue engineered constructs may pose great challenges. Such biomaterials can be of any of the three material types, metals, ceramics or polymers, depending on the tissue to be regenerated, which means a much larger variation compared to the materials frequently used in microfluidic systems. Needless to say, these materials do not meet requirements of transparency, gas-permeability and processability, making their introduction into microfluidic systems not trivial. Furthermore, these bioactive materials dynamically interact with the biological systems, through protein adsorption, degradation, etc. which makes it imperative to study the level of miniaturisation required to have them match the on-chip microenvironment, but also to integrate them into the device in a relevant way. Concerning the latter, coating technologies offer a relatively simple solution, although the aspect of 3D is partially lost. But also microfluidic systems themselves can be applied to develop gradients or arrays of relevant biomaterials to be studied, for example as demonstrated by Burdick et al.[240] and Zaari et al.[241]

Surely, 3D microenvironments with heterogeneous cell populations, room for ECM production over a longer period of time, possibility to create relevant tissue injuries and study regeneration by any type of regenerative strategy, without compromising the advantages of microfluidic systems in general, and possibility to increase throughput of screening in particular, would be a dream come true to anyone working in the field of RM.

This increase in complexity will undoubtedly also introduce challenges regarding applicability and reliability of assays, which may not be suitable for that level of complexity in 3D. Van der Meer and van den Berg recognised this issue and suggested that enhancement of complexity should be accompanied by further technological advancements in terms of integration of microelectrical, micromechanical and microfluidic components.[70] While the in this review indicated end-users of such advanced organs-on-chips systems are identified as biologists, toxicologists and pharmaceutical industry, they will be of great interest to scientists developing regenerative strategies as well.

3 Standalone microfluidic cell culture.

"The essence of the independent mind lies not in what it thinks, but in how it thinks."

Christopher Hitchens

Microtiter plate-sized standalone chip holder for microenvironmental physiological control in gas-impermeable microfluidic devices

In this chapter, the development of a microtiter plate-sized standalone chip holder is presented that allows for precise control of physiological conditions inside closed microfluidic cell culture systems, made from gas-impermeable materials. The suitability of the standalone chip holder to support cell growth was demonstrated in a closed gas-impermeable glass chip, while performing time-lapse imaging. The viability of the cells was tested with a live/dead stain, demonstrating the ability to perform in situ assays. To investigate the ability to change the gas tension inside the chip, a hypoxia responsive reporter cell line was used, and imaged before and after changing the gas environment from normal to hypoxic condition. The chip holder has been found suitable for performing cell-based in vitro experiments in closed microfluidic devices.

This chapter is based on the publication: "Microtiter plate-sized standalone chip holder for microenvironmental physiological control in gas-impermeable microfluidic devices", Lab Chip 2014

Standalone microfluidic cell culture.

Microtiter plate-sized standalone chip holder for micro-environmental physiological control in gas-impermeable microfluidic devices

Microfluidic systems are successfully applied to create tailored chemical and physical microenvironments with high fidelity at the micrometre scale, enabling in-depth analysis of cell behaviour, in a milieu that mimics their natural biological environment.[242] As such, microfluidic systems have become highly relevant tools for fundamental (cell) biological studies, diagnostics, and pharmacological screens. As discussed in Chapter 2, microfluidic systems may become widely used in regenerative medicine (RM) research.[243] Microfluidics based *in vitro* systems for RM research should allow for tailoring of the biological environment by controlling gas-exchange, temperature, pH, nutrient supply, and metabolite removal. Another important aspect to be taken into account when developing such a system is the possibility to perform continuous and real-time assays, for example based on live or time-lapse imaging, increasing therewith the throughput of screening. Finally, such systems are preferably compatible with standard laboratory equipment, such as microscopes and plate readers.

The majority of currently applied microfluidic systems intended for biological studies are made from polydimethylsiloxane (PDMS). It has the advantage of being gas-permeable, and therefore cells grown in PDMS based systems can be cultured using conventional laboratory incubators.[244–246] Furthermore, PDMS is relatively inexpensive and its fabrication is straightforward.[247] The use of PDMS is, however, also associated with important drawbacks, such as limited fluidic control due to the porous nature of the material, and unpredictable and unstable surface chemistry.[248] Furthermore, severe concerns are shared by many biologists regarding the incomplete biological characterisation of the effects of this material.[248] Other materials exist that are better characterised from this perspective, such as glass and polystyrene (PS), owing to their widespread use in conventional *in vitro* systems.[248] However, they are not or poorly gas-permeable, which limits their applicability to closed cell-culture systems, where CO_2 and O_2 must be tightly regulated. Closed *in vitro* systems are of particular importance in the RM research, where, among others, interactions of cells with various natural and synthetic biomaterials are studied, the majority of which are gas-impermeable.[243,249] Such closed systems require alternative ways to control physical parameters inside the cell culture device, for example, in the form of a standalone incubator.

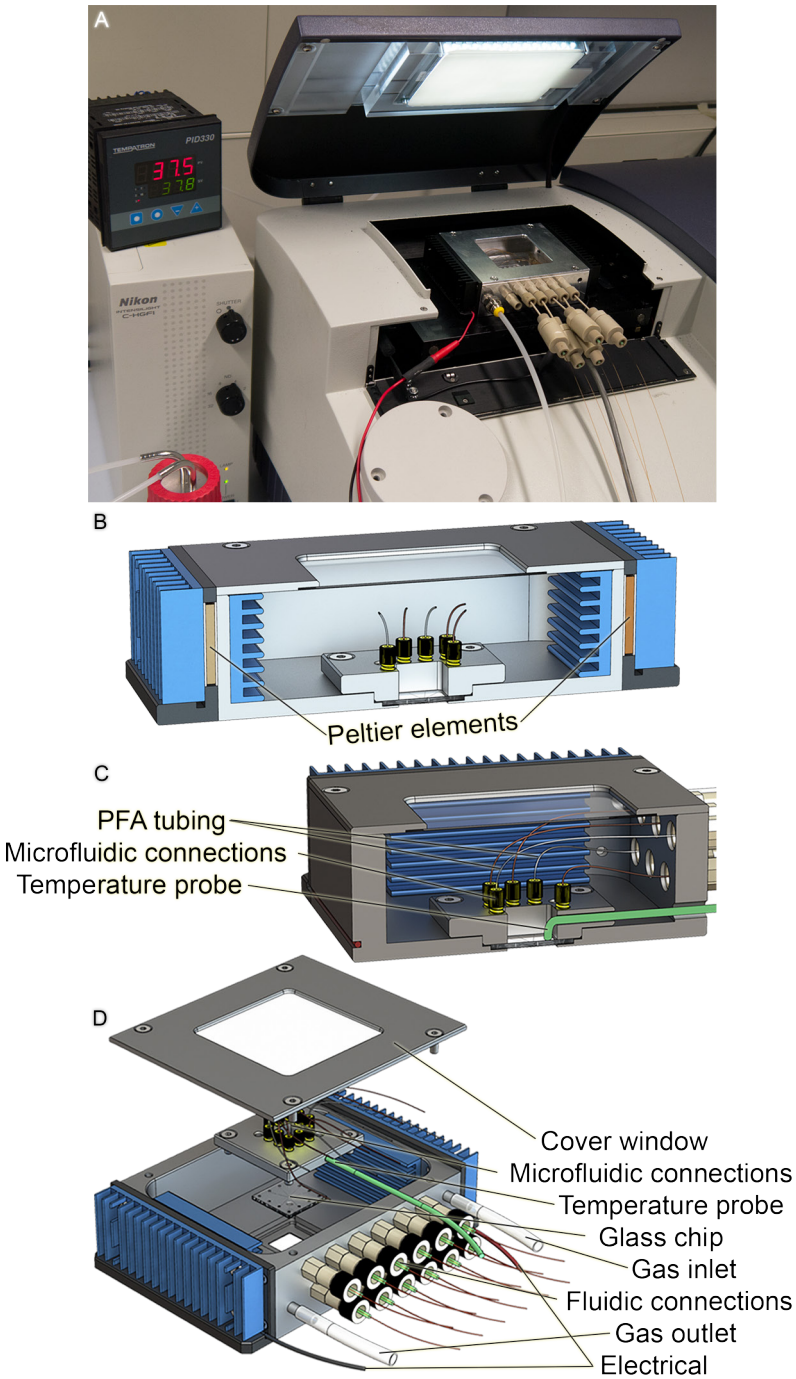

Fig. 3.1 (A) Picture of the chip holder inside a microtiter plate microscope with electrical, gas and fluidic connections. The bottle in the bottom left corner is the bubbler to keep the humidity high to prevent evaporation through the gas-permeable tubing. (B) Schematic depiction of a longitudinal cut-through of the chip-holder, showing the position of the two Peltier elements and heat sinks. (C) Depiction of a transverse cut-through, showing the position of the temperature probe, the chip, and its connections to the gas-permeable PFA tubing. (D) Exploded view, showing the different separable parts. The lid includes a glass window for top illumination for contrast microscopy.

Current commercially available standalone culture systems, such as microscope stage incubators (e.g. Okolab, Pecon), are bulky, limiting control of the microenvironment. In addition, they require modifications of the microscope, they are dedicated, not portable, and do not readily accommodate microfluidic connections. Systems that facilitate microfluidic connections do not allow for control of temperature and gas conditions in closed systems (e.g. Micronit, microLIQUID) or are mainly meant for PDMS cell culture devices.[250–252]

To overcome these issues, a platform was developed in which entirely closed microfluidic systems made from gas-impermeable materials can be used for cell culture under varying physiological conditions (Fig. 3.1). The complete system consists of a glass microfluidic chip inserted into a microtiter plate-sized chip holder, which also functions as a standalone incubator, allowing gas-tension and temperature control. The system is suitable for *in situ* time-lapse or live imaging of cells, and is compatible with standard laboratory (imaging) equipment. Control on the gas composition inside the glass cell culture chip is achieved by using gas-permeable tubing inside the closed chip holder. As such, the system supports cell growth, but it can also be used to mimic deviating physiological conditions, such as oxygen deprivation, also known as hypoxia.

3.1. Chip holder

The chip holder consists of an aluminium chamber, into which the chip can be inserted, allowing for fluidic interfacing using a manifold connected to an array of capillaries. The whole platform was designed, fabricated and assembled in-house. Aluminium was chosen for its high thermal conductivity and machinability. The whole aluminium chamber is used as a heat sink and is kept at a stable temperature using two square 20 mm Peltier elements (MULTICOMP, Farnell, The Netherlands) placed on either side of the chamber, and each containing an attached outer heat sink (Fig. 3.1B). The chamber and heat sinks are thermally insulated using polyoxymethylene (POM) spacers. Since the whole chip holder is precision milled, it is fully symmetrical and involves a relatively small temperature difference (37 - RT = 12 K), with negligible temperature gradient over a distance of 1 mm, as measured using conventional probes (<±0.05°C). To ensure stable temperature and fast response, the Peltier elements are powered by a computer programmable controller, capable of delivering pulse-width modulated and polarisable output (TCM, Electro Dynamics Ltd, Southampton, United Kingdom). The feedback temperature sensor (NTC) is placed on the side of the chip (Fig. 3.1C-D) not to block the light, and an offset of 0.8 K was determined using an external temperature probe near the micro chamber. This resulted in a stable temperature at a desired value

(37°C) with a tested SD of ± 0.003°C over a period of 20 h. This feature is particularly important for the stability of the cell culture, and imperative for the stability and predictability of the fluidics.

Gas exchange is ensured through the microfluidic connections with the chip inside the closed chip holder, using perfluoroalkoxy (PFA) capillaries (150 µm ID and 360 µm OD PFA HP Plus, DuPont, USA), each having an internal volume of 6 µL (Fig. 3.1C-D). Fused silica capillaries (200 µm ID and 360 µm OD, PolyMicro, France) are used for outlet connections and collection of (waste) medium, since medium is passed only once. By controlling the flow rate through the PFA tubing, the residence time of the medium inside the tubing can be set to ensure gas equilibrium is reached before medium enters the chip, as is elaborated in the next section. Even though fluoropolymers are not known for their inherent gas-permeability, they provide a good compromise between chemical resistance, thermal stability, and gas exchange. The gas mixture is provided by 5% CO_2 supplemented compressed air (Linde Group, The Netherlands) and reduced oxygen mixture is obtained by partial mixing with N_2. To provide sufficient humidity, to avoid possible evaporation through the PFA tubing, the gas mixture is flown through a water bubbler before entering the chip holder (Fig. 3.1A).

The whole platform has the footprint of a microtiter plate (127.5 mm x 85.5 mm) and a height of 32 mm. These dimensions make it compatible with a variety of read-out equipment meant for microtiter plates. For live imaging, the chip holder is placed in a microtiter plate microscope (BD Pathway 435, USA) capable of fully automated fluorescence and bright-field microscopy (Fig. 3.1A) or in a fully automated DIC/confocal microscope (NIKON Ti-Eclipse with A1 Confocal, Japan).

Perfluoroalkoxy tubing oxygen mass transfer

To elaborate the oxygen transfer through the PFA tubing, finite element modelling (FEM) was used (COMSOL-MEMS, Sweden). With a flow rate of the medium in the 1 $\mu L \cdot h^{-1}$ range, the pressure gradient over the wall of the PFA tubing, between air and liquid, is negligible, making diffusion dominant in mass transfer. The diffusion coefficient of O_2 through PFA, is approximately 22 x 10^{-8} $cm^2 \cdot s^{-1}$ (at 25°C),[253] as compared to water 2.4 x 10^{-5} $cm^2 \cdot s^{-1}$ (at 25°C) and air 0.22 $cm^{-2} \cdot s^{-1}$ (at 25°C). In a 20% oxygen environment, medium contains approximately 200 µM dissolved oxygen at equilibrium, or 1.2 nmol in 6 µL.[254] To reach this oxygen level in water, it would take approximately 5 minutes through 360 OD and 150 ID PFA tubing at 1 $\mu L \cdot h^{-1}$ in a 20% O_2 air environment (at 25°C and 1 atm), as demonstrated in the plot in Fig. 3.2. In conventional, static flask culture, the change in oxygen content could require > 3 h before an equilibrium is reached, which

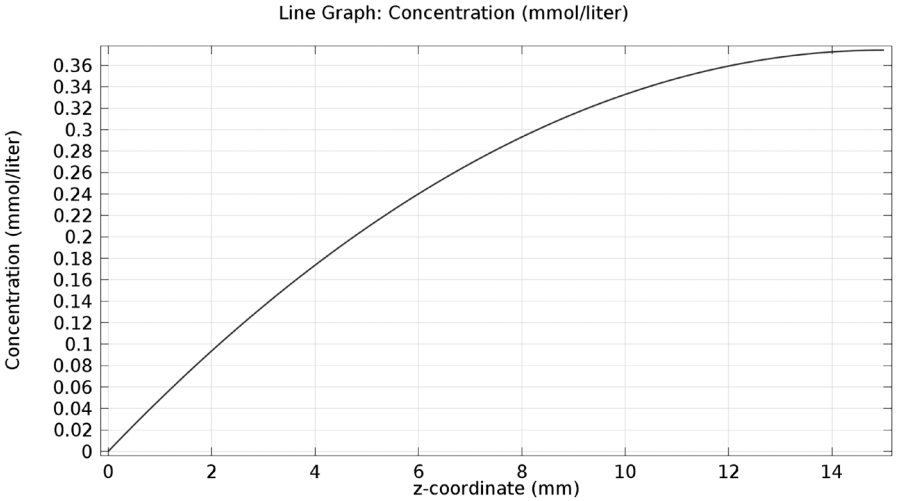

Fig. 3.2 Graph depicting finite element analysis (COMSOL), using incompressible laminar flow (Navier-Stokes) and diluted species diffusion, of a 15 mm piece of PFA tubing (360 µm OD and 150 µm ID) in a 20% oxygen air environment and flowing water at a flow rate of 1 µL·h^{-1}(at 25°C and 1 atm).

makes absorption of oxygen into medium the limiting factor.[255] Since the surface-to-volume ratio in the tubing (160 mm^2 / 6 mm^3 ≈ 27 m^{-1}) is much larger than in classical culture conditions, the equilibrium is reached faster. Therefore, a residence time of 6 h selected for the experiments in the presented study is more than sufficient to ensure that the desired oxygen tension in the medium is reached.

3.2. Chip designs

Two different chip designs were tested to demonstrate the effectiveness of the platform: (i) a device with two 650 µm x 4 mm rectangular chambers connected to two supply channels (Fig. 3.3A), via an array of 1 µm x 3 µm x 10 µm diffusion channels; and (ii) a device with a 650 µm square chamber surrounded by four supply channels (Fig. 3.3C), also connected to the chamber by a similar array of diffusion channels (Fig. 3.3D). Thereby, diffusion is dominant over convection between the supply channel and the chamber due to the high relative resistance of the connecting diffusion channels. This configuration allows for shear stress-free culture of cells, which is essential for delicate mammalian cells.

Chip Fabrication

When designing platforms in which a chemical microenvironment is to be generated with high fidelity, the choice of materials and fabrication methods is of great importance. To ensure stability and prevent deformation, and consequently advection, rigid materials are preferred over elastomeric materials such as polydimethylsiloxane (PDMS), which is widely used

in microfluidics.[29] Elastomeric materials present important limitations in this regard, because of their relatively porous nature.[256] Finally, the platform should be amenable to further chemical modification to introduce biomaterials of interest, which, in general are not gas-permeable. The material of choice for the presented platform was therefore glass, which is chemically stable and inert, better characterised in cell-culture systems than PDMS and applicable for high resolution fabrication.[257] A major issue when using glass, however, is the processing, which is mostly based on wet etching that is associated with low lateral etch control, since this is mainly based on wet etching techniques. Dry etching is possible, however, this is a slow process (<1 μm min^{-1}) that requires harsh and complex masking techniques. Furthermore, it requires working with more expensive materials such as quartz or fused silica to ensure the final surface is smooth, which in turn brings about other processing limitations. Therefore, a two-step wet etching process was developed for common float glass, to produce both shallow nanometre size features (< 1 μm) and deeper micrometre size features (> 50 μm), while dealing with the adhesion challenges by using better controlled low etch rate solutions (hence, prolonged chemical exposure) for small features.

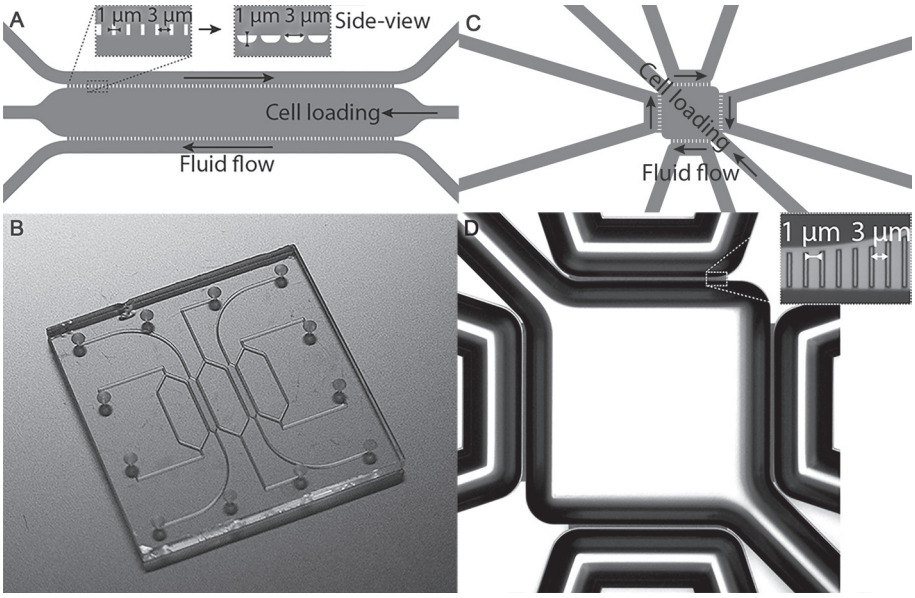

Fig. 3.3 (A) Schematic diagram of the rectangular chamber, showing the flow directions in the supply channels and cell loading channels, with as inset an enlargement and side-view of the diffusion channels. (B) Photograph of the 2 cm square die with two rectangular chambers. (C) Schematic diagram of the square chamber. (D) Bright-field microscopy image of the glass chip, depicting the chamber with the surrounding supply channels, with as inset an enlargement of the diffusion channels that connect the supply channel with the chamber.

Conventionally, wet-etching of glass uses hydrogen fluoride (HF) with a masking layer of > 200 nm gold, together with a 10-15 nm chromium adhesion layer. For features larger than 10 μm this method is usually adequate, but combining features smaller than 10 μm with sub-micron features, as in the platform presented here, required a modified method. First of all, the small-sized diffusion channels possess a very small surface area compared to the end feature size, making adhesion of the masking material to the substrate a challenge. One way to improve adhesion is to reduce the thickness of the gold layer, making it less top-heavy and smaller in comparison to the feature. However, this approach would increase the chance of introducing pinholes caused by imperfections in the sputtering of gold. An alternative is to use a relatively thick chromium layer for masking. Since very 'thick' chromium layers introduce stress, the thickness was optimised to 50 nm, as the best balance between adhesion, low-stress and sufficient masking. To control the etch rate, buffered hydrogen fluoride (BHF) was used, rather than hydrogen fluoride (HF), resulting in an etch rate of approximately 60 nm min^{-1}.

Finally, the microfluidic features of chips were fabricated in thin glass substrates (0.21 mm D263, Schott, Germany), for use with high resolution optical microscopy, using the two-step wet etching process. Masks were designed using CleWin (WieWeb, The Netherlands), and fabricated in-house on 5" soda-lime glass substrates with chromium masking layer using laser lithography (DWL2000, Heidelberg Instruments, Germany). In the first etch step, all shallow features with a depth of 1 μm were realised, (masking layer: 50 nm sputtered chromium; etchant: buffered hydrogen fluoride (etch rate of 60 $nm \cdot min^{-1}$, BHF, BASF, Germany). An etching time of 16.5-min resulted in a diffusion channel depth of approximately 1 μm, and a width of 3 μm. In the second step, the chamber and the surrounding supply channels were created, using a standard wet etching protocol (masking layer: 15 nm sputtered chromium and 200 nm gold; etchant: 10% hydrogen fluoride (HF, BASF, Germany) with an etch-rate of approximately 1 $\mu m \cdot min^{-1}$). Since HF is not buffered, etch rates are unpredictable and decline in time. Therefore, the etching was performed in several steps and the height of the structures measured after each step using a profilometer (DEKTAK, USA), until a depth of 75 μm was reached. In the top glass substrate (1.1 mm D263), via-holes were powder-blasted, using 29 μm alumina particles. Finally, both glass substrates were thermally bonded in an oven (6 h ramp-up, 1 h at 570°C, 6 h ramp-down). After bonding, the wafers were cut in 2 cm x 2 cm dies with a dicing saw (DAD 321, Disco, Japan) followed by polishing (Fig. 3.3B).

3.3. Cell culture

To demonstrate the possibility to perform live or time-lapse imaging, murine myoblastic C2C12 cells were cultured over 2 days and imaged using an automated DIC microscope (NIKON Ti Eclipse, Japan). C2C12 cells were cultured in Dulbecco's-Minimum Essential Medium (DMEM, Invitrogen) supplemented with 10% fetal bovine serum (FBS, Invitrogen), 100 mg mL^{-1} penicillin and 100 mg mL^{-1} streptomycin (Pen/Strep, Invitrogen). After expansion culture, they were dissociated using trypsin (Invitrogen), resuspended to a concentration of approximately 5 million cells·mL^{-1}, and injected into the chip using a syringe through the cell loading channels into the chamber. Cells were left to proliferate for 2 days, while flowing cell culture medium in the supply channels (single pass), at a flow rate of 8 µL·h^{-1} using a precession syringe pump (Nexus, Chemyx, USA).

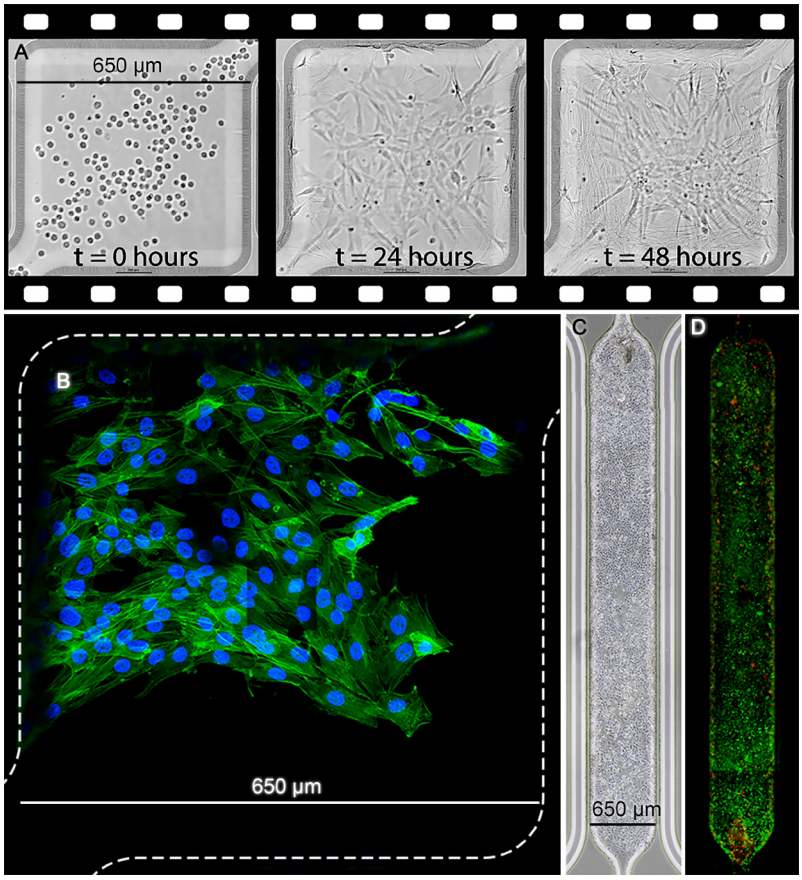

Fig. 3.4 (A) Bright-field microscopy images taken from 2 day time-lapse series of C2C12 cells, with t=0 taken just after cell loading. (B) Confocal fluorescence microscopy image of MG63 cells in the square chamber after 2 days of proliferation, with stained nucleus (DNA, DAPI, blue) and cytoskeleton (F-actin, Phalloidin, green). (C) Bright-field microscopy stitched image of the rectangular chamber with CHO cells after 5 days of culture. (D) Epi-fluorescence image of the same CHO cells with live/dead staining, live cells being green and dead cells red.

Fig. 3.4A presents snapshots taken from a 2 day time-lapse series on the growth of C2C12 cells in the square chamber at different time points: at time point 0, just after loading of the cells, and at time points 22 and 48 h, where the attachment and spreading of cells can be observed, as well as the formation of a cell monolayer.

To demonstrate culture of more delicate human cells, osteoblastic MG-63 cells were cultured for 2 days, subsequently fluorescently stained with Phalloidin (cytoskeleton, F-actin) and DAPI (nuclei), and imaged by confocal microscope. MG-63 cells were cultured in αMEM supplemented with 10% FBS and Pen/Strep. After culture, cells were rinsed with phosphate buffered saline (PBS, Invitrogen), and fixed with 4% paraformaldehyde (PF, Sigma-Aldrich) for 10 minutes, before being stained *in situ* by flushing the staining solutions through the chamber via the cell loading channels. As shown in Fig. 3.4B, MG63 cells were successfully stained inside the chip, which demonstrates the suitability of the platform for *in situ* cell staining and fluorescence imaging.

3.4. Viability assay

Cell viability was assessed using a standard live/dead assay on Chinese hamster ovary (CHO) cell line, cultured in DMEM with 10% FBS and Pen/Strep. All channels and the chamber were first flushed with PBS, and subsequently a mixture of 2 μM calcein AM and 4 μM ethidium homodimer-I (EthD-I, Invitrogen), to stain live and dead cells respectively, was introduced into the chamber via the cell loading channels, and left for 20

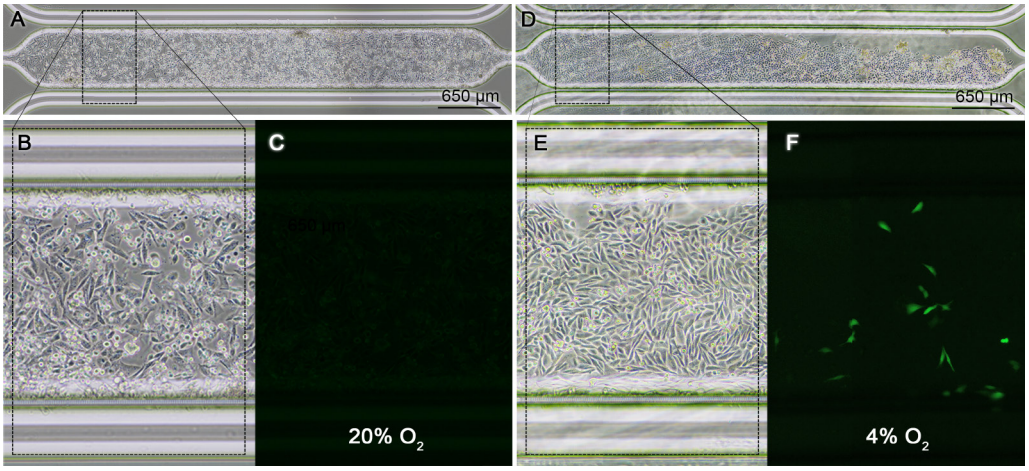

Fig. 3.5 CHO cells with hypoxia GFP reporter (green) inside a gas-impermeable glass chip, using the chip holder, after 48 h culture in normoxic condition (20% O_2), on the left (A-C) and after 22 h under hypoxic condition (approximately 4% O_2) on the right (D-F). For both experiments the following images are provided: bright-field microscopy stitched overview image of the rectangular chamber, with CHO cells inside (A&D); close-up of one section of the rectangular chamber (B&E); and epi-fluorescence microscopy image of the same section of the culture chamber (C&F). After 48 h under normoxic condition, limited or no fluorescence was observed (C), while under hypoxic condition increased fluorescence was observed, indicating the gene reporter is activated.

minutes, before washing again with PBS. Samples were imaged using an epi-fluorescence microscope (TS100, NIKON, Japan), and overview images created by stitching multiple images together. After 5 days of culture, in the rectangular culture chamber, the large majority of cells were found viable, with few dead cells homogenously spread through the chamber (Fig. 3.4C-D), similar to conventional cell culture, proving that cells could be kept viable inside the platform for multiple days. Due to the seeding method, the entrance and exit of the chamber show slightly more red fluorescence due to cell debris flowing back from the dead-volume of the loading channels.

3.5. Hypoxia assay

Oxygen is a critical nutrient for cell survival, which is likely the first one to become limited due to its high uptake and low solubility. Therefore, it is frequently used as a model nutrient.[258] When cells are subjected to low oxygen conditions (hypoxia), numerous genes are up- or down-regulated, like angiogenesis related genes to promote cell survival.[259] To study this, a CHO cell line (CHO HRE-GFP cells) transfected with a green fluorescence protein (GFP) hypoxia reporter, was employed to demonstrate the ability of our microfluidic platform to recapitulate normal and hypoxia conditions. The cells fluoresce in case of limited availability of oxygen. More specifically, hypoxia-inducible factor-1 (HIF-1) translocates into the nucleus and binds to the hypoxia responsive element (HRE) promoter, thereby activating GFP transcription (for details on transfection and clonal procedure, please see the earlier work by Liu and co-workers).[259]

CHO cells were cultured in the chip, under normal and reduced oxygen conditions inside the chip holder, using regular culture medium supplied at a flow rate of 1 $\mu L \cdot h^{-1}$ through the supply channels. Under these conditions, the residence time of 6 h, was sufficient for the medium to reach equilibrium through the PFA tubing. The cells were introduced in the chamber by the cell loading channels and left to attach under normoxic conditions for 8 h. Cell culture either continued at 20% O_2, or the culture condition was switched to hypoxic, whereby the gas mixture flowing in the chip holder contained approximately 4% O_2. After only 22 h of culture under hypoxia, cells showed increased expression of GFP (Fig. 3.5D-F), demonstrating that by varying the oxygen level inside the chip holder, cells in the culture chamber of the chip are affected. In contrast, after 48 h of culture in normoxia, limited or no fluorescence was observed (Fig. 3.5A-C), showing that under normal conditions, the cells inside the gas-impermeable glass chip have sufficient amount of oxygen not to turn to a hypoxic state. These results showed that the platform can be utilised in a standalone fashion with chips made of gas-impermeable materials and that gas composition inside the chip can be varied for mimicking specific *in vivo* conditions, like hypoxia.

3.6. Conclusion

In this study standalone chip holder was presented, particularly meant for microfluidic platforms made from gas-impermeable materials, to control the cell physical microenvironment without the necessity of using a separate incubator. The system is compatible with standard imaging laboratory equipment, making it suitable for live or time-lapse imaging. Various adherent cell types have been successfully cultured over a period of at least 5 days, and both stained and imaged *in situ*. The platform also proved to be suitable to control gas tension, e.g., to induce hypoxic conditions inside the microfluidic chip to reproduce *in vivo* conditions. In the future, this chip holder will particularly be applied to screen interactions between cells and biomaterials for regenerative medicine applications inside microfluidic platforms.

4 Orthogonal multi-gradient generation.

"Imagination is more important than knowledge. For knowledge is limited to all we now know and understand, while imagination embraces the entire world, and all there ever will be to know and understand."

Albert Einstein

Microfluidic Platform with Four Orthogonal and Overlapping Gradients

In this chapter, the development of a multi-gradient microfluidic platform is presented, which can generate four orthogonal and overlapping concentration gradients of soluble compounds. The device includes a square chamber, in which adherent cells can be grown, and four independent supply channels along the sides of the chamber, which are connected through small diffusion channels. Compounds introduced through the supply channels diffuse through the diffusion channels into the chamber, to create a gradient inside the chamber. Further, the chamber is connected to two channels intended for introduction of cells and in situ staining. The dimensions of the different channels were optimised through finite element modelling. Upon fabrication, the chip was used to validate the finite element model by generating and analysing gradients of fluorescent dyes.

This chapter is based on the publication: "Microfluidic Platform with Four Orthogonal and Overlapping Gradients for Soluble Compound Screening in Regenerative Medicine Research", Electrophoresis 2014

Orthogonal multi-gradient generation.

Microfluidic Platform with Four Orthogonal and Overlapping Gradients

When attempting to screen concentration-dependent effects of a bioactive compound or combined effects of different compounds, one faces the challenge of vastly increasing numbers of conditions. For example, screening the individual and combined effect of only 10 compounds at a single concentration would require testing 1,023 unique conditions (Formula (1.1)). Including different time-points and replicates would increase this number even further. Although modern library screening technologies already allow screening of large numbers of compounds, these normally do not take into account combinations, concentration dependence and temporal effects. A model in which all these parameters are embedded would not only increase the throughput of screening, but would possibly also enhance *in vitro* to *in vivo* data translatability. Microfluidics offers a multitude of possibilities to increase throughput of screening, owing to extensive opportunities for integration, parallelisation and miniaturisation.[13,260] Moreover, it allows tailoring of (biological) microenvironments with high fidelity, closely mimicking the *in vivo* situation.[261] The biological microenvironment is of great importance for the fate of the individual cell, as well as for communication among individual cells in the 3D environment of a tissue or organ.[15–17,262]

One very attractive capability of microfluidic systems is their possibility to create and control (multiple) gradients of soluble compounds, which allows the testing a range of concentration in a single assay, increasing thereby the overall screening throughput. For example, Atencia and co-workers successfully created a multi-gradient system that was used to study migration of bacteria.[64] Devices have been developed that can offer complete cell culture, biological assay and analysis, such as multiple single cell gene expression,[263] and have shown promising results.[45] However, these are usually complex devices with integrated valves and external control systems, which present many technical challenges.

Here a closed microfluidic platform is presented that is capable of creating up to four orthogonal and overlapping gradients of compounds inside a chamber, where cells can be cultured. The platform, which is designed for application in regenerative medicine (RM) research, is built from glass, to allow introduction of relevant biomaterials into the system in the future. The microfluidic platform was inserted into a stand-alone chip holder for cell culture outside the incubator and for time-lapse, or real-time imaging

of cell behaviour. Finite element modelling (FEM) was used to aid the creation of the desired microenvironment and then compared to empirically generated fluorescent gradients, to verify and use this model to predict the concentration and combination in each location inside the chamber.

4.1. Materials and methods

The microfluidic platform

The core of the platform is a microfluidic chip with a square chamber having 650 µm sides, in which cells are cultured (Fig. 4.1A). The gradients are generated via diffusion by supplying compounds through four supply channels (75 µm high x 160 µm wide) surrounding the culture chamber. These supply channels are connected to the culture chamber through arrays of smaller diffusion channels (0.5-1 µm high x 2-3 µm wide x 10 µm long, each 4 µm apart, Fig. 4.1 Insets and Fig. 3.3D). By flowing different compounds through these four supply channels at equal pressure and flow rate, and due to the high relative resistance between the chamber and supply channels, the compounds enter the chamber primarily by diffusion. Each supply channel acts as a source of one compound as well as a sink for compounds from each of the other supply channels. Therefore, overlapping gradients of the four compounds are generated inside the chamber. The gradient can be tuned by changing the size of the channels connecting the main chamber to the supply channels. Two channels (75 µm high x 160 µm wide) that directly connect to the chamber are meant for inserting, collecting and *in situ* staining of cells. The glass chip (Fig. 4.1B) was fabricated using the same method as described in Chapter 3, using the same glass for the features (0.21 mm D263, Schott, Germany) and via-holes (1.1 mm D263). The device was then inserted into the in Chapter 3 described standalone chip holder to precisely control the temperature.

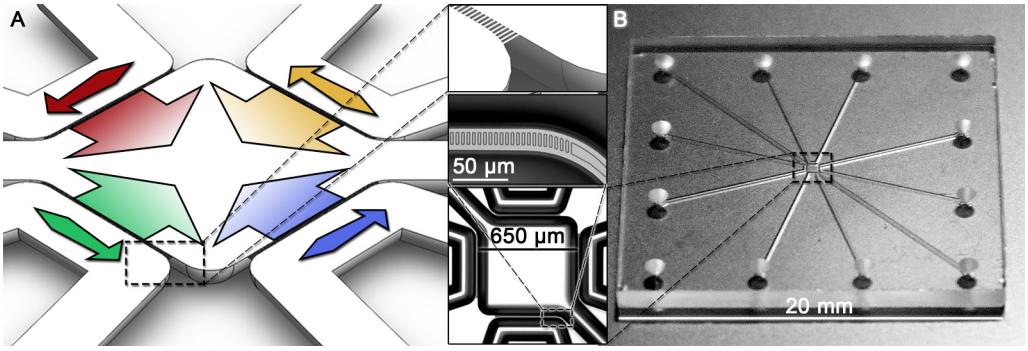

Fig. 4.1 (A) Schematic isometric representation of the four-gradient microfluidic platform, with the four supply channels connected to the chamber by channel arrays. Arrows in the supply channels depict the direction of the flow, and the arrows inside the chamber depict the direction of the gradients. The top inset shows an enlargement of the diffusion channels. (B) Picture of the 2 cm x 2 cm die, depicting the via-holes, channels, and chamber in the middle. The middle inset is an enlargement of a fabricated diffusion channels and the bottom inset shows a bright-field microscopy image of the fabricated chamber.

Finite element modelling

To predict the gradient conditions and aid the design of the gradient platform, FEM was used (COMSOL-MEMS, USA). For the flow, the Navier-Stokes differential equations were used, with the assumptions of: (i) incompressible flow, since liquids in the applicable pressure range have negligible compressibility; (ii) laminar flow, due to the low flow rates and channel dimensions ($Re << 1$); and (iii) Stokes flow whereby inertial terms can be neglected, resulting in:

$$\nabla \cdot [pI + \mu(\nabla u + (\nabla u)^{\tau})] + F = 0 \ \cup \ \rho \nabla \cdot u = 0 \tag{4.5}$$

with pressure p, dynamic viscosity μ, velocity vector u, the applied force F, and density ρ. This was then coupled to transport of diluted species, convection and diffusion, with the assumptions of: (i) neglecting molecular crowding; and (ii) concentration effects, since low concentrations are used with respect to the bulk ($c_i << 1\ \mathrm{M}$):

$$\nabla \cdot \left(-D_i \nabla_{C_i}\right) + u \cdot \nabla_{C_i} = R_i \ \cup N_i = -D_i \nabla_{C_i} + u c_i \tag{4.6}$$

with diffusion coefficient D, species concentration c_i, velocity vector u, species source R_i, species flux N_i, and species number i. Models with different dimensions were studied to optimise the design. The final designs were modelled with different parameters and subsequently compared to the experimental results obtained with fluorescent dyes, to verify and use the model for gradient prediction. Experimentally, four different fluorescent dyes were used to demonstrate the ability to simultaneously generate four overlapping gradients. These dyes are derivatives of rhodamine (CF Dyes, Sigma) excited at four different excitation wavelengths (405 nm, 488 nm, 543 nm and 633 nm), specifically selected for the laser lines of the laser scanning confocal microscope (NIKON Ti-Eclipse with A1 Confocal, Japan). All final concentrations were 10 μM in DI water (Milli-Q, Millipore), and each solution was pumped through one of the supply channels of the chip at a flow rate of 12 $\mu L \cdot h^{-1}$. For the FEM model, the diffusion constant of rhodamine 6G (D = 400 $\mu m \cdot s^{-1}$) was used.[264] Both FEM and experiments with dyes were performed at 37°C and 1 atm. The dimensions of the diffusion channels used were 3 μm width x 1 μm height, and a length of 10 μm. Using confocal microscopy, scans were taken at half-height of the chamber (35 μm) and compared to the FEM data at the same flow speed, concentration and position (Fig. 4.2C-F). The shape of the gradient was compared by matching the maximum excitation of the known concentration in the confocal scan with the maximum in the model.

4.2. Results and discussion

Finite element modelling

Generation of more than two overlapping orthogonal gradients is only possible by applying a solely diffusion-based gradient generator,[85] and not by other approaches such as the flow-based T-cell[265] or mixing based devices.[266] In the current study, to ensure that diffusion is the dominant force of compound influx into the chamber from the supply channels, three conditions had to be taken into consideration: (i) matching flow conditions in all four supply channels, to prevent pressure gradients over the chamber, and therefore advection; (ii) creating high relative resistance between the supply channels and the chamber, to minimise the influence of flow disturbances and restrict advection even further; and (iii) low Reynolds number, to ensure laminar flow, thus excluding lateral flow.

To match flow conditions in different flow channels as closely as possible, a single high precision pump with multiple syringes was used, ensuring that any remaining pulsatile flow and other disturbances were comparable in all syringes. To achieve high relative resistance, the cell culture chamber was connected to the supply channels through an array of smaller diffusion channels in the sub-micron range. An approximation of the resistance (R_h) in a rectangular channel is given by the following formula:

$$\nabla \cdot \left(-D_i \nabla_{C_i}\right) + u \cdot \nabla_{C_i} = R_i \cup N_i = -D_i \nabla_{C_i} + uc_i \tag{4.7}$$

given the conditions that the width (w) is larger than the height (h) and the Reynolds (Re) number much lower than 2000. For instance, resistance in a 50 µm x 100 µm x 1 mm channel is approximately 1.4 x 10^6 Pa·s·m^{-3} and in a 0.5 µm x 1 µm x 1 mm channel 1.4 x 10^{14} Pa·s·m^{-3} per micrometre, using a dynamic viscosity (η) of 1.0 mPa·s for water, thus an eight order of magnitude difference, which ensures that the bulk of the flow passes through the supply channel and not into the chamber. Furthermore, it was important to reach a compromise between the dimensions of the diffusion channels and the flow stability, which could be affected by mechanical disturbances from the pump or moving of tubing. With larger channels, steeper gradients could be achieved, however, with increasing channel size, flow stability was negatively affected, and analogously, with smaller channel size, the flow stability was improved. Low Reynolds number can be obtained by using a syringe pump with high-resolution stepper motor, such that stable low flow rates can be achieved, well within the laminar flow range (± 10 µL·h^{-1}).

Although the gradients are generated by diffusion, the diffusion coefficient of the compound in the solution does not have an influence on the final steady state shape of the generated gradient. It does, however, influence

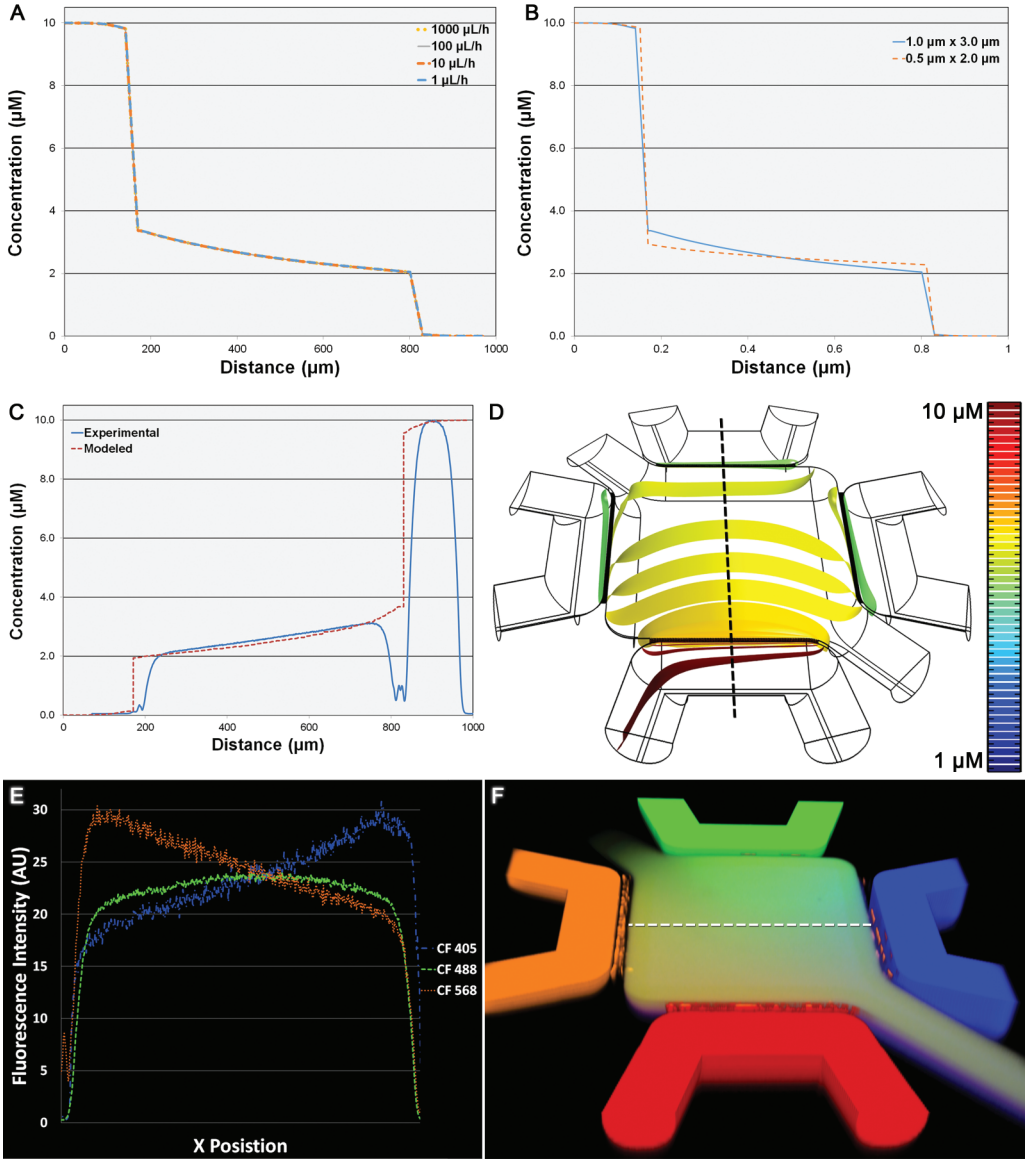

Fig. 4.2 (A) Graph of FEM model depicting the gradient profiles of different flow rates in a chip with a diffusion channel cross-section of 1 µm x 3 µm (10 µM rhodamine 6G), which shows that at different low flow rates (< 1mL·h^{-1}) the gradient profile practically stays the same. (B) Graph of FEM model depicting different diffusion channel cross-sections (12 µL·h^{-1}), showing difference in gradient profiles. (C) Graph depicting the comparison of FEM model gradient (dotted red line) with a fluorescent gradient (solid blue line), using a chip with 3 µm x 1 µm x 10 µm diffusion channels (both 10 µM rhodamine 6G at 12 µL·h^{-1}). The experimental data was obtained from a line profile of a confocal microscopy image, taken at a height of 35 µm from the bottom of the device (dotted black line in D). Since the concentration in the supply channel is known (right peak), and the dye has approximately linear fluorescence emission to concentration in the range used, this peak was used for normalisation. (D) 3D plot of the FEM model depicting a single gradient starting from the bottom, using the same parameters. Coloured lines represent concentration iso-lines. (E) Right to left confocal line scan of the same chamber (horizontal), depicting generated overlapping fluorescent gradients (red, green and yellow). (F) Confocal 3D volume scan image with all four gradients overlapped.

the time required to reach the equilibrium. Similarly, the initial concentration of the compound does not influence the shape of the gradient either, as long as it is diluted with respect to the solvent. The flow rate has a minor impact on the shape, provided that it remains well within the laminar flow regime, and well above the diffusion rate (Fig. 4.2A). Therefore, in the design on the platform presented here, the only parameters that had a significant influence on the generated gradients were the area and length of the diffusion channels. Since the length of the channels was selected and fixed, the only parameter that could be varied was the area of the channel. With a channel area of 0.9 μm^2 (semi-spherical channel of 0.5 µm x 2 µm) a gradient of 2.9 to 2.3 µM (using 10 µM solution) was achieved, and an increase of the channel area size to 2.6 μm^2 (semi-spherical channel of 1 µm x 3 µm) resulted in a steeper gradient of 3.4 to 2.0 µM (Fig. 4.2B).

The FEM model and the experiment with fluorescent dyes, in which the channel size of 1 µm x 3 µm was selected (Fig. 4.2C), indicated that the modelled gradient overlaps with the experimental fluorescent gradient. Therefore, the model is valid for predicting the generation of the gradient and the concentration of the compound can be correlated to the distance from the source of the gradient. As stated before, this specific device gives a gradient ranging from approximately 3.4 to 2.0 µM at a flow rate of 12 $\mu L \cdot h^{-1}$. Fig. 4.2E shows a confocal line scan, taken through the middle of the chip, from left to right, at half the height of the chamber (see line, Fig. 4.2F). Fig. 4.2D shows 3D (z-stack) confocal image depicting four overlapping gradients generated simultaneously.

A stability test performed over a period of 24 h, while controlling the temperature within a +/- 0.05°C range (major contributor to diffusion speed change),[267] indicated stable gradients with variations in concentration below 4% (Fig. 4.3). The stability test was performed by taking a line scan with a laser confocal microscope (LSM510, Zeiss, Germany) every 10 minutes.

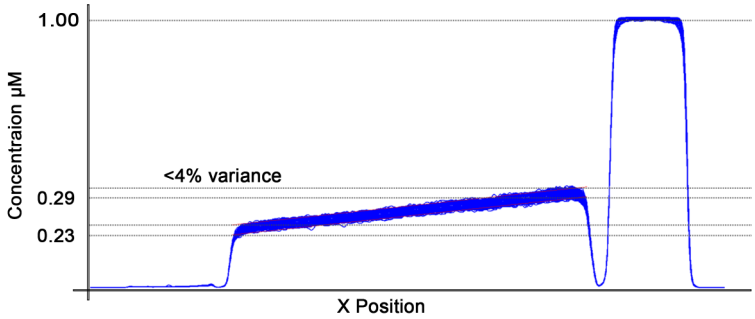

Fig. 4.3 Graph showing overlapping line profiles taken from confocal microscopy images, taken every 10 minutes for 24 hours, using a chip with a diffusion channel cross-section of 0.5 µm x 2 µm (1 µM FITC, 250 $\mu L \cdot h^{-1}$).

4.3. Conclusion

This study demonstrated the possibility to simultaneously generate four identical but orthogonal gradients in a single microfluidic chamber. It also showed the applicability of the developed FEM model to predict the concentration gradients, as validated by comparison to gradients created using fluorescent dyes. The model and fluorescent experiments showed that flow rate (1-1000 $\mu L \cdot h^{-1}$), diffusion constant (steady-state) and initial concentration are of minor or no influence on the final gradient profile. The only major parameter influencing the gradient profile, in this device, is the cross-section of the diffusion channels. Finally, in a test over 24 h, the gradient stability was found to be high, with maximal variation in concentration below 4%. Therefore, this platform is suitable for generating predictable orthogonal and overlapping gradients.

5 Soluble compound screening.

"I have had my results for a long time: but I do not yet know how I am to arrive at them."

Carl Friedrich Gauss

Soluble Compound Screening for Regenerative Medicine Research

In this chapter, the microfluidic platform from Chapter 4, combined with the chip holder from Chapter 3, was used to develop a screening method for cell behaviour upon exposure to soluble compounds, using automated and in situ image analysis. The platform was applied to assess the concentration-dependent response of an osteoblastic cell line exposed to a hypoxia mimicking molecule phenanthroline, using an in situ fluorescent staining assay in combination with image analysis, applicable to closed microfluidic devices. The on-chip assay showed that it was possible to determine differences in expressions between cells in different positions inside the microfluidic gradient, comparable to those observed in conventional culture, where a range of concentrations was tested in independent microwells. In the future this method is intended to complement or replace current research approaches in screening soluble compounds for RM.

This chapter is based on the publication: "Microfluidic Platform with Four Orthogonal and Overlapping Gradients for Soluble Compound Screening in Regenerative Medicine Research", Electrophoresis 2014

Soluble compound screening.

Soluble Compound Screening for Regenerative Medicine Research

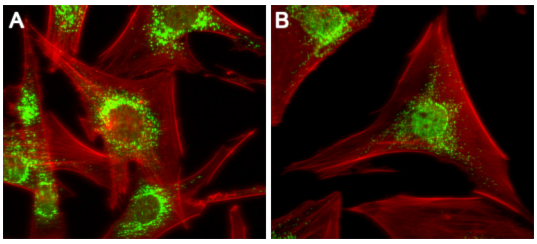

Fig. 5.1 Epi-fluorescence microscopy images of MG63 cells stained for HIF1α (green) and Phalloidin F-actin staining (red) in standard cell culture microwell plates. (A) Negative, non-induced state, where HIF1 only resides in the cytoplasm. (B) Upon 24 h exposure to 100 µM of Phenanthroline, HIF1 is induced and translocates to the nuclei, as shown by the shift of green fluorescence from the cytoplasm to the nuclei.

As a first proof-of-concept to show the applicability of the platform (Chapter 4) in regenerative medicine research, in this study, the concentration-dependent effects of phenanthroline were investigated. Phenanthroline is a compound previously shown by Doorn et al. to positively affect angiogenesis, i.e. new blood vessel formation, a process that is of great relevance for regeneration of most tissues and organs.[268] Specifically, vascularisation is of crucial importance in bone regenerative strategies, in particular for treatment of large bone defects.[269] Phenanthroline is a small molecule from the LOPAC library (Sigma) that was proposed as a relatively inexpensive and stable alternative to growth factors such as vascular endothelial growth factor (VEGF), in stimulating angiogenesis. Phenanthroline has been shown to induce hypoxia-inducible factor 1 (HIF1) expression in a dose dependent manner. HIF1 is a transcription factor expressed by mammalian cells when they are in a hypoxic (low oxygen) state. It plays an essential role in the systemic response to hypoxia and the release of angiogenic factors, including VEGF.[270] When hypoxia is induced in mammalian cells HIF1 translocates from the cytoplasm to the nucleus (Fig. 5.1), which can be visualised by HIF1 immunostaining. For the presented screen, we have used HIF1α immunostaining, a sub-unit of HIF1, followed by quantification of the level of translocation in each cell, by employing high content screening based on imaging algorithms and demonstrated that this can be a powerful *in situ* assay, which can be used in closed microfluidic systems.

Here we present a screening method that is based on the microfluidic platform of Chapter 4, to investigate in time the concentration-dependent effects of phenanthroline on a human osteoblastic cell line. The *in situ* screening routine was developed to analyse epi-fluorescence microscopy images to retrieve information at the single cell level in an automated way, using image analysis. The standalone chip holder (Chapter 3), which also functions as an incubator, was used to enable on-chip cell culture and *in situ* screening.[267] First, the image-based screening method was tested

using conventional microtiter plate cell culture. These results were then used as a starting point to test the method in the microfluidic platform.

5.1. Materials and methods

Cell culture

Human osteoblast-like MG63 cells were expanded and cultured in alpha minimal essential medium (αMEM 41061-029, Gibco) supplemented with 10% fetal bovine serum (FBS, Gibco), 100 $mg \cdot mL^{-1}$ penicillin and 100 $mg \cdot mL^{-1}$ streptomycin (Pen/Strep, Gibco). To determine the concentration range of interest, and to optimise the imaging analysis, MG-63 cells were first cultured in conventional well-plates. Therefore, cells were dissociated from the culture flask using 0.05% trypsin (Trypsin-EDTA, Gibco), seeded in a 96-well microtiter plate at a density of 3,000 $cells \cdot cm^{-2}$, and left to attach and proliferate using normal culture medium. For experiments in the microfluidic device, MG63 cells were dissociated in the same way, and resuspended to a concentration of approximately 5 million $cells \cdot mL^{-1}$. The suspension was injected into the device via the cell loading channel into the chamber using a 250 µL glass syringe. The cells were left to attach for 24 h, while flowing cell culture medium through the side channels at a flow rate of 8 $\mu L \cdot h^{-1}$, using four 500 µL syringes and a precision syringe pump (Nexus Performance, Chemyx, USA).

Phenanthroline, a hypoxia-mimicking small molecule

To test the cell response to hypoxia in the 96-well microtiter plate, after 48 h of regular culture, normal cell culture medium was replaced by culture medium supplemented with different concentrations of phenanthroline (1,10-Phenanthroline monohydrate, Sigma-Aldrich), ranging from 1.5 to 10 µM, prepared from a 1 mM stock solution in methanol (Sigma-Aldrich). The concentration was complemented with a negative, positive (100 µM) and secondary antibody (SAB) control, by leaving out the primary antibody. In the on-chip experiments, normal cell culture medium in the syringes was replaced after 24 h by medium with reduced serum concentration (1% FBS) for a period of 24 h. This was done to arrest the cell proliferation cycle, with the rationale to improve and equalise response, reducing expression differences among cells, since the number of cells in the chip was much lower than that in the wells of the microtiter plate. It also has the added advantage that MG63 cells stop migrating, therefore remaining in the same part of the gradient for the duration of the experiment. After 24 h in normal and 24 h in serum-reduced medium, reduced-serum medium supplemented with 10 µM phenanthroline was added in one syringe, to create a gradient from 2.9 to 2.3 µM inside the chamber (using a chip with diffusion channels of 2 µm width x 0.5 µm height predicted with FEM modelling: $D_{phenanthroline}$ = 620 $\mu m^2 \cdot s^{-1}$; Q = 12 $\mu L \cdot h^{-1}$; C = 10 µM).[271] This concentration range was

selected for being at the beginning of the slope of the S-curve (shape of a sigmoid function) where concentration-dependent effects of phenanthroline were observed in the well plate experiment (Fig. 5.2D).

Cell staining and imaging

After 24 h of exposure to phenanthroline in either the chip or in the well plate, cell culture was stopped and cells were fixed and stained. On-chip, first, the chamber was flushed through the access channels with phosphate buffered saline (PBS, Invitrogen), using a syringe, to remove medium. Subsequently, a 4% paraformaldehyde (PF, Sigma-Aldrich) solution was added for 10 minutes to fix the cells, after which the cells were permeabilised with 0.1 w/v % Triton-X for 4 minutes at 37°C. Following this, cells were stained with primary antibody Mouse anti-Human Anti-HIF1α (Abcam) to locate HIF1, which stains the alpha sub-unit of HIF1, for 2 h at 37°C; and secondary antibody Goat anti-Mouse IgG – Alexa Fluor 488 to stain the located HIF1α, for 1 h at 37°C. In addition, 4',6-diamidino-2-phenylindole (DAPI, Sigma-Aldrich) counter-stain was used, to stain the nuclei of the cells. Image acquisition was performed using an automated plate-reading epi-fluorescence microscope (BD Pathway 435, BD Biosciences, USA).

Image analysis

To analyse the results, high content screening and image recognition were used to locate the nucleus of each cell, based on DAPI stain, with high-content imaging software (CellProfiler, Broad Institute, USA). The localised and outlined nuclei were used as overlay on the HIF1α images (Fig. 5.2BC), and the average fluorescence intensity in the nuclei area was measured. When the transcription-factor HIF1 translocates into the nucleus, when the hypoxia pathway is induced, it is visible and measurable as a fluorescence intensity change of the HIF1α stain in the nucleus. By measuring the mean fluorescence intensity of each individual cell nucleus the level of translocation was determined for each concentration of phenanthroline. In the case of the on-chip experiments the nuclei stain was also used for normalizing the fluorescence intensity of the HIF1α stain, to reduce focal plane effects, since the cells in the grow in a 3D fashion. Graphs and statistics on the resulting data were performed using a statistical software package (SPSS, IBM, USA) and relevant tests were performed as described in the discussion section.

5.2. Results and discussion

Concentration-dependent effects of phenanthroline

MG63 cells cultured in 96-well plates were treated with phenanthroline in concentrations ranging from 1.5 to 10 μM for 24 h, in duplicates. A 3 by 3 montage epi-fluorescence microscopy image was taken at 200x magnification for each condition. Fig. 5.2A displays a zoom-in of these images. By plotting the mean fluorescence intensity of the nuclei over

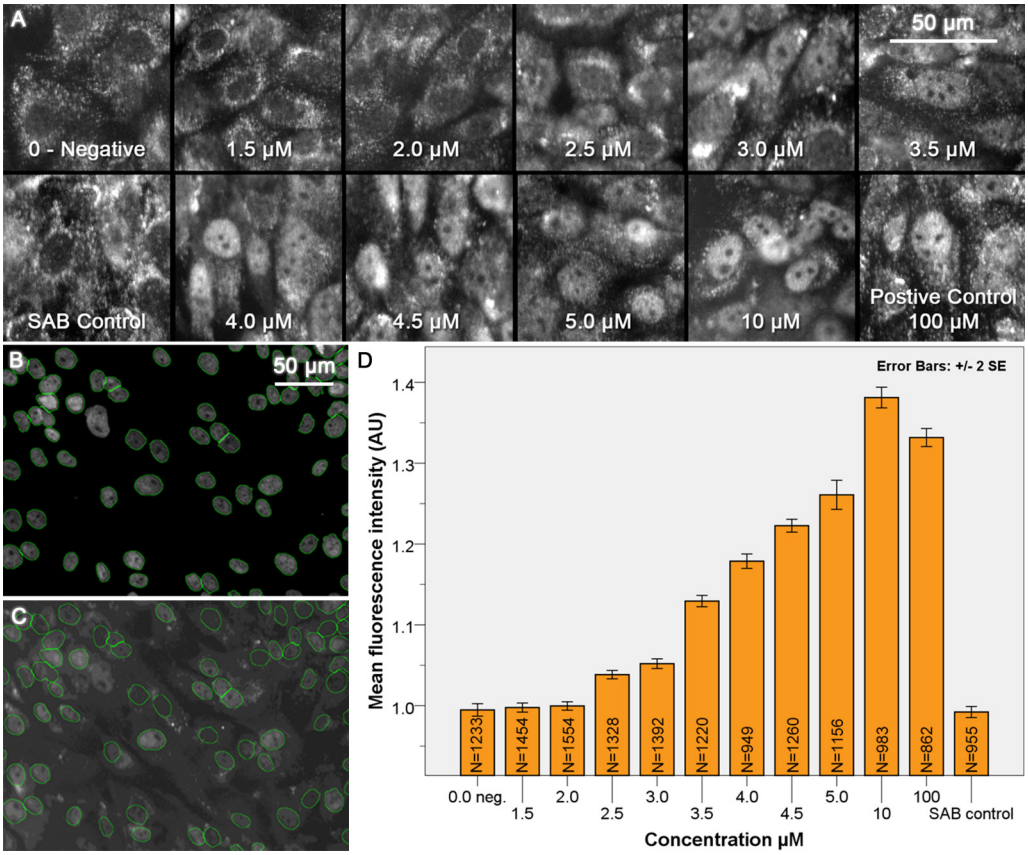

Fig. 5.2 (A) Close-ups of epi-fluorescence microscopy images taken from each of the concentration steps from the microtiter plate experiment. (B) Image analysis of cells treated with 10 µM phenanthroline, as an example, where the DAPI stain was used to visualise the nuclei, with surrounding lines depicting how the location of nuclei was determined. (C) HIF1α stain image of the same area with the overlay of the located nuclei, allowing for determination of the mean fluorescence intensity of the nuclei, and therefore the level of translocation. (D) Graph depicting the relative fluorescence intensity, normalised to the negative control, in arbitrary units (AU), inside the nuclei of the HIF1α staining as response to different concentrations of phenanthroline, including negative (0 µM), positive (100 µM) and secondary antibody (SAB) control.

the concentration, a concentration dependent effect was observed in the 2.5-10 µM range (Fig. 5.2D). All tested concentrations in the 2.5-100 µM range were significantly different from each other and the rest ($p < 0.05$). Only the experiments at 0 (negative control), 1.5 and 2.0 µM, and the secondary antibody (SAB) control did not show statistically different levels of translocation. These results translate into a dose dependent S-curve response to phenanthroline in the range of 2.5-10 µM. At concentrations of 100 µM and higher, the compound becomes cytotoxic and more cell death was observed (Fig. 5.2D), which could explain the reduction in average fluorescence intensity in the nuclei.

Effect of a microfluidic gradient of phenanthroline

Following the proof-of-principle experiments in microtiter plates, a phenanthroline gradient was generated in the microfluidic platform, using the steep part of the S-curve in the dose response of phenanthroline. Accordingly, the chip with diffusion channels of 0.5 µm x 1 µm was used. After 24 h exposure of a phenanthroline gradient (2.9-2.3 µM, from left to right, Fig. 5.3) MG63 cells the culture was stopped, and DAPI and HIF1α staining was performed. We observed that cells attached to both the bottom and the top of the chip, which is probably due to the fact that in a 3D microfluidic environment cells experience more forces from the walls, while the effect of gravity is negligible. Furthermore, such a confined environment is more favourable for the formation of multilayers than it is the case in a well plate. For this reason images were taken from both the bottom and top of the chamber. Furthermore, to avoid imaging difficulties, only non-overlapping cells were selected for the analysis, making the number of cells selected for the analysis lower than the total number of cells in the chip. Fig. 5.3 shows the resulting images after staining of cells upon exposure to the microfluidic gradient, with in A-C the top and in D-F the bottom of the chip. By applying a threshold of the intensity of the nucleus stain (Fig. 5.3A&D) the nuclei out of the focal plane of that layer were discarded, resulting in only located nuclei in focus (Fig. 5.3B&E). Further selection discarded the nuclei that were in a too close proximity to one another, out of focus, too large, too small, or on the edge of the image.

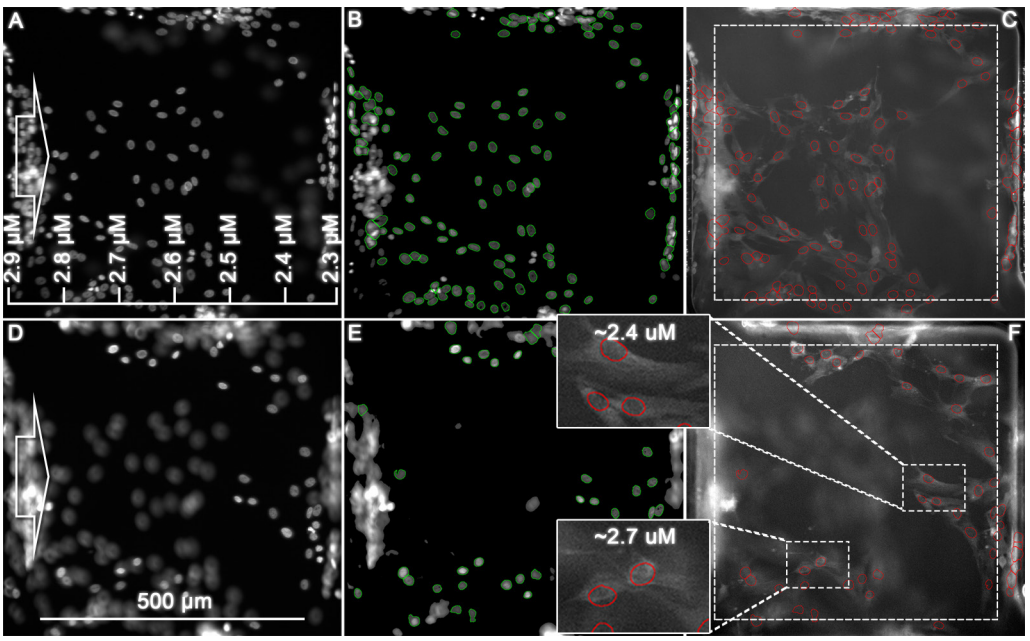

Fig. 5.3 HIF1α and DAPI stain images and analysis in the microfluidic device after 24 h of exposure to a phenanthroline gradient of 2.9-2.3 µM (arrows depict direction of the gradient). (A-C) Top and (D-F) bottom of the chamber. (F) Insets show cells where differences in intensity were measured.

From the image analysis, the remaining mean intensity values of the HIF1α stain in each cell nucleus were measured. This intensity was normalised for the nucleus stain intensity, to correct for focal differences between cells. All values 50 µm from the rim of the chamber (See dotted line Fig. 5.3C&F) were used for further analysis, and outliers were removed (2.5 x SD, 5 values removed), leaving N=119 cells. The values were then placed in a scatter plot for visualisation (Fig. 5.4). Statistical analysis of these data showed that increasing distance from the gradient source, thus decreasing concentration of phenanthroline, had a moderate negative 2-tailed correlation ($r = -0.237$, $P < 0.01$) with normalised HIF1α fluorescence intensity, and linear regression (thick line = regression line, dotted line = 95% confidence interval), as depicted in Fig. 5.4, demonstrated a significant negative relationship ($R^2 = 0.056$, $F(1,117) = 6.957$, $P < 0.01$). Although the number of cells is low compared to the conventional culture, and each cell is an experiment instead of treating the whole culture as an experiment, these results indicated that differences in response could be detected in a relatively shallow diffusive gradient of 2.9 to 2.3 µM in the microfluidic chip.

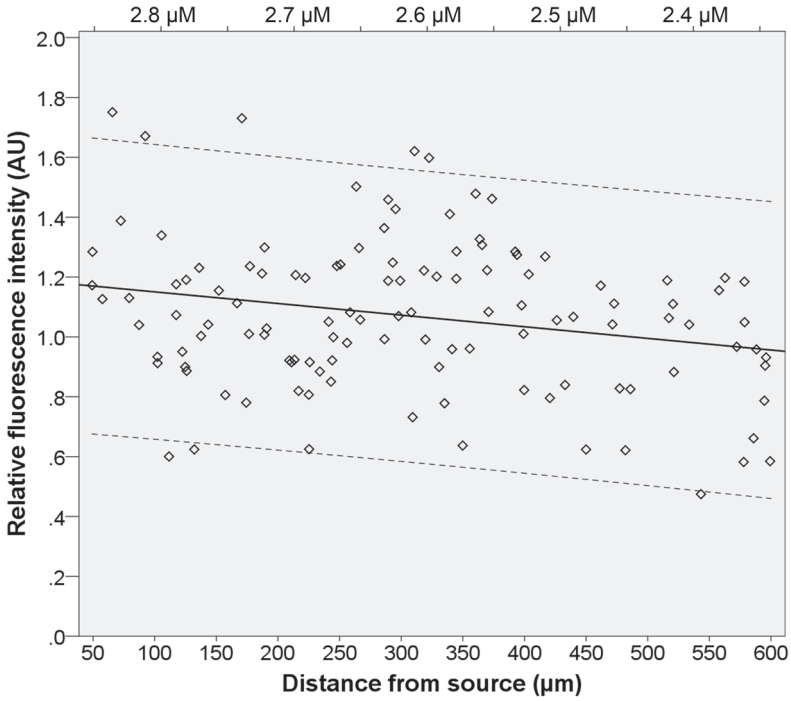

Fig. 5.4 Scatter plot depicting the mean fluorescence intensity of HIF1α stain in the nucleus of each cell (normalised with the DAPI stain) related to the distance from the gradient source. The thick line is the regression line with a moderate negative correlation ($r = -0.237$, $P < 0.01$) and significant negative relationship ($N=119$, $R^2 = 0.056$, $F(1,117) = 6.957$, $P < 0.01$). The dotted line depicts the 95% confidence interval.

5.3. Conclusion

In this study, the first steps were made towards screening of soluble compounds in a concentration-dependent manner applicable to the field of regenerative medicine. A proof-of-concept of the device was provided by testing the biological effect of one compound, in a microfluidic platform that is capable of generating four orthogonal and overlapping gradients. In the presented device, the gradient was relatively shallow, which precludes the study of compounds in which subtle concentration differences are effective, and which obviously still limits the analysis throughput if a large range of concentrations needs to be assessed. Therefore, a second-generation device is being developed, exhibiting a wider concentration gradient. Furthermore, due to this limitation in concentration range, applying the current device for testing combinations of compounds and assessing any synergistic effects is not straightforward, since a selection of concentration ranges for the different compounds needs to be made in advance. On other aspects, the number of cells in one cell culture chamber is low, and therefore challenging to yield statistically relevant data. In the future, this limitation can be addressed by using several identical chambers in parallel, run under the same experimental conditions. In addition to the microfluidic platform, this study was mainly aimed at developing an accompanying *in situ* image analysis method that allows time-lapse or real-time imaging of cell behaviour upon exposure to soluble compounds. In an initial experiment conducted in a microtiter plate, a routine was developed based on image analysis of nuclei and HIF1α staining to study concentration-dependent responses of mammalian cells to phenanthroline exposure. In a subsequent experiment, a comparable image analysis was performed in the microfluidic platform where a shallow gradient of phenanthroline was created, enabling testing of a given range of concentration in a single experiment. This second experiment demonstrated that the proposed method can be used to detect dose response differences inside a shallow diffusive gradient, while retaining the spatial information.

Acknowledgements
For this chapter I would like to thank Hugo Fernandes, then from the Tissue Regeneration department of the University of Twente, for advice and help on the development of the hypoxia assay.

6 Conclusions and outlook.

"The good thing about science is that it's true whether or not you believe in it."

Neil deGrasse Tyson

Conclusions and outlook on alternative applications and microfluidic gradients in regenerative medicine research

With the development of a chip holder that allows control over physiological conditions inside gas-impermeable devices, a multi-gradient microfluidic platform in which long-term cell culture can be performed and an assay and analysis routine to study cell behaviour in situ, it can be concluded that the main objectives of this thesis have been achieved. The screening method, however, still possesses a number of limitations: the gradient range that can be generated is relatively shallow and as a consequence, functional proof-of-concept for screening combined effects of different compounds could not been demonstrated yet. Furthermore, the number of cells is relatively limited to allow statistically powerful analysis of biological response. These limitations can be used as starting points for further development of the platform for use in RM research. In addition, new application areas for the platform with its highly versatile features should be explored.

Conclusions and outlook.

Conclusions an outlook on alternative applications and microfluidic gradients in regenerative medicine research

As stated in the introduction section, the aim of this thesis was the development of a strategy that enables screening of the biological effects of soluble factors on the behaviour of mammalian cells, for use in regenerative medicine (RM) research. To this end, the following requirements for the development of the platform were set: (i) screening cell behaviour in time; (ii) screening of concentration-dependent effects of individual soluble compounds as well as effects of combinations of compounds; (iii) *in situ* assay and analysis; and (iv) mimicking of the biological microenvironment.

In this chapter, the progress towards this aim is discussed, with an overview of the achievements as well as limitations of the platform developed. In addition, an outlook is given towards continuation of the platform development and its applications, as well as a more general view on the importance of use of microfluidic gradients in RM research.

6.1. Aim and objectives

Temporal screening

To allow temporal screening, a standalone chip holder was developed, as presented in Chapter 3. This chip holder enabled the use of microfluidic devices made from gas-impermeable materials for cell-based experiments, by allowing control over physical microenvironment properties, such as gas tension and temperature. Various adherent cell lines were tested and it was demonstrated that cell culture over a period of more than 5 days was possible, while continuously imaging the cells inside the microfluidic device. The control over the gas tension inside the microfluidic device was demonstrated by using a reporter cell line that fluoresces green when in a hypoxic state. Changing the oxygen content from normoxic to hypoxic, while culturing cells inside the glass chip was successful and the changes in cell behaviour could be monitored in real-time.

Concentration-dependent and combination screening

In Chapter 4, fluorescent dyes were used to show that the developed multi-gradient platform enabled generation of four simultaneous overlapping and orthogonal gradients inside the microfluidic culture chamber. A finite element model (FEM) was developed and verified using fluorescent gradients, demonstrating the ability to predict the gradient generation, and to determine the local concentration of each compound inside the culture chamber of the microfluidic device.

In the study described in Chapter 5, first steps were made towards a

method for screening biological effects on mammalian cells of soluble compounds in a concentration-dependent manner, by using the developed microfluidic platform. A proof-of-concept was provided by testing the effect of one compound, phenanthroline, on a human osteoblast-like cell line. Together with the developed *in situ* assay, which combines a fluorescent staining method with automated image analysis, cell response differences inside the diffusive gradient of phenanthroline were detected. This result was achieved while retaining the spatial information from the FEM, which enabled the correlation of cell response to the compound concentration.

The main limitation of the device presented in Chapter 5 is the relatively shallow concentration gradient, which still limits the analysis throughput, and precludes the study of compounds with subtler dose responses. For this reason a second generation device needs to be developed, in which a broader gradient can be created. To increase the gradient range the size of the diffusion channels (Chapter 3) could be increased, which, however, decreases gradient stability introduced by disturbances from, for example, pulsatile flow of the pump or moving of the tubing. More importantly, increase of the channel size may enable the cells to invade the channels, therefore blocking the gradient generation. The feature of the platform developed to test combinations of different compounds for synergistic effects, using the orthogonal and overlapping gradients, has not been tested in this thesis. To validate this feature, one should use compounds with known effects, effective in the concentration range of the gradient that can be generated inside the chamber.

Another limitation of the platform in its current form is the limited number of cells inside the chamber. Although the platform as such allows the collection of information for each individual with regard to time, location, concentration and combination, in order to draw conclusions regarding the biological effect, statistical data is needed from multiple cells under the same condition. In a single culture chamber, the combined information of all the cells can be used to determine a trend, but this does not yield statistically relevant information on different concentrations or combinations of compounds. This limitation can be addressed by using several identical chambers in parallel, in the same experimental conditions are kept. By clustering information from different chamber on individual cells or groups of cells that were exposed to identical compound concentrations or combinations, more powerful statistical information can be derived. This will still yield lower numbers compared to conventional culture, however, it should be emphasised that many different concentrations are tested within a single chamber, in contrast to the conventional culture in which one culture well is one condition.

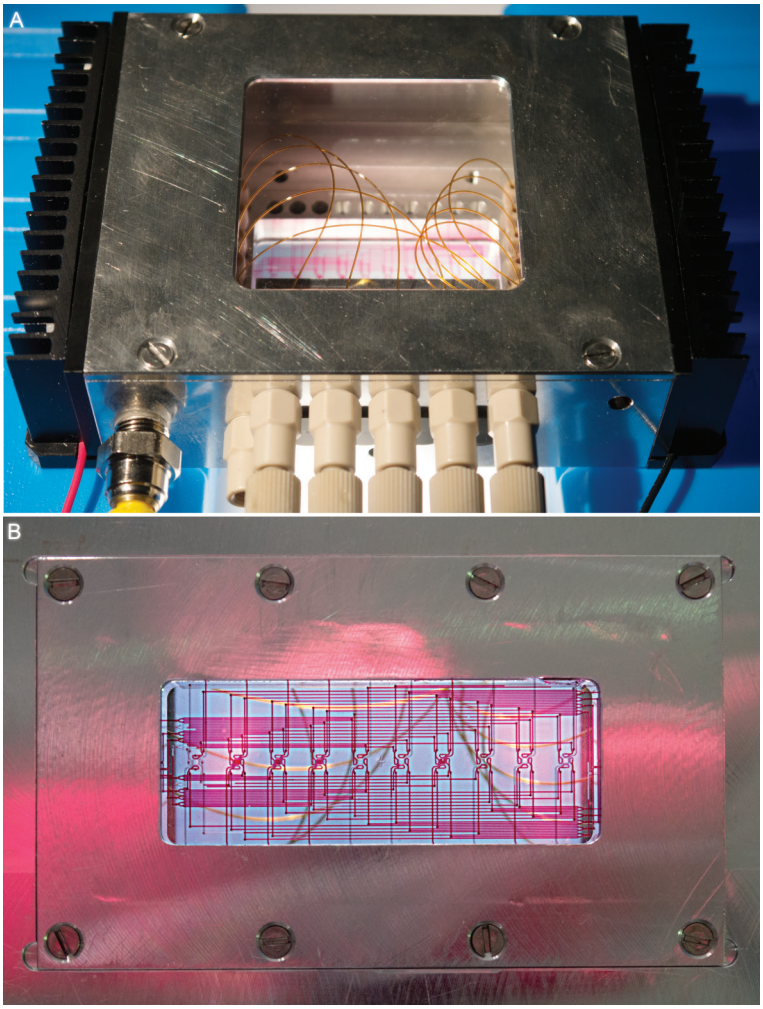

Fig. 6.1 (A) Picture of the chip holder for the 10 chamber microfluidic device (3 cm x 6 cm) with the ability for liquid handling using normal laboratory pipettes. (B) Photograph taken from the bottom of the chip holder, depicting the microfluidic device with the 10 larger chambers (1150 µm x 1150 µm), where the channels and chambers are made visible by using a red dye.

First steps towards the development of a multiplexed version of the platform have been undertaken, as is shown in Fig. 6.1. This platform was specifically designed without the use of complex valve systems, which require additional external pneumatic actuation. Supply of cells and liquids can be achieved by pipetting, avoiding complex syringe injection procedures. The platform consists of 10 similar, but larger (1150 µm x 1150 µm), culture chambers with broader gradients (about one order of magnitude). In each chamber, combinations of 4 different gradients can be created, comparable with the single-chamber platform. In total, supply of 5 different compounds is possible, yielding 5 unique combinations, which are created in duplicate.

***In situ* assay and analysis**

Since the main platform is a closed system, not allowing off-chip subsequent analysis without losing temporal and spatial information, an *in situ* assay needed to be developed. Different assays were successfully applied throughout this research. Readily applicable methods were employed, such as the use of reporter cell lines and *in situ* staining, shown in Chapter 3. In this study, a hypoxia responsive GFP cell line was used and could be imaged live while switching from oxygen-rich to oxygen-poor environment. Also a conventional live/dead fluorescent stain was applied, showing the possibility of *in situ* staining.

In addition to the microfluidic platform that enables *in situ* imaging and staining, an *in situ* imaging based analysis method was developed. In Chapter 5 a routine was presented based on image analysis of translocation of HIF1α stain from cytoplasm to nuclei, to study concentration-dependent responses of mammalian cells to phenanthroline. This removed human assessment and allowed per cell analysis, gaining more in-depth information on the response homogeneity. The results demonstrated that such a method could be used to detect dose response differences inside a shallow microfluidic gradient, while retaining spatial information.

Mimicking biological microenvironment

In general, an important advantage of microfluidics is considered to be the ability to tailor (biological) microenvironments with high fidelity, closely mimicking the *in vivo* situation. The biological microenvironment is a complex environment, which comprises different cell types surrounded by a milieu of physical and chemical signals. This environment is of great importance for the fate of the individual cell, as well as for communication among individual cells in the 3D environment of a tissue or organ.[15–17] Regarding the current platform, the experiments performed in the microfluidic chips (Chapter 3, 4 and 5) showed a distinct cell behaviour as compared to conventional tissue plastic cell culture. The cells tend to readily attach and grow on the bottom and "ceiling" of the devices, making image analysis more complex, but, on the other hand, naturally generating matrix in a 3D fashion, which more closely resembles the intrinsic 3D biological environment than cell monolayer in conventional 2D structure. Furthermore, the ability to closely control the gas tension, like oxygen content inside the microfluidic device aids the mimicking of the natural biological microenvironment making the oxygen distribution around a cell more closely resembling that of natural tissue, than is the case in conventional culture with air-saturated oxygen.[73]

In conclusion, the results of this thesis showed that, by using the platform presented here, it is possible to obtain and study concentration-dependent biological response of mammalian cells to soluble compounds in a closed

device. This last aspect is particularly important for further development of the platform by introducing relevant biomaterials, which are widely used in the field of regenerative medicine. Although screening of combined effects of multiple compounds has not been demonstrated yet, the platform is promising, but it requires further investigation in combination with a second-generation microfluidic platform, with a larger gradient range and more cells.

The optimised image-based assay and analysis method are readily applicable in both the conventional culture and any closed microfluidic device, making it a valuable tool for obtaining more in-depth information on the culture. The method generates data for each individual cell, in a reproducible and unbiased way, as compared to human visual inspection, making the data more readily comparable to other culture methods.

6.2. Outlook

Alternative platform applications

The platform presented here was developed with the aim to screen soluble compounds for regenerative medicine research. Nevertheless, its unique features make it applicable to many other research settings, which could be as interesting as the screening of soluble factors on mammalian cells. A number of attempts to use the platform for other applications are described here.

The aim of the first experiment, performed in collaboration with Eindhoven University of Technology, was to use the platform to spatially control and study nucleation and growth of calcium carbonate crystals, a widely studied topic in the field of biomineralisation. When mixing high concentration aqueous solutions of sodium carbonate (Na_2CO_3) and calcium chloride ($CaCl_2$), the reaction is virtually instantaneous and the resultant calcium carbonate will immediately precipitate. The exact process through which final, stable crystalline mineral phases are formed is still a topic of extensive study, in part because experiments that rely on bulk mixing of the solutions are poorly controlled. In the experiment performed here using the microfluidic gradient platform, solutions of 1M Na_2CO_3 and 1M $CaCl_2$ at neutral pH were introduced into the microfluidic chamber through arrays of channels on opposite sides (Fig. 6.2). The following reaction occurs when calcium carbonate is formed:

$$Na_2CO_{3(aq)} + CaCl_{2(aq)} \rightarrow CaCO_{3(s)} + 2\ NaCl_{(aq)} \qquad (6.8)$$

Since the microfluidic chip was made of high purity glass, carefully cleaned using Piranha solution (H_2O_2 + H_2SO_4), and all chemicals were of ultrapure chemical grade, the number of nucleation sites was reduced to a minimum.

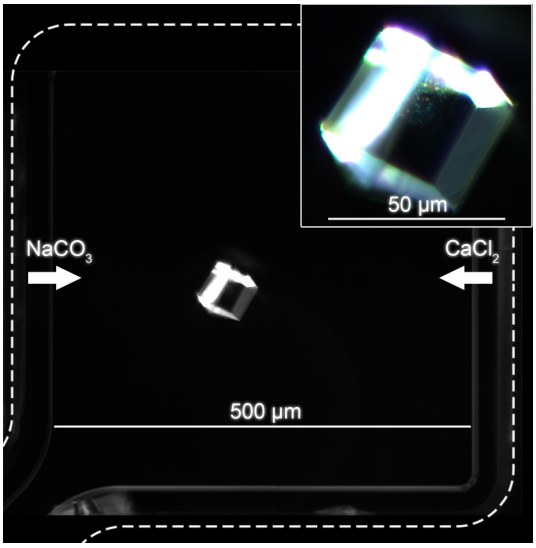

Fig. 6.2 Optical dark-field microscopy image of 'single' crystal growth after 72 h flowing 1M Na_2CO_3 (left) and 1M $CaCl_2$ (right) solutions through the side channels.

Since both solutions entered the chamber solely by diffusion, advective disturbances were eliminated, extending the reaction from one second to several days. To image the reaction in the chip, optical dark-field microscopy was used, which employs the refraction properties of the material to register small refraction changes even for sub-wavelength particles.

Although not verified in multiple experiments or through follow-up analyses, tiny particle spots were observed in the chip after a few hours that continuously appeared and disappeared over time. This phenomenon is extensively studied in fundamental crystallography, following the hypothesis that different crystals are formed by dissolution and reprecipitation of amorphous nanoparticles. When a crystal eventually reaches a critical size, dissolution does not occur anymore, leading to crystal growth, by the uptake of the surrounding dissolved nanoparticles.[272–275] In the experiment presented here eventually one cube-shaped crystal formed in the middle of the chamber (Fig. 6.2), which, after 72 h of the experiment, had a size of about 30 µm. Based on the crystal shape and double refraction it is suggested that the crystal phase is calcite, which is also the most thermodynamically stable form of calcium carbonate.[273] This could not be verified since the current design of the microfluidic device is closed, not allowing subsequent physicochemical analysis. Nevertheless, this result suggests the potential of the platform for use in biomineralisation studies.

While biomineralisation as such is a highly interesting research field, results from these types of studies can also be of great use for regenerative medicine strategies, with emphasis on skeletal tissue, which for 60 wt% consists of calcium phosphate. Crystal formation in living tissues is known to be guided or influenced by proteins or bioinorganics in trace amounts. By using the microfluidic platform developed here, the effects on crystal formation of multiple of such compounds, alone or in combinations can be studied. An additional interesting feature is the possibility of controlling temperature inside the chip, which is another well-known factor influencing mineral formation. An example of a study in which microfluidic gradient generation was used to study the process of biomineralisation is the one by

Ji and co-workers,[276] who demonstrated the control over calcium carbonate crystal formation by using an extra-pallial (EP) protein, which is involved in the shell formation of molluscs. In their study, the authors used a flow-based T-cell (Chapter 1 for more information), which enables testing of two compounds in opposing concentration gradients, with a third compound as background. The device presented in this thesis could provide the third (and fourth) compound as an orthogonal concentration gradient, all in a solely diffusive manner. Another interesting application of the platform could be study on the effect of various cations and anions on crystal formation, for example through ionic substitution in crystal lattice.[277]

3D gradient generation

Aiming at a closed system, with close control over the design features, the microfluidic chip presented in this thesis was made in glass. Nevertheless, for the future, it would be advantageous to produce the device in a material that is more familiar to biologists, and that enables production in larger quantities against lower cost, such as polystyrene. An additional advantage of such a material is that it can easily be shaped in any form providing an even better control over the 3D microenvironment.

In collaboration with Karlsruhe Institute of Technology (KIT), first attempts were made to create three-dimensional microfluidic devices with localised gradient generation. The device was entirely made in polymer, by applying different techniques (Fig. 6.3). By combining an imprinted channel array, shaped into a cavity by thermal forming (Fig. 6.3A Inset), with a partially porous membrane, multiple localised diffusion sources were created in 3D fashion. The partially porous membrane was produced by partially track-etching an ion-irradiated polymer film by masking the required non-porous areas. The different parts and covers were then glued together. The device is designed such that all the imprinted channels are individually addressable, making it possible to make different chemical cues in different parts of

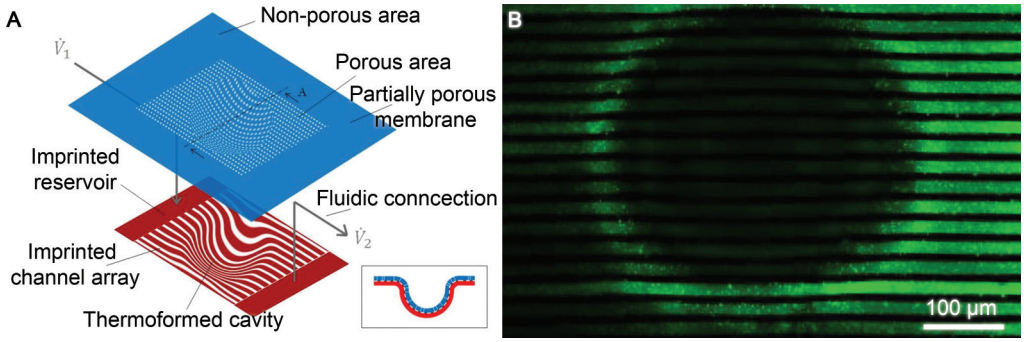

Fig. 6.3 (A) Schematic representation of the different layers of the 3D microfluidic gradient generation device. The inset shows a longitudinal cut-through of the same device. (B) Fluorescent microscopy image of the device while flowing fluorescein through the imprinted channels. Courtesy of Karlsruhe Institute of Technology (KIT).

the cavity. This type of device could be used to study, for instance, cell migration in 3D structures by chemotaxis, or organisation and development of tissues in 3D, in a process called morphogenesis, which is governed by locally secreted signalling molecules, named morphogens (see Chapter 1 for more information on these processes).

6.3. Future of microfluidics in RM research, a personal view

Many microfluidic systems remain too complex to be easily implemented in the field of RM (or biology in general), which is often sceptical, or at best hesitant when it comes to applying new research methods and tools from other fields. This is mainly due to uncertainty when it comes to inter-research reproducibility and comparison to other methods. Methods based on microfluidics do not always take into account the fundamental requirements for biological experiments, and need specialised knowledge to operate, modify and interpret the data. One reason could be that engineers and biologists do not always understand each other's passions, desires and needs. However, the awareness exists and it is growing, as is witnessed by interesting titles of articles, like "Engineers are from PDMS-land, Biologists are from Polystyrenia",[248] and conferences, like Micro- and Nanofluidics for Cell Biology,[278] where engineers and biologists get the chance to meet. Nowadays, biologists are invited to join the traditionally engineering-oriented microfluidics groups, and micro- nanotechnology engineers become a clear asset to classical biology-oriented groups. Referring to the aim of this thesis, this endeavour was not only about finding an alternative for soluble factor screening, but also finding a place for such systems in a RM research environment. From my point of view, as a biomedical engineer, the most important ingredients for successful application of microfluidics in RM research remain dedication, personal as well as monetary capital and appreciation for biology, the science in general as well as the scientist as a person.

Acknowledgements

For this chapter I would like to thank Vladimir Dmitrovic, from the University of Eindhoven, for advice on the calcium carbonate experiments, and Martina Cihova and Stefan Giselbrecht, from Karlsruhe Institute of Technology (KIT), and Roman Truckenmüller, from the University of Twente, for the images on the 3D microfluidic gradient device.

7 Acknowledgements.

"No one who achieves success does so without acknowledging the help of others. The wise and confident acknowledge this help with gratitude."

Alfred North Whitehead

Acknowledgements.

Some words of gratitude

First of all I want to thank Pamela Habibovic for the opportunity to do my doctoral research in her group, and Clemens van Blitterswijk of being part of his department, Tissue Regeneration (TR). Pamela, I want to thank you for giving me the space and responsibility to find my own path in research. Our collaboration did have its twists, but it did deliver this thesis with an already cited review, two well received papers, and a chapter for an important book series we can barely afford ourselves. For the many hours of work for that chapter we received a generous donation, which we spent on a group dinner, luckily we were only with four at that time. Clemens, although we did not speak to each other often, the few times we did I enjoyed the discussions we had. I would also like to thank you for your efforts to show my research, and that of my fellow TR members, around the globe in your numerous presentations.

For this thesis, I have to equally thank Séverine Le Gac, from the BIOS Lab-on-a-Chip group. Séverine, without your efforts this thesis was not imaginable. Thank you for the great time, discussions and dinners in Montreux (Nanotech, Switzerland) and on Jeju-Do (μTAS, South Korea), and introducing me to interesting people in and outside the Lab-on-a-Chip field.

From the TR group I would like to thank everybody for the great time, discussions, drinks, complaints, and more. It was a pleasure working with you. In particular I want to thank the members of Pamela's group: Ana Barradas, Anand Kumar, Ana Rodriques, Charlène Danoux, David Barata, Niloofar Tahmasebi and Ziryan Othman. Charlène, thank you for being my officemate for most of my time in TR. We both started around the same time, and although we are two very different persons, we got along very well from the beginning. Thank you for all the discussions about work, life and other important stuff. Don't forget: life is not always a big pink fluffy bunny! Good luck with the finalising your thesis. David, you are the continuation to this research, thank you for your help and enthusiasm. I wish you all the best and success finishing your own research and thesis. Furthermore, I would like to thank Roman Truckenmüller for your tireless input and ideas in research, and beyond. Hugo Fernandes, for your tremendous help and insight on the hypoxia assays. Lorenzo Moroni, for your advice, and off course the company at numerous salsa parties, in competition or fun. Jan de Boer, although at first I thought we would be two worlds apart, I found out the exact opposite, thank you for sharing your ideas on future research and the philosophical discussions from biology to astrophysics.

During my time at TR I rented out rooms in my house to other PhD fellows, therefore I made many new friends from around the world, better known as my Pathmos family. Thank you: Dietrich (Didi) Kohlheyer for helping me lay the tiles of my terrace and the *Michelin* star dinners; Giovane (Gio) Moura for teaching me the Portuguese words that matter, asking me difficult questions about Dutch culture, and teaching me about yours; Ignacio (Nacho) Hernández Vera giving me insight in the great cultural heritage of Spain by teaching me the Paquito Chocolatero; Sebastian Lipari for changing your favourite football team to FC Twente (for a day); Alicia Martinez for doing me on the *Wii*® (I'm talking about bowling), and the many serious and funny conversations we had; Adithya (minions-have-spawned) Sridhar for teaching me another language (British), and the great philosophical discussions on subjects that matter to the both of us; Rui (Rio) Carvalho, for being a great friend, inviting me to your home in Portugal and teaching me there is always a smaller place than Enschede; Paul (Half-Weird) Wieringa, for the numerous discussions about work and life, while enjoying a fine frosty brew. I love gooold!; Ana Rodrigues and Sara Neves, for teaching me everything about Portugal there is to know; Giuseppe (Princess) Criscenti, for teaching me the Italian way; Alessia Longoni, although we were only housemates for a short time, I really enjoyed our late night talks. Good luck with your future career!; João Crispim and Vanessa Florant, the latest additions to the Pathmos family, we are already having a lot of fun, let's keep on doing that for the foreseeable future.

Mijn familie: Henk Jan, Itie, Manoj, Ishanka, Dennis and Chamali. Pa, wij hebben samen een uitdagende tijd gehad het afgelopen jaar. Voor mij is een nieuwe tijd aangebroken, deze tijd zal voor jou ook snel aanbreken, daar geloof ik in, nu jij nog. Ma, ook jij hebt een aantal leuke en minder leuke uitdagingen gehad afgelopen jaren. Bedankt voor je steun en dat je altijd het positieve de boventoon hebt laten voeren. Manoj, bedankt voor de wederdienst om mij mee te nemen naar een aantal van jou studentenfeesten en de altijd memorabele gezamenlijke verjaardagsfeesten de afgelopen jaren. Ishanka en Dennis, bedankt voor de heerlijke etentjes die voor de noodzakelijke afleiding hebben gezorgd. Chamali, je kunt het misschien nog niet lezen, maar ook jou moet bedanken, je brengt altijd een lach op mijn gezicht als ik je zie.

Also, thank you brew-masters, 1nists and support-crew: Bart Fischer, Corina Ghebes, Febriyani Damanik, Giovane Moura, Jörg Dahlhaus, Juan Amiguet, Michiel Kooiman, Nils Auffermann, Rui Carvalho and Vincent Kickert.

Finally, thank you Dr. Pieter de Jong en Dr. Tim Gorter, for the 'quality' discussions on the couch in the TG building. Tim, thank you in return for all the support, as you can see mine is finally ready too!

I thought I said 'Finally'. OK, since you flipped the page and are still reading, I still need to thank two more important people:

Burcu Çelikkol and Ioana (Nana) Ilie.

Burcu and Nana, without you two the last two years would have been unimaginable. The mojito conferences, dinners and retreats, in your company, are to thank for that. I wish you both good luck with your respective theses and future plans, and I hope there will be numerous more mojito conferences in the future.

Now the real one: Finally, I would like to thank the University Council of 2010-2012 and the PhD Network University of Twente (P-NUT) for a great time. Especially, I would like to thank all the P-NUT old-farts: Anja, Moshin, Nana, Adithya, Burcu, Febriyani, Rong, Parinaz, Mitra, Rense, Harmen, Victor, Juan Carlos, Juan, Bijoy, Giovane, Silja, Raja, Nicole, Josine, Sérgio, Nikolay, Shashank, Anika, Aimee, Nicolas, Maryana and Marije.

To all of you reading this, and I did not mention you by name, probably you have been a part of my life the past few years, somewhere, sometime. That does not mean that I forgot about you. I would like to thank you as well for being part of my life, without you I would not have come this far.

Bedankt!

Thanks!

Danke!

Obrigado!

Gracias!

Grazie!

Merci!

Makasih!

நன்ற ?

با تشکر

8 In short.

"A moral lesson is better expressed in short sayings than in long discourse."

Johann Georg Ritter von Zimmermann

In short.

Summary of this work in English and Dutch

8.1. Summary

This thesis presents a novel method for screening effects of soluble factors on the behaviour of mammalian cells that has been developed as an alternative to the classical candidate approach in regenerative medicine (RM) research. The method covers the entire route from the development of a cell culture platform, to biological assay optimisation and data analysis. The method is based on a microfluidic multi-gradient platform that is capable of temporal screening, combination and concentration screening, in situ assay and analysis, and mimicking of the biological microenvironment.

Chapter 1 – Introduction
The aim of RM is to restore or establish normal function of damaged tissues or organs, using cell therapy, tissue engineered constructs and synthetic graft substitutes. Since the population of the western world is ageing, there is an increasing need for RM therapies, which are readily available in large quantities. In general, the search for such strategies is based on the candidate approach, in which a limited number of candidates (e.g. biomaterials, growth factors and cells) are selected, based on a rationale. As a result, a limited number of candidates is investigated, and therefore development and clinical implementation of novel, significantly improved strategies is relatively slow. Microfluidics is a field that offers new tools to accelerate progress in RM research, by enabling higher throughput of screening through parallelisation, miniaturisation, and tailoring of a physical and chemical microenvironment. One such a tool is the use of microfluidic concentration gradients that can be generated using flow- or diffusion-based techniques.

Chapter 2 – Regeneration-on-a-Chip?
Currently, tremendous efforts are made in development of novel regenerative strategies, which are becoming increasingly important as a consequence of ageing. To facilitate accelerated development of new strategies, fast and reliable assessment of (biological) performance is sought for, not only to select the potentially promising candidates, but also to rule out poor ones at an early stage of development. Microfluidics can provide the tools to accelerate RM research, as proven in its maturity for the realisation of high-throughput screening platforms. In addition, microfluidic systems are suitable for recreating *in vivo*-like microenvironments. Application of microfluidics to RM research is, however, a challenging process. One needs to take into account the complexity of organs or tissues that need to be regenerated, but also the complexity of regenerative strategies themselves.

The question therefore arises whether so much complexity can be integrated into microfluidic systems without compromising reliability and throughput of assays.

Chapter 3 – Standalone microfluidic cell culture
In Chapter 3, the development of a microtiter plate-sized standalone chip holder is presented that allows for precise control of physiological conditions inside closed microfluidic cell culture systems, made from gas-impermeable materials. The suitability of the standalone chip holder to support cell growth was demonstrated in a closed gas-impermeable glass chip, while performing time-lapse imaging. The viability of the cells was tested with a live/dead stain, demonstrating the ability to perform in situ assays. To investigate the ability to change the gas tension inside the chip, a hypoxia responsive reporter cell line was used, and imaged before and after changing the gas environment from normal to hypoxic condition. The chip holder has been found suitable for performing cell-based *in vitro* experiments in closed microfluidic devices.

Chapter 4 – Orthogonal multi-gradient screening
In Chapter 4, the development of a multi-gradient microfluidic platform is presented, which can generate four orthogonal and overlapping concentration gradients of soluble compounds. The device includes a square chamber, in which adherent cells can be grown, and four independent supply channels along the sides of the chamber, which are connected through small diffusion channels. Compounds introduced through the supply channels diffuse through the diffusion channels into the chamber, to create a gradient inside the chamber. Further, the chamber is connected to two channels intended for introduction of cells and in situ staining. The dimensions of the different channels were optimised through finite element modelling. Upon fabrication, the chip was used to validate the finite element model by generating and analysing gradients of fluorescent dyes.

Chapter 5 – Soluble compound screening
In Chapter 5, the microfluidic platform from Chapter 4, combined with the chip holder from Chapter 3, was used to develop a screening method for cell behaviour upon exposure to soluble compounds, using automated and in situ image analysis. The platform was applied to assess the concentration-dependent response of an osteoblastic cell line exposed to a hypoxia mimicking molecule phenanthroline, using an in situ fluorescent staining assay in combination with image analysis, applicable to closed microfluidic devices. The on-chip assay showed that it was possible to determine differences in expressions between cells in different positions inside the microfluidic gradient, comparable to those observed in conventional culture, where a range of concentrations was tested in independent microwells.

In the future this method is intended to complement or replace current research approaches in screening soluble compounds for RM.

Chapter 6 – Conclusion and outlook
With the development of a chip holder that allows control over physiological conditions inside gas-impermeable devices, a multi-gradient microfluidic platform in which long-term cell culture can be performed and an assay and analysis routine to study cell behaviour in situ, it can be concluded that the main objectives of this thesis have been achieved. The screening method, however, still possesses a number of limitations: the gradient range that can be generated is relatively shallow and as a consequence, functional proof-of-concept for screening combined effects of different compounds could not been demonstrated yet. Furthermore, the number of cells is relatively limited to allow statistically powerful analysis of biological response. These limitations can be used as starting points for further development of the platform for use in RM research. In addition, new application areas for the platform with its highly versatile features should be explored.

8.2. Samenvatting

In dit proefschrift wordt een nieuwe methode beschreven voor het screenen van het effect van oplosbare factoren op het gedrag van zoogdiercellen, ter vervanging van de gebruikelijke kandidaat-aanpak in regeneratieve geneeskunde (RG) onderzoek. Deze methode omvat het hele traject, van de ontwikkeling van een celkweek platform, tot aan de biologisch assay en gegevensanalyse. De methode is gebaseerd op een microfluïdisch multi-gradiënt platform dat in staat is om tijdsafhankelijk combinaties en concentraties van factoren te screenen. Daarnaast is het platform ook geschikt voor het nabootsen van de biologisch micro-omgeving en voor het uitvoeren van in situ assays.

Hoofdstuk 1 – Introductie
Het doel van RG is het herstellen van de functie van beschadigde weefsels en organen, door middel van celtherapie, synthetische weefsel constructen en transplantaat substituten. Aangezien de bevolking van de westerse wereld vergrijst, is er een toenemende behoefte aan RG therapieën die snel en in grote hoeveelheden beschikbaar zijn. In het algemeen is het zoeken naar dergelijke strategieën gebaseerd op de kandidaat-aanpak, waarbij een beperkt aantal kandidaten (e.g. biomaterialen, groeifactoren, cellen) zijn geselecteerd op basis van een redenering. Hierdoor wordt een beperkt aantal kandidaten onderzocht en derhalve verloopt de ontwikkeling en klinische implementatie van nieuwe verbeterde strategieën relatief traag. Microfluidica is een gebied dat nieuwe mogelijkheden biedt om de vooruitgang in RG onderzoek te versnellen, door de screening doorvoer te versnellen door middel van parallellisatie, miniaturisatie, en het afstemmen

van een fysische en chemische micro-omgeving. Een van de mogelijkheden is het gebruik van microfluïdische concentratie gradiënten die kunnen worden gegenereerd met behulp van perfusie of diffusie-gebaseerde technieken.

Hoofdstuk 2 – Regeneratie-in-een-Chip
Momenteel worden enorme inspanningen gedaan in de ontwikkeling van nieuwe regeneratieve strategieën, gezien die steeds belangrijker worden als gevolg van de vergrijzing. Om de ontwikkeling van nieuwe strategieën te versnellen is snelle en betrouwbare evaluatie nodig ter beoordeling van de (biologische) prestatie, niet alleen om het potentieel veelbelovende kandidaten te selecteren, maar vooral om slechte kandidaten in een vroeg stadium van de ontwikkeling uit te sluiten. Microfluidica kan de tools bieden om RG onderzoek te versnellen, zoals bewezen in de ontwikkeling en realisatie van high-throughput screening platformen. Bovendien zijn microfluïdische systemen in staat de *in vivo* micro-omgeving na te bootsen. Het toepassen van microfluïdische systemen in RG onderzoek is echter een uitdagend proces. Men moet rekening houden met de complexiteit van organen, of weefsels, die moeten worden geregenereerd, maar ook met de complexiteit van regeneratieve strategieën zelf. De vraag is of zo veel complexiteit in microfluïdische systemen kan worden geïntegreerd, zonder afbreuk te doen aan de betrouwbaarheid en de doorvoer van assays.

Hoofdstuk 3 – Standalone microfluïdisch celkweek systeem
In hoofdstuk 3 wordt de ontwikkeling van een standalone chip houder, met het formaat van een microtiterplaat, beschreven dat in staat is nauwkeurig de fysiologische omstandigheden te beheersen in gesloten microfluïdisch celkweek systemen, gemaakt van niet gasdoorlatend materiaal. De geschiktheid van de standalone chip houder voor celkweek werd aangetoond in een gesloten, niet gasdoorlaatbare, glazen chip door middel van time-lapse microscopie. De levensvatbaarheid van de cellen werd getest met een zogenaamde levend/dood assay, wat tevens de geschiktheid van in situ testen aantoonde. Om te onderzoeken of de gasdruk in de chip geregeld kan worden, is een hypoxie (zuurstofgebrek) reporter cellijn gebruikt en het resultaat voor en na het veranderen van de gasomgeving vergeleken, van normale naar hypoxische toestand. De chip houder is geschikt bevonden voor het uitvoeren van cel-gebaseerde *in vitro* experimenten in een gesloten microfluïdische systeem.

Hoofdstuk 4 – Orthogonaal multi-gradiënt screening
In hoofdstuk 4 wordt de ontwikkeling van een multi-gradiënt microfluïdische platform beschreven, waarin vier orthogonale en overlappende concentratiegradiënten van oplosbare factoren kunnen worden gegenereerd. Het platform omvat een vierkante ruimte, waarin hechtende cellen kunnen worden gekweekt, en vier onafhankelijke toevoerkanalen langs de

zijwanden van de kamer, die verbonden zijn met de kamer door middel van kleine diffusie-kanalen. Factoren die door de toevoerkanalen stromen diffunderen door de diffusie-kanalen in de celkweekkamer, waardoor een concentratiegradiënt ontstaat. Daarnaast is de kamer verbonden met twee kanalen voor het inbrengen van cellen en in situ kleuring. De afmetingen van de verschillende kanalen zijn geoptimaliseerd door eindige elementen modellering. Na vervaardiging werd de chip gebruikt om het eindige elementen model te valideren door het genereren en analyseren van gradiënten van fluorescente kleurstoffen.

Hoofdstuk 5 – Oplosbare factor screening
In hoofdstuk 5 is het microfluïdische platform van hoofdstuk 4, in combinatie met de chip houder uit hoofdstuk 3, gebruikt om een screening methode te ontwikkelen om het gedrag van cellen te bestuderen bij blootstelling aan verschillende oplosbare factoren, met behulp van geautomatiseerde en in situ beeldanalyse. Het platform werd gebruikt om de concentratie-afhankelijke respons van een osteoblast cellijn, blootgesteld aan het molecule fenantroline dat hypoxie kan nabootsen, te bestuderen met behulp van een in situ fluorescerende assay in combinatie met beeldanalyse, specifiek voor gesloten microfluïdische systemen. Uit de on-chip analyse bleek dat het mogelijk was om verschillen in expressie vast te stellen tussen cellen in verschillende posities in het microfluïdische gradiënt, vergelijkbaar met die waargenomen in conventionele kweek, waarbij een reeks concentraties werd getest in onafhankelijke microwells. Deze methode is bedoeld om in de toekomst te dienen als aanvulling of vervanging van de huidige aanpak van het screenen van oplosbare factoren voor RG onderzoek.

Hoofdstuk 6 – Conclusies en vooruitzicht
Met de ontwikkeling van een chip houder die de fysiologische omstandigheden in niet gasdoorlaatbare microfluïdische systemen kan beheersen, een multi-gradiënt microfluïdisch platform waarin langdurige celkweek kan worden uitgevoerd met een assay en analyse routine die het in situ cel gedrag kan bestuderen, kan worden geconcludeerd dat de belangrijkste doelstellingen van dit proefschrift zijn bereikt. Het screening platform heeft echter nog een aantal beperkingen: het gradiënt bereik is beperkt en dientengevolge kan een functioneel proof-of-concept experiment voor het screenen van gecombineerde effecten van verschillende factoren, nog niet worden uitgevoerd. Bovendien is het aantal cellen relatief laag om sterke statistisch analyse van een biologische respons mogelijk te maken. Deze beperkingen kunnen worden gebruikt als uitgangspunten voor de doorontwikkeling van het platform voor gebruik in RG onderzoek. Daarnaast moeten nieuwe toepassingsgebieden voor het platform, met zijn zeer veelzijdige mogelijkheden, worden verkend.

9 Lists.

"The list is the origin of culture. It's part of the history of art and literature. What does culture want? To make infinity comprehensible. It also wants to create order."

Umberto Eco

Lists.

List of publications and figures

9.1. Publications

Journal papers

2014

Microfluidic platform with four orthogonal and overlapping gradients for soluble compound screening in regenerative medicine research
Björn Harink, Séverine Le Gac, David Barata, Clemens van Blitterswijk, and Pamela Habibovic
Electrophoresis, 2014, DOI: 10.1002/ELPS.201400286

Microtiter plate-sized standalone chip holder for microenvironmental physiological control in gas-impermeable microfluidic devices
Björn Harink, Séverine Le Gac, David Barata, Clemens van Blitterswijk, and Pamela Habibovic
Lab Chip, 2014, DOI: 10.1039/C4LC00190G

2013

Regeneration-on-a-Chip? The Perspectives on Use of Microfluidics in Regenerative Medicine
Björn Harink, Séverine Le Gac, Roman Truckenmüller, Clemens van Blitterswijk, and Pamela Habibovic
Lab Chip, 2013, DOI: 10.1039/C3LC50293G

Book contributions

2011

Calcium Phosphate Ceramics with Inorganic Additives
Comprehensive Biomaterials by *Paul Ducheyne*, Volume 1, Chapter 18
Liang Yang, Björn Harink, and Pamela Habibovic
Oxford: Elsevier, 2011, ISBN: 978-0-08-055294-1

International conference proceedings

2012

Microfluidic Platform for Combinatorial Biochemistry and Biomaterials Research
Björn Harink, David Barata, Clemens van Blitterswijk, and Pamela Habibovic
BioNanoTech 2012 in Montreux, Switserland

Microfluidic Platform for Simultaneous Generation of Four Independent Gradients: Towards High Throughput Screening in Bone Tissue Engineering
Björn Harink, Clemens van Blitterswijk, and Pamela Habibovic
9th World Biomaterials Congress 2012 in Chengdu, China

2011

Microfluidic Platform for Simultaneous Generation of Four Independent Gradients: Towards High Throughput Screening in Tissue Engineering
Björn Harink, Séverine Le Gac, Clemens van Blitterswijk, and Pamela Habibovic
Tissue Engineering and Regenerative Medicine International Society (TERMIS) 2011 in Granada, Spain

Microfluidic Platform for Simultaneous Generation of Four Independent Gradients: Towards High Throughput Screening of Trace Elements for Bone Tissue Engineering
Björn Harink, Clemens van Blitterswijk, and Pamela Habibovic
Bone-Tec 2011 in Hannover, Germany

2010

Microfluidic Platform for the Simultaneous Generation of Four Independent Gradients: Towards the High Throughput Screening of Trace Elements for Bone Tissue Engineering
Björn Harink, Séverine Le Gac, Clemens van Blitterswijk, and Pamela Habibovic
14th International Conference on Miniaturized Systems for Chemistry and Life Science (μTAS) 2010 in Groningen, The Netherlands, 2010

Microfluidic Platform for Simultaneous Generation of Four Independent Gradients: Towards High Throughput Screening of Trace Elements for Bone Tissue Engineering
Björn Harink, Séverine Le Gac, and Pamela Habibovic
Micro- and Nanofluidics for Cell Biology 2010 in Leiden, The Netherlands

9.2. Figures and tables

Figures

Page 5

Fig. 1.1 (A) Microfluidic device with different colour dies. (B) Zoomed-in image of the different colour dyes meeting in a single channel, showing laminar flow behaviour, therefore the colours do not readily mix. (C) Switching different streams and changing pumps speeds can results in complex fluidic flow-patterns. Courtesy of Albert Foclh LAB ART.

Page 6

Fig. 1.2 Schematic depiction of a microfluidic T-sensor with two fluidic entrances and one exit. The red and green colours depict different dies entering from either side into a single channel with a laminar flow. The yellow colour is the region where the two dies meet and mix solely due to diffusion. The arrows depict the flow directions.

Page 6

Fig. 1.3 (A) Local delivery of trypsin over a monolayer of endothelial cells, including an added fluorescent dye for visualisation. (B) Effect after local trypsin delivery: removing part of endothelial monolayer. Reproduced with permission, copyright 2010 American Physiological Society.[23] (C) Fluorescence images of a single cell after treatment with Mitotracker Green FM on the left and Mitotracker Red on the right. (D) Image of the same cell 2.5 h after staining, showing intermixing of red and green subpopulations of mitochondria. Reproduced with permission, copyright 2001 Macmillan Publishers Ltd.[24]

Page 7

Fig. 1.4 (A) Scanning electron microscope (SEM) image of a captured chondrocyte in complex spatial design, using corner lithography.[25] Courtesy of the University of Twente. (B) SEM image of a spatial design of a liver lobule in a so-called Liver-on-a-Chip. (C) Hepatocytes in the culture area of the artificial liver lobule. Reproduced with permission, copyright 2011 AIP Publishing LLC.[26]

Page 8

Fig. 1.5 Comparative list of materials used in microfluidics and their apparent advantages or disadvantages in fabrication, cell culture and application. Reproduced with permission, copyright 2012 The Royal Society of Chemistry.[36]

Page 10

Fig. 1.6 Multiplexed microfluidics system with 256 individually addressable chambers using 2,056 microvalves. Reproduced with permission, copyright 2007 AAAS.[13]

Page 10

Fig. 1.7 Microscopy image of triple labelled Drosophila embryo, 2 h after fertilisation. The Bicoid protein (blue) gradient, emanating from the left, produces a shallow gradient towards the right, resulting in a sharp difference of expression in Hunchback protein (green), seen by the sharp transition from green to red (DNA). Reproduced with permission, copyright 2007 Elsevier.[53]

Page 12

Fig. 1.8 (A) Original schematic drawing of the Boyden chamber. Compartment B holds a membrane with the test solution on top. Compartment A holds the cells, migrating towards or away from B.[56] (B) Zigmond chamber, which uses lanes divided by shallow bridges, to limit mass transport.57 (C) Dunn chamber, similar to the previous chamber, but in the form of concentric rings.[58]

Page 14

Fig. 1.9 (A) Schematic representation of a diffusion-based multi-gradient microfluidic device, depicting sources and sinks from different entry-points, and the positions of inlets and outlets. (B) Microscope image of the device with three different colour dyes, creating three overlapping gradients solely by diffusion. Reproduced with permission, copyright 2009 Royal Society of Chemistry.

Page 15

Fig. 1.10 Schematic representation of a microfluidic device with a hydrogel membrane sandwiched between two different fluidic layers, which enables the creation of complex shaped chemical gradients by diffusion. Reproduced with permission, copyright 2006 American Society of Chemistry.[66]

Page 17

Fig. 1.11 Schematic representation of microfluidic diffusion-based multi-gradient device. White arrows depict the flow directions and gradient-filled arrows the direction of the overlapping gradients.

Page 20

Fig. 2.1 The needs of regenerative medicine research and the tools microfluidics offers to meet them.

Page 31

Fig. 2.2 Schematic diagram of a Campenot chamber. (A) Top-view with cell-bodies in the centre and axons spreading to the outer chambers by scratches in the surface or through vacuum grease. (B) Side-view of situation in A. (C) Alternative seeding possibility from the left chamber, so the middle part of the axons can be exposed to treatment, separately. Reproduced with permission, copyright 2005 Macmillan Publishers Ltd.[151]

Page 32

Fig. 2.3 Fluorescent microscopy image of a compartmentalised microfluidic device in which two chambers are connected with micro-grooves of 7.5 µm x 3 µm x 900 µm. Neurons, from rat hippocampus, on the left produce Green Fluorescent Protein (GFP) and neurons on the right Red Fluorescent Protein (RFP). Such a system allows the investigation and manipulation of synapses between neurons. Reproduced with permission, copyright 2010 Elsevier.[152]

Page 32

Fig. 2.4 Gel-based 3D microvascular network made of collagen type-I gel. (A) Schematic representation of research possibilities on this platform. (B) Fluorescent microscopy image of human umbilical vein endothelial cells (HUVEC) on the walls of the gel-based networks, stained for the nuclei (blue) and CD31 (red), an angiogenic marker. (C) Schematic side-view representation of the microvascular networks. Reproduced with permission, copyright 2012 National Academy of Sciences, U.S.A.[180]

Page 36

Fig. 2.5 High-throughput screening platform for compression analysis of cells in hydrogel materials. (A) Schematic representation of the compression array in rest and (B) in compressed state. Reproduced with permission, copyright 2010 Elsevier.[196]

Page 37

Fig. 2.6 High-throughput screening platform for cell-biomaterial interactions, using parallel microfluidic chambers with different inkjet printed materials. (A) Photograph of the microfluidic platform, depicting multiple chambers. (B) Schematic representation of a single chamber with printed micropatterns. Reproduced with permission, copyright 2012 Elsevier.[200]

Page 47

Fig. 3.1 (A) Picture of the chip holder inside a microtiter plate microscope with electrical, gas and fluidic connections. The bottle in the bottom left corner is the bubbler to keep the humidity high to prevent evaporation through the gas-permeable tubing. (B) Depiction of a transverse cut-through, showing the position of the temperature probe, the chip, and its connections to the gas-permeable PFA tubing. (C) Exploded view, showing the different separable parts. The lid includes a glass window for top illumination for contrast microscopy. (D) Schematic depiction of a longitudinal cut-through of the chip-holder, showing the position of the two Peltier elements and heat sinks.

Page 50

Fig. 3.2 Graph depicting finite element analysis (COMSOL), using incompressible laminar flow (Navier-Stokes) and diluted species diffusion, of a 15 mm piece of PFA tubing (360 µm OD and 150 µm ID) in a 20% oxygen air environment and flowing water at a flow rate of 1 $\mu L \cdot h^{-1}$ (at 25°C and 1 atm).

Page 51

Fig. 3.3 (A) Schematic diagram of the rectangular chamber, showing the flow directions in the supply channels and cell loading channels, with as inset an enlargement and side-view of the diffusion channels. (B) Photograph of the 2 cm square die with two rectangular chambers. (C) Schematic diagram of the square chamber. (D) Bright-field microscopy image of the glass chip, depicting the chamber with the surrounding supply channels, with as inset an enlargement of the diffusion channels that connect the supply channel with the chamber.

Page 53

Fig. 3.4 (A) Bright-field microscopy images taken from 2 day time-lapse series of C2C12 cells, with t=0 taken just after cell loading. (B) Confocal fluorescence microscopy image of MG63 cells in the square chamber after 2 days of proliferation, with stained nucleus (DNA, DAPI, blue) and cytoskeleton (F-actin, Phalloidin, green). (C) Bright-field microscopy stitched image of the rectangular chamber with CHO cells after 5 days of culture. (D) Epi-fluorescence image of the same CHO cells with live/dead staining, live cells being green and dead cells red.

Page 54

Fig. 3.5 CHO cells with hypoxia GFP reporter (green) inside a gas-impermeable glass chip, using the chip holder, after 48 h culture in normoxic condition (20% O_2), on the left (A-C) and after 22 h under hypoxic condition (approximately 4% O_2) on the right (D-F). For both experiments the following images are provided: bright-field microscopy stitched overview image of the rectangular chamber, with CHO cells inside (A&D); close-up of one section of the rectangular chamber (B&E); and epi-fluorescence microscopy image of the same section of the culture chamber (C&F). After 48 h under normoxic condition, limited or no fluorescence was observed (C), while under hypoxic condition increased fluorescence was observed, indicating the gene reporter is activated.

Page 61

Fig. 4.1 (A) Schematic isometric representation of the four-gradient microfluidic platform, with the four supply channels connected to the chamber by channel arrays. Arrows in the supply channels depict the direction of the flow, and the arrows inside the chamber depict the direction of the gradients. The top inset shows an enlargement of the diffusion channels. (B) Picture of the 2 cm x 2 cm die, depicting the via-holes, channels, and chamber in the middle. The middle inset is an enlargement of a fabricated diffusion channels and the bottom inset shows a bright-field microscopy image of the fabricated chamber.

Page 64

Fig. 4.2 (A) Graph of FEM model depicting the gradient profiles of different flow rates in a chip with a diffusion channel cross-section of 1 µm x 3 µm (10 µM rhodamine 6G), which shows that at different low flow rates (< 1mL·h^{-1}) the gradient profile practically stays the same. (B) Graph of FEM model depicting different diffusion channel cross-sections (12 µL·h^{-1}), showing difference in gradient profiles. (C) Graph depicting the comparison of FEM model gradient (dotted red line) with a fluorescent gradient (solid blue line), using a chip with 3 µm x 1 µm x 10 µm diffusion channels (both 10 µM rhodamine 6G at 12 µL·h^{-1}). The experimental data was obtained from a line profile of a confocal microscopy image, taken at a height of 35 µm from the bottom of the device (dotted black line in D). Since the concentration in the supply channel is known (right peak), and the dye has approximately linear fluorescence emission to concentration in the range used, this peak was used for normalisation. (D) 3D plot of the FEM model depicting a single gradient starting from the bottom, using the same parameters. Coloured lines represent concentration iso-lines. (E) Right to left confocal line scan of the same chamber (horizontal), depicting generated overlapping fluorescent gradients (red, green and yellow). (F) Confocal 3D volume scan image with all four gradients overlapped.

Page 65

Fig. 4.3 Graph showing overlapping line profiles taken from confocal microscopy images, taken every 10 minutes for 24 hours, using a chip with a diffusion channel cross-section of 0.5 µm x 2 µm (1 µM FITC, 250 µL·h^{-1}).

Tables

10 Bibliography.

"If I have seen further it is by standing on the shoulders of giants."

Isaac Newton

Bibliography.

A list of all references used in this thesis

1. A. Daar and H. Greenwood, *J Tissue Eng Regen Med*, 2007, **1**, 179–184.
2. J. Ellman, B. Stoddard, and J. Wells, *Proc. Natl. Acad. Sci. U. S. A.*, 1997, **94**, 2779–82.
3. M. Lebl, *J. Comb. Chem.*, 1999, **1**, 3–24.
4. J. Klein, T. Zech, J. M. Newsam, and S. A. Schunk, *Appl. Catal. A Gen.*, 2003, **254**, 121–131.
5. J. C. Meredith, J.-L. Sormana, B. G. Keselowsky, A. J. García, A. Tona, A. Karim, and E. J. Amis, *J. Biomed. Mater. Res. A*, 2003, **66**, 483–90.
6. J. D. Hoheisel, *Nat Rev Genet*, 2006, **7**, 200–210.
7. A. A. Borisy, P. J. Elliott, N. W. Hurst, M. S. Lee, J. Lehar, E. R. Price, G. Serbedzija, G. R. Zimmermann, M. A. Foley, B. R. Stockwell, and C. T. Keith, *Proc. Natl. Acad. Sci. U. S. A.*, 2003, **100**, 7977–82.
8. M. A. Held, C. G. Langdon, J. T. Platt, T. Graham-Steed, Z. Liu, A. Chakraborty, A. Bacchiocchi, A. Koo, J. W. Haskins, M. W. Bosenberg, and D. F. Stern, *Cancer Discov.*, 2012, **3**, 1–16.
9. H. Kitano, *Science (80-.).*, 2002, **295**, 1662–4.
10. M. Simpson-Brose, J. Treisman, and C. Desplan, *Cell*, 1994, **78**, 855–65.
11. P. Ripphausen, B. Nisius, and J. Bajorath, *Drug Discov. Today*, 2011, **16**, 372–6.
12. B. K. Shoichet, *Nature*, 2004, **432**, 862–5.
13. T. Thorsen, S. J. Maerkl, and S. R. Quake, *Science (80-.).*, 2002, **298**, 580–4.
14. J. Melin and S. R. Quake, *Annu. Rev. Biophys. Biomol. Struct.*, 2007, **36**, 213–31.
15. J. Y. Park, S. Takayama, and S.-H. Lee, *Integr. Biol. (Camb).*, 2010, **2**, 229–40.
16. P. M. Gilbert, K. L. Havenstrite, K. E. G. Magnusson, A. Sacco, N. A. Leonardi, P. Kraft, N. K. Nguyen, S. Thrun, M. P. Lutolf, and H. M. Blau, *Science (80-.).*, 2010, **329**, 1078–81.
17. J. A. Burdick and G. Vunjak-Novakovic, *Tissue Eng. Part A*, 2009, **15**, 205–19.
18. G. M. Whitesides, *Nature*, 2006, **442**, 368–73.
19. U. Moran, R. Phillips, and R. Milo, *Cell*, 2010, **141**, 1262–1262.e1.
20. H. Bruus, *Theoretical microfluidics*, Oxford University Press, USA, 2007, vol. 18.
21. T. M. Squires, *Rev. Mod. Phys.*, 2005, **77**, 977–1026.
22. A. E. Kamholz, B. H. Weigl, B. A. Finlayson, and P. Yager, *Anal. Chem.*, 1999, **71**, 5340–7.
23. A. D. van der Meer, K. Vermeul, A. A. Poot, J. Feijen, and I. Vermes, *Am J Physiol Hear. Circ Physiol*, 2010, **298**, H719–25.
24. S. Takayama, E. Ostuni, P. LeDuc, K. Naruse, D. E. Ingber, and G. M. Whitesides, *Nature*, 2001, **411**, 1016.
25. E. J. W. Berenschot, N. Burouni, B. Schurink, J. W. van Honschoten, R. G. P. Sanders, R. Truckenmuller, H. V Jansen, M. C. Elwenspoek, A. a van Apeldoorn, and N. R. Tas, *Small*, 2012, **8**, 3823–31.
26. Y. Nakao, H. Kimura, Y. Sakai, and T. Fujii, *Biomicrofluidics*, 2011, **5**, 22212.
27. A. D. van der Meer and A. van den Berg, *Integr. Biol.*, 2012, **4**, 461–70.
28. C. S. Effenhauser, G. J. Bruin, A. Paulus, and M. Ehrat, *Anal. Chem.*, 1997, **69**, 3451–7.
29. D. C. Duffy, J. C. McDonald, O. J. Schueller, and G. M. Whitesides, *Anal. Chem.*, 1998, **70**, 4974–84.
30. J. C. Mcdonald, D. C. Duffy, J. R. Anderson, and D. T. Chiu, *Electrophoresis*, 2000, **21**, 27–40.
31. Y. Xia and G. M. Whitesides, *Angew. Chemie Int. Ed.*, 1998, **37**, 550–575.
32. M. A. Unger, C. Hou-Pu, T. Thorsen, A. Scherer, and S. R. Quake, *Science (80-.).*, 2000, **288**, 113–116.
33. E. Berthier, E. W. K. Young, and D. Beebe, *Lab Chip*, 2012, **12**, 1224–37.
34. K. J. Regehr, M. Domenech, J. T. Koepsel, K. C. Carver, S. J. Ellison-Zelski, W. L. Murphy, L. a

Schuler, E. T. Alarid, and D. J. Beebe, *Lab Chip*, 2009, **9**, 2132–9.
35. M. W. Toepke and D. J. Beebe, *Lab Chip*, 2006, **6**, 1484–6.
36. E. Berthier, E. W. K. Young, and D. Beebe, *Lab Chip*, 2012, **12**, 1224–37.
37. C. J. Bettinger and J. T. Borenstein, *Soft Matter*, 2010, **6**, 4999.
38. A. Paguirigan and D. J. Beebe, *Lab Chip*, 2006, **6**, 407–13.
39. N. W. Choi, M. Cabodi, B. Held, J. P. Gleghorn, L. J. Bonassar, and A. D. Stroock, *Nat. Mater.*, 2007, **6**, 908–915.
40. A. D. Stroock and M. Cabodi, *MRS Bullitin*, 2006, **31**, 114–119.
41. S.-Y. Cheng, S. Heilman, M. Wasserman, S. Archer, M. L. Shuler, and M. Wu, *Lab Chip*, 2007, **7**, 763–9.
42. S. Gobaa, S. Hoehnel, M. Roccio, A. Negro, S. Kobel, and M. Lutolf, *Nat. Methods*, 2011, **8**, 949–957.
43. A. J. DeMello, *Nature*, 2006, **442**, 394–402.
44. J. W. Hong and S. R. Quake, *Nat. Biotechnol.*, 2003, **21**, 1179–83.
45. P. Dalerba, T. Kalisky, D. Sahoo, P. S. Rajendran, M. E. Rothenberg, A. a Leyrat, S. Sim, J. Okamoto, D. M. Johnston, D. Qian, M. Zabala, J. Bueno, N. F. Neff, J. Wang, A. a Shelton, B. Visser, S. Hisamori, Y. Shimono, M. van de Wetering, H. Clevers, M. F. Clarke, and S. R. Quake, *Nat. Biotechnol.*, 2011, **29**, 1120–7.
46. C.-H. Hsu, C. Chen, and A. Folch, *Lab Chip*, 2004, **4**, 420–4.
47. D. M. Cate, C. G. Sip, and A. Folch, *Biomicrofluidics*, 2010, **4**, 44105.
48. K. Lai Wing Sun, J. P. Correia, and T. E. Kennedy, *Development*, 2011, **138**, 2153–69.
49. H. Gerhardt, M. Golding, M. Fruttiger, C. Ruhrberg, A. Lundkvist, A. Abramsson, M. Jeltsch, C. Mitchell, K. Alitalo, D. Shima, and C. Betsholtz, *J. Cell Biol.*, 2003, **161**, 1163–77.
50. H. Gerhardt, *Organogenesis*, 2008, **4**, 241–246.
51. J. B. Gurdon and P. Y. Bourillot, *Nature*, 2001, **413**, 797–803.
52. L. Wolpert, *Development*, 1989, **107 Suppl**, 3–12.
53. T. Gregor, D. W. Tank, E. F. Wieschaus, and W. Bialek, *Cell*, 2007, **130**, 153–64.
54. R. D. Nelson, P. G. Quie, and R. L. Simmons, *J. Immunol.*, 1975, **115**, 1650–1656.
55. L. Köhidai, *Curr. Microbiol.*, 1995, **30**, 251–3.
56. S. Boyden, *J. Exp. Med.*, 1962, 453–466.
57. S. Zigmond, *J. Cell Biol.*, 1977, **75**, 606–616.
58. D. Zicha, G. A. Dunn, and A. F. Brown, *J. Cell Sci.*, 1991, **99**, 769–75.
59. S. Kim, H. J. Kim, and N. L. Jeon, *Integr. Biol.*, 2010, **2**, 584–603.
60. S. K. W. Dertinger, D. T. Chiu, N. L. Jeon, and G. M. Whitesides, *Anal. Chem.*, 2001, **73**, 1240–1246.
61. B. G. Chung, L. A. Flanagan, S. W. Rhee, P. H. Schwartz, A. P. Lee, E. S. Monuki, and N. L. Jeon, *Lab Chip*, 2005, **5**, 401–6.
62. C. Joanne Wang, X. Li, B. Lin, S. Shim, G.-L. Ming, and A. Levchenko, *Lab Chip*, 2008, **8**, 227–37.
63. A. Shamloo, N. Ma, M. Poo, L. Sohn, and S. Heilshorn, *Lab Chip*, 2008, 1292–1299.
64. J. Atencia, J. Morrow, and L. E. Locascio, *Lab Chip*, 2009, **9**, 2707–14.
65. S.-Y. Cheng, S. Heilman, M. Wasserman, S. Archer, M. L. Shuler, and M. Wu, *Lab Chip*, 2007, **7**, 763–9.
66. H. Wu, B. Huang, and R. N. Zare, *J. Am. Chem. Soc.*, 2006, **128**, 4194–5.
67. G. M. Whitesides, *Nature*, 2006, **442**, 368–73.
68. S. J. Maerkl, *Integr. Biol.*, 2009, **1**, 19–29.
69. M. Baker, *Nature*, 2011, **471**, 661–665.
70. A. D. van der Meer and A. van den Berg, *Integr. Biol.*, 2012, **4**, 461–70.
71. H. Yu, C. M. Alexander, and D. J. Beebe, *Lab Chip*, 2007, **7**, 726–30.

72. P. C. Thomas, S. R. Raghavan, and S. P. Forry, *Anal. Chem.*, 2011, **83**, 8821–4.
73. M. Csete, *Ann. N. Y. Acad. Sci.*, 2005, **1049**, 1–8.
74. A. P. Vollmer, R. F. Probstein, R. Gilbert, and T. Thorsen, *Lab Chip*, 2005, **5**, 1059–66.
75. A. Shamloo, D. Ph, H. Xu, and S. Heilshorn, *Tissue Eng. Part A*, 2012, **18**, 320–330.
76. P. Lee and P. Hung, *Biotechnol. Bioeng.*, 2006, **94**, 5–14.
77. E. M. Lucchetta, M. S. Munson, and R. F. Ismagilov, *Lab Chip*, 2006, **6**, 185–90.
78. E. Lucchetta, J. Lee, L. Fu, N. Patel, and R. Ismagilov, *Nature*, 2005, **434**.
79. W.-T. Fung, A. Beyzavi, P. Abgrall, N.-T. Nguyen, and H.-Y. Li, *Lab Chip*, 2009, **9**, 2591–2595.
80. J. Warrick, I. Meyvantsson, J. Ju, and D. J. Beebe, *Lab Chip*, 2007, **7**, 316–21.
81. T. Tabata and Y. Takei, *Development*, 2004, **131**, 703–12.
82. H. L. Ashe and J. Briscoe, *Development*, 2006, **133**, 385–94.
83. S. Zigmond, *J. Cell Biol.*, 1977, **75**, 606–616.
84. D. Zicha, G. A. Dunn, and A. F. Brown, *J. Cell Sci.*, 1991, **99**, 769–75.
85. T. M. Keenan and A. Folch, *Lab Chip*, 2008, **8**, 34–57.
86. C. W. Frevert, G. Boggy, T. M. Keenan, and A. Folch, *Lab Chip*, 2006, **6**, 849–56.
87. T. M. Keenan, C.-H. Hsu, and A. Folch, *Appl. Phys. Lett.*, 2006, **89**, 114103.
88. N. Li Jeon, H. Baskaran, S. K. W. Dertinger, G. M. Whitesides, L. Van de Water, and M. Toner, *Nat. Biotechnol.*, 2002, **20**, 826–30.
89. G. S. Jeong, S. Han, Y. Shin, G. H. Kwon, R. D. Kamm, S.-H. Lee, and S. Chung, *Anal. Chem.*, 2011, **83**, 8454–9.
90. J. Choi, S. Kim, J. Jung, Y. Lim, K. Kang, S. Park, and S. Kang, *Biomaterials*, 2011, **32**, 7013–22.
91. G. Mehta, J. Lee, W. Cha, Y.-C. Tung, J. J. Linderman, and S. Takayama, *Anal. Chem.*, 2009, **81**, 3714–22.
92. K. Ren, W. Dai, J. Zhou, J. Su, and H. Wu, *Proc. Natl. Acad. Sci. U. S. A.*, 2011, **108**, 8162–6.
93. C. J. Bettinger, K. M. Cyr, A. Matsumoto, R. Langer, J. T. Borenstein, and D. L. Kaplan, *Adv. Mater.*, 2007, **19**, 2847–2850.
94. C. J. Bettinger, K. M. Cyr, A. Matsumoto, R. Langer, J. T. Borenstein, and D. L. Kaplan, *Adv. Mater.*, 2007, **19**, 2847–2850.
95. B. Kundu, R. Rajkhowa, S. C. Kundu, and X. Wang, *Adv. Drug Deliv. Rev.*, 2012.
96. P. S. Lienemann, M. P. Lutolf, and M. Ehrbar, *Adv. Drug Deliv. Rev.*, 2012, **64**, 1078–89.
97. S. Allazetta, S. Cosson, and M. P. Lutolf, *Chem. Commun.*, 2011, **47**, 191–3.
98. Y. Xia, E. Kim, X. Zhao, J. Rogers, M. Prentiss, and G. Whitesides, *Science (80-.).*, 1996, **273**, 347–9.
99. S. Kobel, M. Limacher, S. Gobaa, T. Laroche, and M. P. Lutolf, *Langmuir*, 2009, **25**, 8774–9.
100. C. S. Chen, M. Mrksich, S. Huang, G. M. Whitesides, and D. E. Ingber, *Biotechnol. Prog.*, 1998, **14**, 356–63.
101. R. McBeath, D. Pirone, and C. Nelson, *Dev. Cell*, 2004, **6**, 483–495.
102. C. Flaim, S. Chien, and S. Bhatia, *Nat. Methods*, 2005, **2**, 119–125.
103. S. Le Gac and A. van den Berg, *Trends Biotechnol.*, 2010, **28**, 55–62.
104. J. Rouwkema, N. C. Rivron, and C. a van Blitterswijk, *Trends Biotechnol.*, 2008, **26**, 434–41.
105. S. Kobel and M. P. Lutolf, *Biotechniques*, 2010, **48**.
106. S. Kobel and M. P. Lutolf, *Curr. Opin. Biotechnol.*, 2011, **22**, 690–7.
107. A. Ranga and M. P. Lutolf, *Curr. Opin. Cell Biol.*, 2012, **24**, 236–44.
108. C. E. Sims and N. L. Allbritton, *Lab Chip*, 2007, **7**, 423–40.
109. R. Trouillon, M. K. Passarelli, J. Wang, M. E. Kurczy, and A. G. Ewing, *Anal. Chem.*, 2013, **85**, 522–42.
110. H. Yin and D. Marshall, *Curr. Opin. Biotechnol.*, 2012, **23**, 110–9.
111. D. Di Carlo, L. Y. Wu, and L. P. Lee, *Lab Chip*, 2006, **6**, 1445–9.
112. S. A. Kobel, O. Burri, A. Griffa, M. Girotra, A. Seitz, and M. P. Lutolf, *Lab Chip*, 2012, **12**, 2843–9.

113. F. T. G. van den Brink, E. Gool, J.-P. Frimat, J. Bomer, A. van den Berg, and S. Le Gac, *Electrophoresis*, 2011, **32**, 3094–100.
114. K. S. Phillips, H. H. Lai, E. Johnson, C. E. Sims, and N. L. Allbritton, *Lab Chip*, 2011, **11**, 1333–41.
115. J. S. Marcus, W. F. Anderson, and S. R. Quake, *Anal. Chem.*, 2006, **78**, 3084–9.
116. Y.-C. Chen, P. Ingram, X. Lou, and E. Yoon, *16th Int. MicroTAS Proc.*, 2012, 106–108.
117. G. Mehta, A. Y. Hsiao, M. Ingram, G. D. Luker, and S. Takayama, *J. Control. Release*, 2012, **164**, 192–204.
118. J. M. Kelm and M. Fussenegger, *Trends Biotechnol.*, 2004, **22**, 195–202.
119. M. Ingram, G. Techy, and R. Saroufeem, *Vitr. Cell. Dev. Bio.*, 1997, **33**, 459–466.
120. S. L. Nyberg, J. Hardin, B. Amiot, U. a Argikar, R. P. Remmel, and P. Rinaldo, *Liver Transplant.*, 2005, **11**, 901–10.
121. N. C. Rivron, E. J. Vrij, J. Rouwkema, S. Le Gac, A. van den Berg, R. K. Truckenmüller, and C. a van Blitterswijk, *Proc. Natl. Acad. Sci. U. S. A.*, 2012, **109**, 6886–91.
122. Y. Torisawa, B. Chueh, D. Huh, P. Ramamurthy, T. M. Roth, K. F. Barald, and S. Takayama, *Lab Chip*, 2007, **7**, 770–6.
123. H.-J. Jin, Y.-H. Cho, J.-M. Gu, J. Kim, and Y.-S. Oh, *Lab Chip*, 2011, **11**, 115–9.
124. L. Yu, M. C. W. Chen, and K. C. Cheung, *Lab Chip*, 2010, **10**, 2424–32.
125. Y.-C. Tung, A. Y. Hsiao, S. G. Allen, Y. Torisawa, M. Ho, and S. Takayama, *Analyst*, 2011, **136**, 473–8.
126. Y. Torisawa, B. Mosadegh, G. D. Luker, M. Morell, K. S. O'Shea, and S. Takayama, *Integr. Biol.*, 2009, **1**, 649–54.
127. B. G. Chung, K.-H. Lee, A. Khademhosseini, and S.-H. Lee, *Lab Chip*, 2012, **12**, 45–59.
128. A. Khademhosseini and R. Langer, *Biomaterials*, 2007, **28**, 5087–92.
129. T. Takei, N. Kishihara, S. Sakai, and K. Kawakami, *Biochem. Eng. J.*, 2010, **49**, 143–147.
130. U. A. Gurkan, S. Tasoglu, D. Kavaz, M. C. Demirel, and U. Demirci, *Adv. Healthc. Mater.*, 2012, **1**, 149–58.
131. D. Huh, H. Fujioka, Y.-C. Tung, N. Futai, R. Paine, J. B. Grotberg, and S. Takayama, *Proc. Natl. Acad. Sci. U. S. A.*, 2007, **104**, 18886–91.
132. P. Lee, P. Hung, and L. Lee, *Biotechnol. Bioeng.*, 2007, **97**, 1340–1346.
133. D. Huh, B. D. Matthews, A. Mammoto, M. Montoya-Zavala, H. Y. Hsin, and D. E. Ingber, *Science (80-.).*, 2010, **328**, 1662–8.
134. C. Moraes, G. Mehta, S. C. Lesher-Perez, and S. Takayama, *Ann. Biomed. Eng.*, 2012, **40**, 1211–27.
135. W. H. Grover, M. G. von Muhlen, and S. R. Manalis, *Lab Chip*, 2008, **8**, 913–8.
136. M. T. Guo, A. Rotem, J. a Heyman, and D. a Weitz, *Lab Chip*, 2012, **12**, 2146–55.
137. J. Baret, V. Taly, M. Ryckelynck, C. A. Merten, and A. D. Griffiths, *Med Sci*, 2009, **25**, 627–632.
138. W. Gu, X. Zhu, N. Futai, B. S. Cho, and S. Takayama, *Proc. Natl. Acad. Sci. U. S. A.*, 2004, **101**, 15861–6.
139. C. L. Hansen, M. O. A. Sommer, and S. R. Quake, *Proc. Natl. Acad. Sci. U. S. A.*, 2004, **101**, 14431–6.
140. N. Bontoux, L. Dauphinot, T. Vitalis, V. Studer, Y. Chen, J. Rossier, and M.-C. Potier, *Lab Chip*, 2008, **8**, 443–50.
141. C. L. Hansen, E. Skordalakes, J. M. Berger, and S. R. Quake, *Proc. Natl. Acad. Sci. U. S. A.*, 2002, **99**, 16531–6.
142. B. Mosadegh, T. Bersano-Begey, J. Y. Park, M. a Burns, and S. Takayama, *Lab Chip*, 2011, **11**, 2813–8.
143. B. Starly and A. Choubey, *Ann. Biomed. Eng.*, 2008, **36**, 30–40.
144. S. M. Grist, L. Chrostowski, and K. C. Cheung, *Sensors*, 2010, **10**, 9286–316.

145. C. Amatore, S. Arbault, Y. Bouret, B. Cauli, M. Guille, A. Rancillac, and J. Rossier, *Chemphyschem*, 2006, **7**, 181–7.
146. M. Takeda, H. Shiku, K. Ino, and T. Matsue, *Analyst*, 2011, **136**, 4991–6.
147. S. H. Jeong, D. W. Lee, S. Kim, J. Kim, and B. Ku, *Biosens. Bioelectron.*, 2012, **35**, 128–33.
148. W. Chen, M. Lisowski, G. Khalil, I. R. Sweet, and A. Q. Shen, *PLoS One*, 2012, **7**, e33070.
149. E. E. Krommenhoek, J. G. E. Gardeniers, J. G. Bomer, X. Li, M. Ottens, G. W. K. van Dedem, M. Van Leeuwen, W. M. van Gulik, L. a M. van der Wielen, J. J. Heijnen, and A. a van den Berg, *Anal. Chem.*, 2007, **79**, 5567–73.
150. R. B. Campenot, *Proc. Natl. Acad. Sci. U. S. A.*, 1977, **74**, 4516–4519.
151. L. S. Zweifel, R. Kuruvilla, and D. D. Ginty, *Nat. Rev. Neurosci.*, 2005, **6**, 615–25.
152. A. M. Taylor, D. C. Dieterich, H. T. Ito, S. a Kim, and E. M. Schuman, *Neuron*, 2010, **66**, 57–68.
153. D. Kilinc, J.-M. Peyrin, V. Soubeyre, S. Magnifico, L. Saias, J.-L. Viovy, and B. Brugg, *Neurotox. Res.*, 2011, **19**, 149–61.
154. W. W. Liu, J. Goodhouse, N. L. Jeon, and L. W. Enquist, *PLoS One*, 2008, **3**, e2382.
155. K. A. Hosie, A. E. King, C. A. Blizzard, J. C. Vickers, and T. C. Dickson, *ASN Neuro*, 2012, **4**, 47–57.
156. J. W. Park, B. Vahidi, A. M. Taylor, S. W. Rhee, and N. L. Jeon, *Nat. Protoc.*, 2006, **1**, 2128–36.
157. A. M. Taylor and N. L. Jeon, *Crit. Rev. Biomed. Eng.*, 2011, **39**, 185–200.
158. I. H. Yang, R. Siddique, S. Hosmane, N. Thakor, and A. Höke, *Exp. Neurol.*, 2009, **218**, 124–8.
159. L. Li, L. Ren, W. Liu, J.-C. Wang, Y. Wang, Q. Tu, J. Xu, R. Liu, Y. Zhang, M.-S. Yuan, T. Li, and J. Wang, *Anal. Chem.*, 2012, **84**, 6444–53.
160. Y. Kim, K. Karthikeyan, S. Chirvi, and D. P. Davé, *Lab Chip*, 2009, **9**, 2576–81.
161. J. Walter, S. Henke-Fahle, and F. Bonhoeffer, *Development*, 1987, **101**, 909–913.
162. B. Vahidi, J. W. Park, H. J. Kim, and N. L. Jeon, *J. Neurosci. Methods*, 2008, **170**, 188–96.
163. N. Bhattacharjee, N. Li, T. M. Keenan, and A. Folch, *Integr. Biol.*, 2010, **2**, 669–79.
164. A. Kunze, M. Giugliano, A. Valero, and P. Renaud, *Biomaterials*, 2011, **32**, 2088–98.
165. A. Kunze, A. Valero, D. Zosso, and P. Renaud, *PLoS One*, 2011, **6**, e26187.
166. A. Kunze, R. Meissner, S. Brando, and P. Renaud, *Biotechnol. Bioeng.*, 2011, **108**, 2241–5.
167. C. R. Kothapalli, E. van Veen, S. de Valence, S. Chung, I. K. Zervantonakis, F. B. Gertler, and R. D. Kamm, *Lab Chip*, 2011, **11**, 497–507.
168. H. G. Sundararaghavan, G. a Monteiro, B. L. Firestein, and D. I. Shreiber, *Biotechnol. Bioeng.*, 2009, **102**, 632–43.
169. H. G. Sundararaghavan, S. N. Masand, and D. I. Shreiber, *J. Neurotrauma*, 2011, **28**, 2377–87.
170. B. J. Pfister, A. Iwata, D. F. Meaney, and D. H. Smith, *J. Neurosci.*, 2004, **24**, 7978–83.
171. D. H. Smith, J. a Wolf, T. a Lusardi, V. M. Lee, and D. F. Meaney, *J. Neurosci.*, 1999, **19**, 4263–9.
172. M. D. Tang-Schomer, A. R. Patel, P. W. Baas, and D. H. Smith, *FASEB J.*, 2010, **24**, 1401–10.
173. Y.-W. Lin, C.-M. Cheng, P. R. Leduc, and C.-C. Chen, *PLoS One*, 2009, **4**, e4293.
174. S.-M. Ong, C. Zhang, Y.-C. Toh, S. H. Kim, H. L. Foo, C. H. Tan, D. van Noort, S. Park, and H. Yu, *Biomaterials*, 2008, **29**, 3237–44.
175. L. Ziegler, S. Grigoryan, I. H. Yang, N. V Thakor, and R. S. Goldstein, *Stem Cell Rev.*, 2011, **7**, 394–403.
176. P. Shi, M. a Scott, B. Ghosh, D. Wan, Z. Wissner-Gross, R. Mazitschek, S. J. Haggarty, and M. F. Yanik, *Nat. Commun.*, 2011, **2**, 510.
177. X. Tian, S. Wang, Z. Zhang, and D. Lv, *PLoS One*, 2012, **7**, e42804.
178. M. C. Peterman, N. Z. Mehenti, K. V Bilbao, C. J. Lee, T. Leng, J. Noolandi, S. F. Bent, M. S. Blumenkranz, and H. a Fishman, *Artif. Organs*, 2003, **27**, 975–85.
179. R. K. Jain, P. Au, J. Tam, D. G. Duda, and D. Fukumura, *Nat Biotech*, 2005, **23**, 821–823.
180. Y. Zheng, J. Chen, M. Craven, N. W. Choi, S. Totorica, A. Diaz-Santana, P. Kermani, B. Hempstead, C. Fischbach-Teschl, J. a López, and A. D. Stroock, *Proc. Natl. Acad. Sci. U. S. A.*,

2012, **109**, 9342–7.
181. B. M. Gillette, J. a Jensen, B. Tang, G. J. Yang, A. Bazargan-Lari, M. Zhong, and S. K. Sia, *Nat. Mater.*, 2008, **7**, 636–40.
182. B. Carrion, C. P. Huang, C. M. Ghajar, S. Kachgal, E. Kniazeva, N. L. Jeon, and A. J. Putnam, *Biotechnol. Bioeng.*, 2010, **107**, 1020–8.
183. S. Chung, R. Sudo, I. K. Zervantonakis, T. Rimchala, and R. D. Kamm, *Adv. Mater.*, 2009, **21**, 4863–7.
184. W. A. Farahat, L. B. Wood, I. K. Zervantonakis, A. Schor, S. Ong, D. Neal, R. D. Kamm, and H. H. Asada, *PLoS One*, 2012, **7**, e37333.
185. Y. Shin, J. S. Jeon, S. Han, G.-S. Jung, S. Shin, S.-H. Lee, R. Sudo, R. D. Kamm, and S. Chung, *Lab Chip*, 2011, **11**, 2175–81.
186. R. Sudo, S. Chung, I. K. Zervantonakis, V. Vickerman, Y. Toshimitsu, L. G. Griffith, and R. D. Kamm, *FASEB*, 2009, **23**, 2155–64.
187. J. M. Chan, I. K. Zervantonakis, T. Rimchala, W. J. Polacheck, J. Whisler, and R. D. Kamm, *PLoS One*, 2012, **7**, e50582.
188. C.-C. Liang, A. Y. Park, and J.-L. Guan, *Nat. Protoc.*, 2007, **2**, 329–33.
189. M. Felder, P. Sallin, L. Barbe, B. Haenni, A. Gazdhar, T. Geiser, and O. Guenat, *Lab Chip*, 2012, **12**, 640–6.
190. A. D. van der Meer, K. Vermeul, A. A. Poot, J. Feijen, and I. Vermes, *Am J Physiol Hear. Circ Physiol*, 2010, **298**, H719–25.
191. K. Jang, K. Sato, K. Igawa, U. Chung, and T. Kitamori, *Anal. Bioanal. Chem.*, 2008, **390**, 825–32.
192. Y.-T. Xiao, L.-X. Xiang, and J.-Z. Shao, *Biochem. Biophys. Res. Commun.*, 2007, **362**, 550–3.
193. D. Rickard, T. Sullivan, and B. Shenker, *Dev. Biol.*, 1994, **161**, 218–228.
194. E. Leclerc, B. David, L. Griscom, B. Lepioufle, T. Fujii, P. Layrolle, and C. Legallaisa, *Biomaterials*, 2006, **27**, 586–95.
195. B. Riehl and J. Lim, *Cells*, 2012, **1**, 1225–1245.
196. C. Moraes, G. Wang, Y. Sun, and C. a Simmons, *Biomaterials*, 2010, **31**, 577–84.
197. C. Moraes, J.-H. Chen, Y. Sun, and C. a Simmons, *Lab Chip*, 2010, **10**, 227–34.
198. Y.-C. Toh, C. Zhang, J. Zhang, Y. M. Khong, S. Chang, V. D. Samper, D. van Noort, D. W. Hutmacher, and H. Yu, *Lab Chip*, 2007, **7**, 302–9.
199. Y. Li, J. Qin, B. Lin, and W. Zhang, *Tissue Eng. Part C*, 2010, **16**, 1267–1275.
200. J.-H. Lee, Y. Gu, H. Wang, and W. Y. Lee, *Biomaterials*, 2012, **33**, 999–1006.
201. J.-H. Lee, H. Wang, J. B. Kaplan, and W. Y. Lee, *Acta Biomater.*, 2010, **6**, 4422–9.
202. J. Lee and H. Wang, *Tissue Eng. Part C*, 2010, **17**, 39–48.
203. A. Tourovskaia, X. Figueroa-Masot, and A. Folch, *Lab Chip*, 2005, **5**, 14–9.
204. T. F. Kosar, A. Tourovskaia, X. Figueroa-Masot, M. E. Adams, and A. Folch, *Lab Chip*, 2006, **6**, 632–8.
205. A. Tourovskaia, X. Figueroa-Masot, and A. Folch, *Nat. Protoc.*, 2006, **1**, 1092–104.
206. A. Tourovskaia, N. Li, and A. Folch, *Biophys. J.*, 2008, **95**, 3009–16.
207. E. Figallo, C. Cannizzaro, S. Gerecht, J. A. Burdick, R. Langer, N. Elvassore, and G. Vunjak-Novakovic, *Lab Chip*, 2007, **7**, 710–9.
208. L. Shintu, R. Baudoin, V. Navratil, J.-M. Prot, C. Pontoizeau, M. Defernez, B. J. Blaise, C. Domange, A. R. Péry, P. Toulhoat, C. Legallais, C. Brochot, E. Leclerc, and M.-E. Dumas, *Anal. Chem.*, 2012, **84**, 1840–8.
209. P. M. van Midwoud, E. Verpoorte, and G. M. M. Groothuis, *Integr. Biol.*, 2011, **3**, 509–21.
210. Y. Imura, E. Yoshimura, and K. Sato, *Anal. Sci.*, 2012, **28**, 197–9.
211. R. Baudoin, A. Corlu, L. Griscom, C. Legallais, and E. Leclerc, *Toxicol. Vitr.*, 2007, **21**, 535–44.
212. V. N. Goral and P. K. Yuen, *Ann. Biomed. Eng.*, 2012, **40**, 1244–54.

213. S. Kaihara, J. Borenstein, R. Koka, S. Lalan, E. R. Ochoa, M. Ravens, H. Pien, B. Cunningham, and J. P. Vacanti, *Tissue Eng.*, 2000, **6**, 105–17.
214. X. Ju, D. Li, N. Gao, Q. Shi, and H. Hou, *Biotechnol. J.*, 2008, **3**, 383–91.
215. J. H. Sung, J. Choi, D. Kim, and M. L. Shuler, *Biotechnol. Bioeng.*, 2009, **104**, 516–25.
216. A. Carraro, W.-M. Hsu, K. M. Kulig, W. S. Cheung, M. L. Miller, E. J. Weinberg, E. F. Swart, M. Kaazempur-Mofrad, J. T. Borenstein, J. P. Vacanti, and C. Neville, *Biomed. Microdevices*, 2008, **10**, 795–805.
217. E. Leclerc, Y. Sakai, and T. Fujii, *Biomed. Microdevices*, 2003, **5**, 109–114.
218. E. Leclerc, Y. Sakai, and T. Fujii, *Biochem. Eng. J.*, 2004, **20**, 143–148.
219. S. Ostrovidov, J. Jiang, and Y. Sakai, *Biomed. Microdevices*, 2004, **6**, 279–287.
220. M. J. Powers, K. Domansky, M. R. Kaazempur-mofrad, A. Kalezi, A. Capitano, A. Upadhyaya, P. Kurzawski, K. E. Wack, D. B. Stolz, R. Kamm, and L. G. Grif, *Biotechnol. Bioeng.*, 2002, **78**, 257–269.
221. R. Baudoin, G. Alberto, P. Paullier, C. Legallais, and E. Leclerc, *Sensors Actuators B Chem.*, 2012, **173**, 919–926.
222. N. Ye, J. Qin, X. Liu, W. Shi, and B. Lin, *Electrophoresis*, 2007, **28**, 1146–53.
223. N. Ye, J. Qin, W. Shi, X. Liu, and B. Lin, *Lab Chip*, 2007, **7**, 1696–704.
224. J. M. Prot, C. Aninat, L. Griscom, F. Razan, C. Brochot, C. G. Guillouzo, C. Legallais, A. Corlu, and E. Leclerc, *Biotechnol. Bioeng.*, 2011, **108**, 1704–15.
225. B. Altmann, S. Giselbrecht, K.-F. Weibezahn, A. Welle, and E. Gottwald, *Biomed. Mater.*, 2008, **3**, 034120.
226. K. Domansky, W. Inman, J. Serdy, A. Dash, M. H. M. Lim, and L. G. Griffith, *Lab Chip*, 2010, **10**, 51–8.
227. W.-M. Hsu, A. Carraro, K. M. Kulig, M. L. Miller, M. Kaazempur-Mofrad, E. Weinberg, F. Entabi, H. Albadawi, M. T. Watkins, J. T. Borenstein, J. P. Vacanti, and C. Neville, *Ann. Surg.*, 2010, **252**, 351–7.
228. S. F. Wong, D. Y. No, Y. Y. Choi, D. S. Kim, B. G. Chung, and S.-H. Lee, *Biomaterials*, 2011, **32**, 8087–96.
229. K. Nakazawa, Y. Izumi, J. Fukuda, and T. Yasuda, *J. Biomater. Sci. Polym. Edn.*, 2006, **17**, 859–873.
230. J. Fukuda and K. Nakazawa, *Tissue Eng.*, 2005, **11**, 1254–1262.
231. S. Lee, E. Kang, J. Ju, D. Kim, and S. Lee, *Lab Chip*, 2013.
232. Y.-C. Toh, T. C. Lim, D. Tai, G. Xiao, D. van Noort, and H. Yu, *Lab Chip*, 2009, **9**, 2026–35.
233. R. Baudoin, L. Griscom, M. Monge, C. Legallais, and E. Leclerc, *Biotechnol. Prog.*, 2007, **23**, 1245–53.
234. K.-J. Jang, H. S. Cho, D. H. Kang, W. G. Bae, T.-H. Kwon, and K.-Y. Suh, *Integr. Biol.*, 2011, **3**, 134–41.
235. K.-J. Jang and K.-Y. Suh, *Lab Chip*, 2010, **10**, 36–42.
236. T. Kniazeva, J. C. Hsiao, J. L. Charest, and J. T. Borenstein, *Biomed. Microdevices*, 2011, **13**, 315–23.
237. N. Ferrell, K. B. Ricci, J. Groszek, J. T. Marmerstein, and W. H. Fissell, *Biotechnol. Bioeng.*, 2012, **109**, 797–803.
238. J. Park, H. Koito, J. Li, and A. Han, *Biomed. Microdevices*, 2009, **11**, 1145–53.
239. C.-T. Ho, R.-Z. Lin, W.-Y. Chang, H.-Y. Chang, and C.-H. Liu, *Lab Chip*, 2006, **6**, 724–34.
240. J. Burdick, A. Khademhosseini, and R. Langer, *Langmuir*, 2004, **20**, 8–11.
241. N. Zaari, P. Rajagopalan, S. K. Kim, a. J. Engler, and J. Y. Wong, *Adv. Mater.*, 2004, **16**, 2133–2137.
242. A. van der Meer and A. van den Berg, *Integr. Biol.*, 2012, **4**, 461–70.
243. B. Harink, S. Le Gac, R. Truckenmüller, C. van Blitterswijk, and P. Habibovic, *Lab Chip*, 2013, **13**,

3512–28.
244. G. Mehta, K. Mehta, D. Sud, J. Song, T. Bersano-Begey, N. Futai, Y.-S. Heo, M.-A. Mycek, J. Linderman, and S. Takayama, *Biomed. Microdevices*, 2007, **9**, 123–34.
245. S. Oppegard and D. Eddington, *Biomed. Microdevices*, 2013, **15**, 407–14.
246. C.-C. Peng, W.-H. Liao, Y.-H. Chen, C.-Y. Wu, and Y.-C. Tung, *Lab Chip*, 2013, **13**, 3239–45.
247. D. Duffy, J. McDonald, O. Schueller, and G. Whitesides, *Anal. Chem.*, 1998, **70**, 4974–84.
248. E. Berthier, E. Young, and D. Beebe, *Lab Chip*, 2012, **12**, 1224–37.
249. A. Daar and H. Greenwood, *J Tissue Eng Regen Med*, 2007, **1**, 179–84.
250. M. Reichen, R. J. Macown, N. Jaccard, A. Super, L. Ruban, L. D. Griffin, F. S. Veraitch, and N. Szita, *PLoS One*, 2012, **7**, e52246.
251. T. Kirk and N. Szita, *Biotechnol. Bioeng.*, 2013, **110**, 1005–19.
252. L. Hanson, L. Cui, C. Xie, and B. Cui, *Microsc. Res. Tech.*, 2011, **74**, 496–501.
253. C. Extrand and L. Monson, *J Appl Polym Sci*, 2006, **100**, 2122–2125.
254. A. Oller, C. Buser, M. Tyo, and W. Thilly, *J Cell Sci*, 1989, **94**, 43–9.
255. C. Allen, *Am J Physiol Lung Cell Mol Physiol*, 2001, **281**, 1021–27.
256. M. W. Toepke and D. J. Beebe, *Lab Chip*, 2006, **6**, 1484–6.
257. R. Mukhopadhyay, *Anal. Chem.*, 2007, **79**, 3248–3253.
258. J. Malda, J. Rouwkema, D. Martens, E. Le Comte, F. Kooy, J. Tramper, C. van Blitterswijk, and J. Riesle, *Biotechnol. Bioeng.*, 2004, **86**, 9–18.
259. J. Liu, J. Hilderink, T. Groothuis, C. Otto, C. van Blitterswijk, and J. de Boer, *J Tissue Eng Regen Med*, 2013, DOI:10.1002/term.1654.
260. S. J. Maerkl, *Integr. Biol.*, 2009, **1**, 19–29.
261. E. W. K. Young and D. J. Beebe, *Chem. Soc. Rev.*, 2010, **39**, 1036–48.
262. B. Harink, S. Le Gac, R. Truckenmüller, C. van Blitterswijk, and P. Habibovic, *Lab Chip*, 2013.
263. Y. Gong, A. O. Ogunniyi, and J. C. Love, *Lab Chip*, 2010, **10**, 2334–7.
264. P.-O. Gendron, F. Avaltroni, and K. J. Wilkinson, *J. Fluoresc.*, 2008, **18**, 1093–101.
265. F. Lin and E. C. Butcher, *Lab Chip*, 2006, **6**, 1462–9.
266. N. Li Jeon, H. Baskaran, S. K. W. Dertinger, G. M. Whitesides, L. Van de Water, and M. Toner, *Nat. Biotechnol.*, 2002, **20**, 826–30.
267. B. Harink, S. Le Gac, D. Barata, C. van Blitterswijk, and P. Habibovic, *Lab Chip*, 2014, **14**, 1816–20.
268. J. Doorn, H. A. M. Fernandes, B. Q. Le, J. van de Peppel, J. P. T. M. van Leeuwen, M. R. De Vries, Z. Aref, P. H. A. Quax, O. Myklebost, D. B. F. Saris, C. A. van Blitterswijk, and J. de Boer, *Biomaterials*, 2013, **34**, 3053–63.
269. L. Krishnan, N. Willett, and R. Guldberg, *Ann. Biomed. Eng.*, 2014, **42**, 432–444.
270. G. L. Wang, B. H. Jiang, E. A. Rue, and G. L. Semenza, *Proc. Natl. Acad. Sci. U. S. A.*, 1995, **92**, 5510–4.
271. S. Li and H. A. Mottola, *Anal. Chim. Acta*, 1994, **289**, 79–85.
272. P. Bots, L. G. Benning, J.-D. Rodriguez-Blanco, T. Roncal-Herrero, and S. Shaw, *Cryst. Growth Des.*, 2012, **12**, 3806–3814.
273. T. Ogino, T. Suzuki, and K. Sawada, *Geochim. Cosmochim. Acta*, 1987, **51**, 2757–2767.
274. J. Rodriguez-Blanco, S. Shaw, and L. Benning, *Mineral. Mag.*, 2008, **72**, 283–286.
275. J. D. Rodriguez-Blanco, S. Shaw, and L. G. Benning, *Nanoscale*, 2011, **3**, 265–71.
276. B. Ji, M. Cusack, A. Freer, P. S. Dobson, N. Gadegaard, and H. Yin, *Integr. Biol.*, 2010, **2**, 528–35.
277. J. D. Rodriguez-Blanco, S. Shaw, P. Bots, T. Roncal-Herrero, and L. G. Benning, *J. Alloys Compd.*, 2012, **536**, S477–S479.
278. B. Harink, S. Le Gac, and P. Habibovic, in *Micro- and Nanofluidics for Cell Biology*, Lorentz Center, Leiden, The Netherlands, 2010.

The New Gradient Wave

The aim of regenerative medicine (RM) is to restore normal function of damaged tissues or organs, using cell therapy, tissue engineered constructs and synthetic graft substitutes. Since the population of the western world is ageing, there is an increasing need for RM therapies, which are readily available in large quantities. In general, the search for such strategies is based on the candidate approach in which a limited number of candidates (e.g. biomaterials, growth factors and cells) are selected, based on a rationale. As a result, a limited number of candidates is investigated, and therefore development and clinical implementation of novel, significantly improved strategies is relatively slow. In this work the development of a screening method for RM research is presented, based on a multi-gradient microfluidic platform, with the goal to speed up the search for such candidates.

The Author

Björn Harink received his BSc. in Biomedical Engineering at the University of Twente (UT) in 2006, where he worked on microarray spotting techniques for Surface Plasmon Resonance Imaging (SPRI) at the Biophysical Engineering group of Prof. Subramaniam in the MIRA Institute for Biomedical Technology and Technical Medicine. During his master he did an internship at the Korean Institute of Machinery and Materials (KIMM), Daejeon, South Korea, working on sub-cellular laser-ablation. In 2008 he received his MSc. in Materials, Cellular and Tissue Engineering, focused on Micro- and Nanotechnology, also at the UT, where he worked on the coupling of Isoelectric Focusing (IEF) to SPRI, using microfluidics, for the search of biomarkers in autoimmune diseases at the BIOS - Lab-on-a-Chip group of Prof. Van den Berg in the MESA+ Institute for Nanotechnology. Before he started his PhD research, he worked (BIOS) on an alternative fabrication method for silicon nanowires, using E-beam lithography, for the use as biosensors. In 2009 he started his PhD project in the department of Tissue Regeneration of Prof. Van Blitterswijk (MIRA). The result of this project is presented in this book.

www.bjornharink.info

ISBN: 978-90-365-3756-8 DOI: 10.3990/1.9789036537568